

SIGLEC LIGAND EXPRESSION AT THE CHOROID PLEXUS MODULATES  
NEUROINFLAMMATION IN ALZHEIMER'S DISEASE

by

KATELYN ROSENBALM

(Under the Direction of MICHAEL TIEMEYER)

ABSTRACT

The pathology of Alzheimer's disease (AD) is complex and involves incompletely understood inflammatory responses. The contributions of inflammatory cells, either resident in the brain (microglia) or recruited from peripheral sources (monocytes/macrophages), are an emerging interest with regard to the initiation and progression of AD. The choroid plexus (CP), which comprises an important part of the interface between the peripheral blood and the cerebrospinal fluid, functions as an immune gateway in the brain and has been proposed to regulate trafficking, activation, and differentiation of inflammatory cells. In a mouse model for aggressive familial AD, we observed upregulated expression of ligands for Siglec-F on CP epithelial cells. Siglec-F, like other members of the Siglec family, binds sialylated glycans to modulate innate and adaptive immune responses in many inflammatory contexts. To explore the role of Siglec ligand expression in normal human CP and in human neurodegenerative disease progression, we have undertaken targeted glycomic and glycoproteomic analysis of Siglec-F and Siglec-9 counterreceptors expressed by choroid plexus papilloma cells (HIBCPP) as well as by 3-D choroid plexus tissue derived from patient induced pluripotent stem cells (choroid plexus organoids, which we call chorganoids). Specific endoglycosidase digestion and orthogonal biochemical analysis indicates that human CP cells

present keratan sulfate ligands for Siglec-9, as well as structurally related ligands for Siglec-F, on polypeptide backbones including low-density lipoprotein receptor-related protein 1 (LRP1) and galectin-3 binding protein/Mac-2 binding protein/90k tumor associated antigen (Gal-3BP). Gal-3BP ligands for Siglec-9 purified from HIBCPP cell media induce inflammatory cell responses using a murine bone marrow derived hematopoietic cell-based screening platform. The identification of these Siglec ligands in a unique tissue setting presents opportunities for investigating the response of inflammatory cells to disease-related glycan expression.

INDEX WORDS: glycosylation, Alzheimer's disease, choroid plexus, Siglec, innate immunity, glycomics, neuroinflammation

SIGLEC LIGAND EXPRESSION AT THE CHOROID PLEXUS MODULATES  
NEUROINFLAMMATION IN ALZHEIMER'S DISEASE

by

KATELYN ROSENBALM

BA, Lawrence University, 2014

A Dissertation Submitted to the Graduate Faculty of The University of Georgia in Partial  
Fulfillment of the Requirements for the Degree

DOCTOR OF PHILOSOPHY

ATHENS, GEORGIA

2022

© 2022

Katelyn Rosenbalm

All Rights Reserved

SIGLEC LIGAND EXPRESSION AT THE CHOROID PLEXUS MODULATES  
NEUROINFLAMMATION IN ALZHEIMER'S DISEASE

by

KATELYN ROSENBALM

Major Professor:	Michael Tiemeyer
Committee:	Lance Wells
	Fikri Avci
	Carl Bergmann

Electronic Version Approved:

Ron Walcott  
Vice Provost for Graduate Education and Dean of the Graduate School  
The University of Georgia  
August 2022

## DEDICATION

For those across the rainbow bridge.

## TABLE OF CONTENTS

	Page
LIST OF FIGURES .....	vii
CHAPTER	
1 INTRODUCTION AND LITERATURE REVIEW.....	1
Research Gap .....	39
Figures.....	40
References .....	46
2 STEM CELL MODELING OF THE ALZHEIMER'S DISEASE GLYCOME....	62
Abstract .....	63
Introduction.....	63
Experimental Procedures .....	67
Results.....	69
Discussion .....	72
Figures.....	76
References .....	82
3 SIGLEC LIGAND EXPRESSION AT THE CHOROID PLEXUS MODULATES NEUROINFLAMMATION IN ALZHEIMER'S DISEASE .....	90
Abstract .....	91
Introduction.....	92
Experimental Procedures .....	93
Results.....	99
Discussion .....	110
Figures.....	115
References .....	127

4	GLYCOMIC ANALYSIS OF SITE-SPECIFIC GLYCOSYLATION FOR SARS-COV-2 SPIKE PROTEIN.....	140
	Abstract .....	140
	Introduction.....	140
	Experimental Procedures .....	141
	Results.....	151
	Discussion .....	154
	References .....	155
5	CONCLUSIONS AND FUTURE DIRECTIONS.....	157
	Scope of Study .....	157
	Discussion .....	157
	Figures.....	163
	References .....	164

## LIST OF FIGURES

	Page
Fig. 1.1: N-glycan biosynthesis occurs in multiple subcellular compartments .....	39
Fig. 1.2: Structural diversity of mammalian N-glycans .....	40
Fig. 1.3: Structural diversity of mammalian O-glycans.....	41
Fig. 1.4: Structural diversity of mammalian GSLs.....	42
Fig. 1.5: Siglecs are sialic acid receptors expressed by leukocytes .....	43
Fig. 1.6: The choroid plexus is a highly specialized cell type located in the ventricles of the brain .....	44
Fig. 2.1: AD patient-derived stem cells can be differentiated to cortical tissue.....	67
Fig. 2.2: Summarized N-glycome of iPSCs and NI cultures detects differences in glycan classes upon differentiation.....	69
Fig. 2.3: Summarized O-glycome of iPSCs and NI cultures reveals no significant changes in AD glycans through differentiation.....	70
Fig. 2.4: AD NI cultures incorporated greater diversity of sulfated O-glycan structures .	71
Fig. 2.5: Summarized GSL profiles of iPSCs and NI cultures detects subtle differences in GSL biosynthesis .....	72
Fig. 3.1: Siglec-F ligand is increased at the 5xFAD CP .....	101
Fig. 3.2: LRP1 is modified with the ligand for Siglec-F in murine brain tissue .....	103
Fig. 3.3: Siglec-F ligand also modifies LRP1 in human iPSCs .....	105
Fig. 3.4: Gal-3BP is a Siglec ligand carrier at the CP .....	107
Fig. 3.5: Siglec ligand expression is sensitive to TLR signaling.....	110
Fig. 3.6: Siglec-F engagement induces a pro-inflammatory phenotype in mouse leukocytes.....	112

Fig. 5.1: AD pathology produces DAMPS that interact with innate immune receptors to alter cell surface glycosylation at the CP epithelium, which functions to differentiate infiltrating leukocytes at the BCSFB ..... 163

## CHAPTER ONE

### INTRODUCTION AND LITERATURE REVIEW

Glycosylation is one of the most prevalent post-translational modifications (PTMs) implicated in modulating cell signaling, migration, development, transcription, and differentiation. In glycosylation, glycans (also known as carbohydrates, saccharides, or sugars) are covalently linked to macromolecules via a glycosidic bond to a functional group (a glycosyl acceptor). Glycans often decorate the cell surface via attachment to proteins, lipids, and proteoglycans. They can also be secreted as free molecules modifying the extracellular environment. At the cell surface and in the extracellular matrix, glycans modulate and/or mediate cell-cell, cell-matrix, cell-molecule, and host cell-foreign cell interactions. Further, glycans add a layer of quality control and alter the three-dimensional structure of macromolecules, ultimately adding to the complexity and function of proteins, lipids, and other molecules (Varki & Kornfeld, 2015). In this review, glycoproteins, glycolipids, and glycosaminoglycans will be discussed in detail and evaluated in the context of health and disease associated with the central nervous system (CNS).

#### **Protein glycosylation**

Protein glycosylation takes place co-translationally or post-translationally where glycans are covalently linked to amino acids. Serine, threonine, and asparagine residues are often the sites of glycosylation; however, other amino acids can be targeted as well (Moremen, Tiemeyer, & Nairn, 2012). This opens many opportunities for glycosylation to take place and add tremendous variety and complexity to the proteins synthesized. The two main categories of protein glycosylation are N-linked glycosylation and O-linked glycosylation.

## **N-linked glycosylation**

N-linked glycosylation takes place in the secretory pathway in two different compartments of the cell. Initially, in the endoplasmic reticulum (ER) of eukaryotes, synthesis of Dolichol-P-P-GlcNAc<sub>2</sub>Man<sub>9</sub>Glc<sub>3</sub> takes place at the cytoplasmic side of the ER. This precursor matures into Dol-P-P-GlcNAc<sub>2</sub>Man<sub>5</sub> and is flipped across the ER membrane to the lumen for *en bloc* attachment to a protein via a N-glycosidic bond between C-1 of N-acetylglucosamine (GlcNAc) and an Asn residue (GlcNAc $\beta$ 1-Asn). The attachment to a protein occurs via the enzymatic actions of oligosaccharyltransferase (OST) which attaches the 14-sugar glycan to an Asn residue on a glycoprotein with the consensus sequence Asn-X-Ser/Thr where “X” represents any amino acid except proline (Burda & Aebi, 1999; Pless & Lennarz, 1977). The glycans are further processed in the ER lumen and Golgi depending on the cell type and protein type via the actions of glycosidases and glycosyltransferases (**Fig. 1.1**).

The glycoprotein is then processed with  $\alpha$ -I and  $\alpha$ -II glucosidases that trim the glycans by removing two glucose (Glc) residues. ER chaperones calnexin and calreticulin bind glycoproteins containing a single Glc residue. If the protein is properly folded,  $\alpha$ -II glucosidase acts again to remove the final Glc residue. This glycoprotein can be additionally trimmed by ER mannosidases, and one to two mannose (Man) residues respectively are removed (Stanley, Taniguchi, & Aebi, 2015). Most glycoproteins that exit the ER carry N-glycans with eight or nine Man residues.

If not properly folded, following  $\alpha$ -II glucosidase Glc removal, the enzyme UDP-Glc:glycoprotein glucosyltransferase (UGGT1) replaces the previously cleaved Glc residue. This processing sends the glycoprotein through chaperone surveillance again. If the protein is considered terminally misfolded, the protein is marked for ER Associated Degradation (ERAD). Permanently misfolded glycoproteins are transported to the cytoplasm, ubiquitinated, and degraded by the 26S proteasome (Helenius & Aebi, 2004;

Moremen & Molinari, 2006). Among many triggers, accumulation of misfolded proteins in the ER induces ER stress and results in the unfolded protein response (UPR).

If correctly folded, the glycosylated protein will enter the cis-Golgi where it will undergo through further trimming. Specifically, the  $\alpha$ 1-2Man is trimmed further by  $\alpha$ 1-2 mannosidases IA and IB (MAN1A1, MAN1A2) to produce the key intermediate of Man<sub>5</sub>GlcNAc<sub>2</sub>. This intermediate transfers to the medial-Golgi where the hybrid and complex structures of N-linked glycans are produced. The formation of hybrid N-linked glycans entails the addition of a GlcNAc to the C-2 of the  $\alpha$ 1-3Man in the core of Man<sub>5</sub>GlcNAc<sub>2</sub>. This process is catalyzed by the N-acetylglucosaminyltransferase Mannose-GlcNAc-TI (MGAT1). The complex structure of glycans arises from further processing after the action of MGAT1. The  $\alpha$ -mannosidase II enzyme cleaves mannoses off the glycan structure and makes precursors for the formation of complex and biantennary structures. Complex and hybrid glycans demonstrate structural variety on their own; however, the true diversity of these N-linked glycans arises from the addition of different sugar residues that mature these glycans into much more complex structures. Common additions to N-glycans consist of a core fucose (Fuc), addition of galactose (Gal) to the available GalNAc at each of the arms, and capping of the elongated arms with sialic acids, Fuc, Gal, GlcNAc, and sulfate (**Fig. 1.2**). The sugars added by the capping reactions are usually  $\alpha$ -linked, which allows them to play a major role in recognition and binding by various biologically relevant receptors such as lectins and antibodies.

### **O-linked glycosylation**

O-linked glycosylation of proteins is a PTM that attaches a sugar to the side chain oxygen atoms of serine (Ser) and/or threonine (Thr) residues. Further, O-linked glycans are categorized based on the initial sugars that attach to the Ser and Thr and their linkages.

The first and highly prominent category of O-linked glycosylation initiates with a GalNAc sugar, and its members are known as O-GalNAc glycans or mucin type glycans. Mucin type glycans are abundant in the extracellular environment of vertebrates. As presented in **Fig. 1.3**, they are further categorized into eight cores, and among those eight cores, cores 1-4 predominate while cores 5-8 are relatively rare. The addition of mucin type glycans takes place in the Golgi where the core is elongated, branched, and modified with fucose and sialic acid residues. The presence of certain cores is closely associated with the expression patterns of specific GalNAc-transferases (Gill, Clausen, & Bard, 2011). The regulated expression of O-GalNAc cores can be demonstrated using the example of Core 1 GalNAc-transferase and Core 3 and 4 GalNAc-transferase. Core 1 GalNAc-transferase is widely expressed throughout the body while the Core 3 and 4 GalNAc-transferases have high activity in the gastrointestinal tissue (Vavasseur, Yang, Dole, Paulsen, & Brockhausen, 1995). The localization of these cores results in tissue specific modifications and contributes to specialized roles of each core. The role of mucin type glycans is especially prominent in the airway and the luminal space of the intestine. In these tissues, glycoproteins are heavily glycosylated with O-GalNAc glycans which contribute to innate immunity, exposure of protein epitopes, and leukocyte interaction with receptors. Further, they create a charged and lubricating surface that creates a barrier between epithelia and bacteria (Kiwamoto et al., 2015b; Linden, Sutton, Karlsson, Korolik, & McGuckin, 2008).

In addition to the mucin type glycans, O-linked glycans are present in the form of O-linked  $\beta$ -N-acetylglucosamine (O-GlcNAc). O-GlcNAc is attached to proteins within cellular compartments and demonstrates key functions in the mitochondria, the nucleus, as well as to signaling and metabolic proteins. Additionally, O-GlcNAc glycoproteins play important roles in disease state signaling and enzymatic regulation throughout the cell (Bond & Hanover, 2015). For example, reduced O-GlcNAcylation of proteins is correlated

with the pathophysiology of neurodegenerative disorders. This reduced O-GlcNAcylation can result from improper glucose metabolism and altered expression and activity of key enzymes like OGT and OGA; potentially affecting the onset of neurodegenerative disorders like Alzheimer's disease (AD) (N. Zachara, Akimoto, & Hart, 2015).

O-GlcNAcylation modifies proteins at Ser and Thr residues which are also often sites of phosphorylation. A primary function of O-GlcNAcylation is to regulate protein phosphorylation tightly by blocking phosphorylation sites for kinases to act upon. In AD, the balance of phosphorylation and O-GlcNAcylation changes dramatically and corresponds with changes in glucose metabolism, the pathology associated with hyperphosphorylated Tau and the formation of the amyloidogenic  $\beta$ -amyloid 42 ( $A\beta$ -42). In the past few years, the impact of alterations in glucose metabolism on the pathophysiology of AD has been termed type-III diabetes. Similar to the pathology of type-II diabetes, AD CNS tissue has prominent insulin resistance, and the concentration of insulin receptors is much higher in AD compared to wild type (Frolich et al., 1998). The insulin resistance essentially decreases the uptake of glucose in CNS tissue and alters the metabolism inside the cells. O-GlcNAc forms in the hexosamine pathway, a branch of glycolysis, which is initiated with a glucose molecule and forms the precursor UDP-GlcNAc which eventually produces O-GlcNAc (N. E. Zachara, 2018). Since glucose levels decreased in AD are associated with poor glucose uptake, the levels of O-GlcNAc and O-GlcNAcylation decrease in the cell. The disturbance in the phosphorylation and O-GlcNAcylation balance alters protein tendencies and activity and directly contributes to the formation of hyperphosphorylated tau and  $A\beta$ -42 in AD.

In AD, tau protein is abnormally hyperphosphorylated, and this hyperphosphorylated tau has the tendency to form tangles that lead to cellular toxicity (Iqbal et al., 2005). In the healthy state, tau protein is heavily O-GlcNAcylated; however, in AD the balance of phosphorylation and O-GlcNAcylation is disrupted. Due to the

decrease in glucose uptake or through an undiscovered mechanism, the O-GlcNAcylation of tau protein decreases significantly. The decrease in O-GlcNAcylation frees up phosphorylation sites, changing the balance in favor of the pathogenic hyperphosphorylated form of tau (B. E. Lee, Suh, & Kim, 2021).

In addition to tau pathology, O-GlcNAcylation is also connected with the function of  $\gamma$ -secretase, a key enzyme that regulates the formation of A $\beta$ -42. The formation of A $\beta$ -42 initiates with the amyloid precursor protein (APP) which can be cleaved by either  $\alpha$ -secretase or  $\beta$ -secretase. If the APP is cleaved by  $\beta$ -secretase, a sequential cleavage by  $\gamma$ -secretase will occur to generate amyloid- $\beta$  (A $\beta$ ). The  $\gamma$ -secretase cleavage lacks precision and produces several different peptides including the amyloidogenic A $\beta$ -42 (Murphy & LeVine, 2010). In this process, the activity of  $\gamma$ -secretase directly affects the abundance of A $\beta$ -42. Using the 5xFAD mouse model, a link between O-GlcNAcylation and  $\gamma$ -secretase has been established. O-GlcNAcylation is present at the Ser708 residue of nicastrin, a part of the  $\gamma$ -secretase complex, and inhibits activity of  $\gamma$ -secretase. As described earlier O-GlcNAc abundance decreases in AD and most likely correlates with the increase in the activity of  $\gamma$ -secretase. Recently, there have been experiments targeting O-GlcNAc in the 5xFAD model, where they have either inhibited OGA which cleaves O-GlcNAc from proteins or genetically increased O-GlcNAc levels to reduce amyloid pathology and improve cognitive function (B. E. Lee et al., 2021).

Another class of O-linked glycans emerges from the covalent linkage of a mannose sugar to Ser and Thr residues which forms an O-linked mannose glycoprotein. These glycans can be further extended and modified with other sugars and functional groups. With a wide variety of possible modifications, O-mannose glycans have been shown to play a vital role in cellular interactions. An example of the importance of O-mannose glycans is presented by the improper O-mannose glycosylation of alpha-dystroglycan ( $\alpha$ -DG) which leads to multiple congenital muscular dystrophies (also known as  $\alpha$ -

dystroglycanopathies). The insufficient and improper O-mannose glycosylation of  $\alpha$ -DG manifests itself in the form of congenital or non-Duchenne's muscular dystrophy and malformations of the eye and brain. The progressive weakness and muscle loss associated with muscular dystrophy can be devastating, and the malformation of the eye and brain result in serious vision and cognitive issues (Praisman & Wells, 2014).

There are two more classes of O-linked glycans, and they consist of O-glucose linked glycans and O-fucose linked glycans. O-glucose modifications occur between the first and second conserved cysteines of epidermal growth factor-like repeats (EGF-like repeats). This modification has only been found on certain proteins, out of which Notch being the most well-known and understood. In murine Notch1, deleting specific O-glucose sites changes Notch activation, thus showing an important role of O-glucose glycans in Notch functioning (Freeze & Schachter, 2009).

O-fucose glycans modify specific sites that precede the third conserved cysteine of the EGF-like repeat. O-fucose is implicated in various signaling pathways, however, its effect on the Notch pathway is one of the best understood. In developmental studies, Protein O-fucosyltransferase 1 (POFUT1) has been studied extensively. POFUT1 transfers a fucose to properly folded EGF-like repeats on proteins such as the Notch receptor. The fucose added can be further modified with other sugars, and the presence or absence of specific modification to the fucose have implications on the activity of the Notch signaling pathway (Freeze & Schachter, 2009).

### **Lipid glycosylation**

In animals, glycosphingolipids (GSLs) are the primary glycolipids that decorate the cell surface and modulate signaling through various receptors and detect toxins, pathogens, and viruses. GSL biosynthesis begins in the ER with the production of a ceramide. It is then trafficked to the Golgi where it can be elongated by different glycosyltransferases prior to being shuttled to the outer leaflet of the plasma membrane.

The function of GSLs consists of two major categories. First, they mediate cell-cell interaction (trans recognition) by binding complementary molecules on opposing/nearby plasma membranes. Second, they have a cis regulatory function as well, where they modulate the activity of notable proteins like receptor tyrosine kinases via lipid rafts (Schnaar & Kinoshita, 2015). On a cellular level, GSLs are not essential for the survival of a cell, however, for the development of an entire organism, they play an essential role. For example, mice lacking the gene for glucosylceramide (GlcCer) synthesis, arrest into the gastrula stage and fail to develop. GlcCer is modified to make many of the GSLs, demonstrating the importance of GSLs in the life of complex organisms.

The nervous tissue is especially abundant in gangliosides, a class of GSLs, which enrich lipid rafts and modulate cell signaling significantly. For example, Salt-and-Pepper Syndrome is a GM3 ganglioside deficiency that is caused by a mutated and improperly functioning GM3 synthase enzyme. Without the formation of GM3, much of the ganglio-series of glycosphingolipids cannot be synthesized, leaving the patient without vital lipid glycosylation. The absence of complex gangliosides has a drastic impact on normal brain function and can lead to seizures as well as neural crest defects (Boccutto et al., 2014).

### **Proteoglycans and Glycosaminoglycans**

A proteoglycan consists of a core protein that is modified with one or more glycosaminoglycans (GAGs). GAGs are polysaccharides consisting of repeating disaccharide units that consist of an amino sugar (N-acetylated or N-sulfated hexosamine) and a uronic acid (glucuronic acid or iduronic acid) or galactose. Proteoglycans also contain N-linked and O-linked glycans; however, the GAG chains on the proteoglycans are much larger and contain nearly eighty sugar residues which is nearly six to eight times more sugar residues than typical N-linked and O-linked glycans. The major role of proteoglycans and GAGs occurs in the extracellular matrix (ECM) where they interact with ECM fibrillar proteins and glycoproteins to promote ECM synthesis. Additionally,

proteoglycans and GAGs affect the physical properties of the ECM and even act as storage for small proteins like growth factors (Lindahl, Couchman, Kimata, & Esko, 2015).

### **Keratan Sulfate**

Keratan sulfate (KS) is a GAG which was identified first by M. Suzuki in cornea extracts in 1939. KS is described as a sulfated poly N-acetyllactosamine chain and is N- or O-linked to a limited number of proteins. Variations in abundance, specific protein association, GAG chain length, and composition determine the biological effects exerted by KS.

KS has been characterized into three different types: KS I, II, and III. The different types of KS are distinguished by their specific linkages to proteins and not by tissue specificity. KS I, also known as corneal KS, is N-linked to Asn residues. Although known as corneal KS, KS I is not limited to the cornea and has structural differences depending on the tissue. KS II is O-linked to Ser/Thr residues, and more specifically, has a GalNAC-O-Ser/Thr connection. KS III is also O-linked; however, it has a Man-O-Ser linkage (Funderburgh, 2000). In addition to the differences in linkage, the KS-type specific presence of L-fucose and N-acetylneuraminic acid (sialic acid) modifications further distinguishes the three types of KS. Although KS I, II, and III have variations in linkage groups, chain length, and sulfation patterns, there are still considerable structural similarities among them. They all contain variable regions of mono- and disulfated 6-sulfated D-galactose and N-acetylglucosamine, the signature disaccharide units of KS. Further, they all contain stretches of non-sulfated poly-N-acetyllactosamine adding to the similarities of their structure (Caterson & Melrose, 2018).

For non-detailed structural characterization, there are two enzymes, Keratanase I and Keratanase II, that can cleave KS chains at specific sites and release part of the KS molecule. Keratanase I is categorized as an endo-galactosidase that works best in areas of low sulfation. In a typical KS-1 chain, Keratanase I cleaves the  $\beta$ 1-4 linkage between a

D-galactose and a 6-sulfated N-acetylglucosamine. Keratanase II is an endo-N-acetylglucosaminidase that works best in areas of high sulfation. The preference of Keratanase II for regions of high sulfation areas was confirmed by experiments that observed a loss of binding of  $\alpha$ -KS monoclonal antibody clone 5D4 that binds highly sulfated KS. The specific site of cleavage for Keratanase II is the  $\beta$ 1-3 linkage between 6-sulfated N-acetylglucosamine and D-galactose where the galactose may or may not have 6-sulfation (Brown, Huckerby, Morris, Abram, & Nieduszynski, 1994; Brown, Huckerby, & Nieduszynski, 1994; Caterson, Christner, & Baker, 1983; Gonzalez-Gil et al., 2018). Altogether, the sensitivity to either enzyme is ligand specific, and the enzymes allow for the release of ligands associated with KS.

Despite the uncovering of key structural details of KS, it is still the least understood GAG thus far. Current discoveries of KS function present a complex and unique functional role in a diverse set of tissues such as the cornea, nervous system, reproductive system, and connective tissue. Although KS has a diverse role throughout different organ systems, our interest lies in the nervous system. After the cornea, KS is especially abundant in the central and peripheral nervous system. In the nervous system, KS associates with various proteins, leading to a diverse class of proteoglycans that have biological functions such as brain tissue development, neural maintenance, and synapse regulation to give a few examples (Caterson & Melrose, 2018). A prominent example of KS-proteoglycan in the nervous system is the synapse vesicle protein 2 (SV2). SV2 is a transmembrane proteoglycan with long KS additions and plays a major role in neurotransmitter storage and transport. SV2 forms a major protein component of the synaptic vesicles and has KS chain protruding inside the vesicle structure. The KS on SV2 provides a gel matrix to the inside of the synaptic vesicles and assists with the movement of neurotransmitters when the vesicle fuses with the membrane (Caterson & Melrose, 2018). KS has many more

roles in the nervous system that have been discovered, especially in development, however the SV2 example provides a snapshot into the important function KS serves.

### **Siglecs**

Siglecs (Sialic acid-binding immunoglobulin-type lectins) are cell surface receptors on immune cells that bind sialic acid. They are type I transmembrane receptors that are expressed in vertebrates and normally associated with functional roles in mice and primates. Their extracellular domains can contain numerous immunoglobulin domains including the terminal V-set domain that binds sialic acid via coordination with a critical arginine residue. The intracellular domain of the majority of Siglecs contains immunoreceptor tyrosine-based inhibitory motifs (ITIMs) that are phosphorylated by Src family kinases. This signaling cascade initiates recruitment of Src homology region 2 domain-containing phosphatase-1 and -2 (SHP-1 and SHP-2). These tyrosine-protein phosphatases can block cell survival signals and inhibit MAP kinase signaling which dampens inflammatory response (Rashmi et al., 2009). Alternatively, Siglecs can also have immunoreceptor tyrosine-based activating motifs (ITAMs) through recruitment of protein adapter DNAX-activation protein of 12 kD (Dap12) which functions in the activation of immune cells (Siddiqui et al., 2019).

Binding of Siglecs to their ligands can occur as *cis* or *trans* interactions depending on the desired effect on immune cell function. *Cis* interactions are useful for modulating intracellular signaling by sequestering the Siglec from an activating receptor on the cell surface (Muller et al., 2013). *Trans* interactions can directly inhibit an activating receptor as well as recruit Siglec receptors towards or away from cell surface receptors (Macauley, Crocker, & Paulson, 2014). Upon engaging ligands, many Siglecs have been shown to undergo endocytosis, though some are trafficked to recycling compartments and some are trafficked to lysosomal compartments (Tateno et al., 2007).

The family of human Siglecs contains 15 members and has two groups within: evolutionarily conserved Siglecs and CD33-related/rapidly evolving Siglecs. In mice, the family contains 8 members. As implied, many Siglecs do not have true homologs between mouse and human due to gene divergence (**Fig. 1.5**) (Varki, Schnaar, & Crocker, 2015). Some human and mouse Siglecs are historically associated as functionally equivalent paralogs, such as Siglec-E and -8 as well as Siglec-F and -9, while others including Siglec-3/CD33 are very different between species (Crocker & Varki, 2001) (Bhattacharjee et al., 2019; Bochner, 2009b).

Our interest in Siglec involvement in neurological dysfunction stemmed from Siglec-4/myelin-associated glycoprotein (MAG) and CD33. MAG is expressed in the central and peripheral nervous systems on the periaxonal myelin membrane, facilitating glial-neuronal interactions through binding of complimentary ganglioside ligands (Sun et al., 2004). MAG was first discovered in rat myelin in 1973 but wasn't identified as a Siglec until 1994 (Kelm et al., 1994). It is an inhibitor of neurite outgrowth and results in axon growth collapse, making it a potential therapeutic target for regeneration following CNS injury (Siddiqui et al., 2019). CD33, which is expressed on microglia in addition to other immune cell types, was found to have a protective gene variant through genome wide association studies (Hollingworth et al., 2011). *CD33* can be spliced into a short isoform that lacks the sialic acid binding domain. A single nucleotide polymorphism (SNP) that generates the shorter form was found to have increased microglial activity and reduced A $\beta$  accumulation through localization in peroxisomes rather than cell surface mobilization (Siddiqui et al., 2017). Each of these examples provide rationale for previously unexplored notion that additional Siglecs may be involved in the brain as well as neurological disorders such as Alzheimer's disease.

Based on primary structure, murine Siglec-F is considered the ortholog of human Siglec-8. Both receptors are associated mainly with expression on mature circulating

eosinophils and served important functions in allergic inflammation by inducing eosinophil apoptosis (M. Zhang et al., 2007). However, visualizing the counterreceptors using Fc chimeras in mouse and human tissue has demonstrated substantial disparity in binding specificities between Siglec-8 and -F in tracheal cross sections (Yu et al., 2017). Glycan array analysis has suggested that Siglec-8 engagement is highly specific and requires  $\alpha$ 2-3-linked sialic acid and a 6-sulfate on galactose (Bochner et al., 2005). Siglec-F, however, is more promiscuous in its ligand preferences and will bind to human and mouse tissue while Siglec-8 does not demonstrate any engagement of murine tissue. Probing the human airway Siglec-8 ligand with enzymatic digestion has revealed that the ligand includes sialylated keratan sulfate which can decorate subsets of aggrecan or DMBT1 (deleted in malignant brain tumor 1) (Gonzalez-Gil et al., 2021; Gonzalez-Gil et al., 2018).

Distribution of Siglec-9 counterreceptors more closely resembles that of Siglec-F ligands, prompting us to explore Siglec-9 functionality in the human brain rather than Siglec-8 (Yu et al., 2017). Siglec-9 is expressed broadly on leukocytes including but not limited to monocytes, macrophages, neutrophils, and T cells. Siglec-9 engagement can induce neutrophil death and inhibits macrophage phagocytic activity (Delaveris, Chiu, Riley, & Bertozzi, 2021). Like Siglec-8 and -F, Siglec-9 demonstrates binding to sulfated epitopes including 6-sulfated sialyl LewisX. The Siglec-9 ligand has been found to decorate airway mucins and is upregulated in human carcinomas (Laubli, Pearce, et al., 2014).

In cultured human umbilical vein endothelial cells (HUVEC), Siglec-9 ligand expression detected with Siglec-9 Fc overlay was significantly increased by treatment with high glucose (8 g/L) and *E. coli* derived lipopolysaccharide (LPS) (100  $\mu$ g/L). Co-culture experiments of HUVEC expressing Siglec-9 ligands with macrophages demonstrate immunophenotypes including upregulation of macrophage apoptosis as well as downregulation of phagocytic activity (Y. Zhang et al., 2019). Siglec-E ligand expression

was also found to be inducible with LPS treatment of cultured primary mouse aortic endothelial cells (H. Liu et al., 2020). These examples demonstrate that expression and presentation of Siglec ligands is susceptible to the inflammatory milieu.

### **Alzheimer's disease**

AD is a neurodegenerative disorder that is the most common cause of dementia and characterized by decreased cognitive function and loss of neurons in the brain. Currently, about 5.5 million Americans, mostly over 65 years old, are affected by AD. This figure is expected to increase significantly in the future as life expectancy increases (Hebert, Weuve, Scherr, & Evans, 2013). As of now, there are no disease modifying therapies that have slowed the cognitive decline associated with AD. With the growing patient population that is suffering from AD, there is an urgent need for disease modifying treatments and accurate diagnostics to help millions of people around the world.

There are two forms of AD: sporadic AD (SAD) also known as late onset, and familial AD (FAD) also known as early onset. The sporadic form of AD begins over the age of 65 and accounts for over 95% of AD cases. FAD on the other hand accounts for only 5% of AD and manifests itself before the age of 65 (mostly in the 40s and 50s) (Bali, Gheinani, Zurbriggen, & Rajendran, 2012). Sporadic and FAD share similar pathology and clinical presentation, however, the differentiating factor is the stronger and more specific genetic impact in FAD over sporadic AD.

In FAD, a strong genetic influence is prevalent as FAD is characterized as a Mendelian trait with an autosomal dominant inheritance pattern. In FAD, three genes, *amyloid precursor protein (APP)*, *presenilin 1*, and *presenilin 2*, present around 160 highly penetrating rare mutations. For *app* mutations in FAD, different research groups have observed the presence of specific mutations at the chromosomal location: 21q21.3. These mutations have been estimated to contribute about 16% to FAD pathology. The next set of genes affected work closely with APP by altering the activity of  $\gamma$ -secretase which

cleaves APP to produce the amyloidogenic A $\beta$ -42. *Psen1* is present at the chromosomal location 14q24.2, and mutations in this protein lead to an increase in cleavage of APP by  $\gamma$ -secretase. *Psen2* is located on chromosome 1q42.13 and contains a genetic sequence similar to *psen1*. PSEN2 also affects the cleavage of APP in conjunction with PSEN1; however, the mechanism of action is different (Barber, 2012). PSEN1 and PSEN2 associate with active  $\gamma$ -secretase; however, through gel-exclusion chromatography and antibody immunoprecipitation, it has been shown that they both are present in different sites of the active  $\gamma$ -secretase (Kopan & Goate, 2000; Li et al., 2000). *Psen1* and *psen2* show variability in the number of mutations, but the overall effect of their mutations renders their protein products to ultimately increase the production of A $\beta$ -42 (Barber, 2012).

In the sporadic form of AD, the disease is etiologically heterogeneous with several contributing causes but has similar pathology and prognosis. The genetic component of sporadic AD has significant variance where only the  $\epsilon$  allele in the apolipoprotein E (APOE) gene has been reliably shown to increase the risk of sporadic AD. In addition to APOE, there are nearly 2,000 genes that have been implicated in the development of sporadic AD. These genes encode for proteins serving important functions such as acting as chaperone proteins, immune complex regulation, signal transduction, and tumor suppression. However, patients may present changes in only some of these genes, making the etiology of sporadic AD quite complicated (Barber, 2012).

The classical contributors of AD are the misfolded amyloid proteins that deposit A $\beta$  plaques and neurofibrillary tangles (NFTs) caused by hyperphosphorylated tau proteins. The pathology of the A $\beta$  plaques is hypothesized to arise from the incorrect cleavage products of APP that produce A $\beta$  monomers that aggregate to form oligomers which further aggregate to create the A $\beta$  plaques (J. A. Hardy & Higgins, 1992). Normally, APP is cleaved into smaller monomers by  $\alpha$ -secretase and  $\gamma$ -secretase that produce non-amyloidogenic soluble fragments. The formation of the toxic A $\beta$  that aggregate together

occurs through a different cleavage of the APP where the proteolysis occurs via  $\gamma$ -secretase followed by  $\beta$ -secretase (Anderson, Chen, Kim, & Robakis, 1992). Although the specific role of  $A\beta$  plaques in AD is unknown, it is reasonably hypothesized that these plaques can disrupt neuron function and connectivity as well as possibly induce inflammation that can exacerbate AD pathology.

In addition to the plaques from  $A\beta$  oligomerization, NFTs are the second key contributor to AD pathology where hyperphosphorylation of tau proteins inside neurons forms tangles which can severely disrupt normal neuron function. Tau is a microtubule associated protein that regulates the stability of microtubules that are a key component of the cytoskeletal structure of a cell. In AD, tau is hyperphosphorylated (ptau) in comparison to the non-diseased state and that leads to a misdirection of tau protein from primarily axonal to somatodendritic subcellular location. This change negatively affects the normal function of the microtubules and leads to polymerization and aggregation of the tau proteins forming the NFTs (Alonso, Li, Grundke-Iqbal, & Iqbal, 2008). Although there is a close correlation between the NFT pathology severity and AD severity, the mechanism of neuronal death is disputed. In previous studies, markers of cell death were not found in NFT neurons in ptau mice, but instead, aggregate-prone tau shows association with cell death (Khlistunova et al., 2006; X. Wang et al., 2009). Nevertheless, the contribution of ptau to AD pathology has a long way to be completely understood, but its role in AD progression is prominent.

The  $A\beta$  and NFT pathologies have been shown to play an important correlational role in AD, but both pathologies are inconsistent with the onset of clinically observable symptoms. The  $A\beta$  plaques can be present in asymptomatic or unaffected individuals and in patients the plaques can form as many as ten years before any symptoms of AD are present (J. Hardy & Selkoe, 2002). The NFT, although showing a strong correlation between progression of AD and tangle load, is also present much earlier than the

pathology of AD is visible for diagnosis (Guillozet, Weintraub, Mash, & Mesulam, 2003). The discrepancy between the onset of the disease and presence of the two core pathologies calls for the need of additional participants that must be playing a role in the onset and progression of AD. In recent years, inflammation is assessed as a key player in exacerbating the neurodegeneration associated with AD.

The clinical diagnosis of AD generally relies on the early symptoms of issues with most commonly memory, cognition, movement, and sense of smell. AD diagnosis is often difficult because the symptoms listed above can be consistent with other disorders and scans of AD brains show significant variation between patients. However, there are biomarkers being researched for the use of clinical diagnosis of AD, and the biomarkers are studied through positron emission tomography (PET) scans and cerebrospinal fluid (CSF) analysis that can be utilized to support the diagnosis. The CSF markers include A $\beta$  1-42, total tau, and ptau which have been incorporated into the diagnostic criteria. However, the process of obtaining CSF requires an invasive lumbar puncture/spinal tap, making it difficult to use this tool often. To solve this issue, many attempts have been made to use biomarkers in the blood, but as of now, there has been no blood biomarker that has sufficient predictability for clinical use (Keshavan, Heslegrave, Zetterberg, & Schott, 2017). Further, these biomarker tools cannot be exclusively used to diagnose AD, but they do aid clinicians in making their diagnosis more reliable. For instance, PET scans have been developed that can detect a classical contributor to AD pathology, A $\beta$ . Such techniques have the potential to aid diagnostic accuracy but currently they are not widely used due to approval limitations, interpretation conflicts, and other regulation problems.

### **Neuroinflammation**

Inflammation is an essential part of the mechanism utilized by the immune system to respond to stimuli that appear harmful such as pathogens, toxins, and damaged cells. Induced through the innate immune response, it is usually the first response to harmful

stimuli, and the purpose is to recruit peripheral leukocytes to the area of tissue damage to heal and repair the damaged tissue and defend against foreign invaders. The inflammatory mechanism follows a general pattern where tissue-resident immune cells and antigen presenting cells release cytokines in response to recognition of specific sugars and proteins presented on the surfaces of bacteria, damaged cells, and other pathogenic entities. The release of cytokines leads to the expression of selectins in the capillaries that initiates a low affinity interaction between the selectin and glycoproteins on leukocytes in the bloodstream. This tethers and rolls the leukocytes to slow them down, allowing integrin binding to induce adhesion near the site of inflammation. This process brings increased circulation of blood to the site of inflammation and many more leukocytes (Freire & Van Dyke, 2013). In the CNS, this process is noted as neuroinflammation and involves additional layers of complexity due to the immunoprivileged status of the CNS.

Historically, the brain was considered to have immune privilege with physical separation from circulating pathogens, immune cells, and blood factors established by the blood-brain barrier (BBB), specialized endothelial cells that are joined by protein complexes forming tight junctions. Immune cell entry into the CNS was thought to be slow and deliberate, only in cases of pathological incidence. However, in recent years, the idea of CNS immune privilege has evolved. One of the most prominent and emerging ideas regarding CNS immune privilege proposes that the CNS parenchyma receive an immunoprivileged status to retain proper neuronal function. However, the ventricular, subarachnoid, and perivascular spaces contain significant immune cell activity (Mapunda, Tibar, Regragui, & Engelhardt, 2022).

The primary resident immune cells of the CNS are microglia. Microglia are immune cells of the CNS that constitute 5-20% of the brain cell population in adults and are maintained throughout life by self-renewal (Soulet & Rivest, 2008). Native microglia are ramified cells that contribute to brain homeostasis by actively scanning their environment

for distress signals from other cells, phagocytosing debris, secreting cytokines, and presenting antigens to lymphocytes. In normal homeostatic conditions, microglial immune responses are regulated for initiation followed by resolution. However, in pathological conditions, this tuning of immune responses is unbalanced, resulting in chronic neuroinflammation.

The origin of microglia has been controversial throughout history, leading to two main hypotheses: resident vs. peripheral. Resident/brain-derived microglia have been reported to originate during development from hematopoietic precursors from the yolk sac, matrix cells from the neuroectoderm, and pericytes (Ginhoux et al., 2010).

Peripheral/bone marrow-derived microglia are infiltrating monocytes that are recruited to the CNS during development, injury, or disease. It is believed some bone marrow-derived cells are present during development, but many are recruited to the CNS by stressed neurons likely via TLR signaling (Soulet & Rivest, 2008). Though controversial, these cells have been shown to differentiate to ramified microglia in some studies (Ling, 1979). Bone marrow-derived microglia are considered crucial for repair to acute injury and may be candidates for drug delivery.

Like M1/M2 monocyte-derived macrophages and Th1/Th2 lymphocytes, microglia are also characterized with a polar inflammatory response paradigm. M1 microglia, described as originating from classical activation, are associated with the production and secretion of pro-inflammatory cytokines such as TNF- $\alpha$ , IL-1 $\beta$ , nitric oxide, reactive oxygen species (ROS), and proteases. M2 microglia, derived from alternative activation or acquired deactivation, are associated with production and secretion of anti-inflammatory cytokines such as IL-4, IL-13, IL-10, and TGF- $\beta$  as well as phagocytosis and extracellular matrix reconstruction. M1 microglia are thought to be the first line of defense in the CNS, responding to injury and infection but also contributing to neurotoxicity and cell death via hyperinflammation. Following acute inflammation induced by M1 microglial response, M2

microglia are intended to dampen the M1 response and to induce repair that restores tissue homeostasis. However, The M1/M2 activation states for microglia is not a universally accepted paradigm (Ransohoff, 2016).

In addition to microglia, other cells of the CNS (astrocytes, oligodendrocytes, endothelial cells, and neurons) have been observed to have roles in modulating the immune response in the CNS. Astrocytes are star shaped glial cells that primarily regulate brain functions affecting neurogenesis, synaptogenesis, BBB permeability, and maintain extracellular homeostasis. Astrocytes outnumber neurons by greater than five fold and are essential components of a healthy CNS (Siracusa, Fusco, & Cuzzocrea, 2019). In addition to regulating everyday functions of the CNS, astrocytes also regulate neuroinflammation. Astrocytes primarily affect neuroinflammation by actively exacerbating or inhibiting inflammatory reactions via interactions with microglia associated compounds (Priego & Valiente, 2019). Therefore, astrocytes act in association with microglia to modulate inflammation in the CNS.

Oligodendrocytes are known as myelinating cells of the CNS. In addition to primary function of myelinating neurons, oligodendrocytes also have immune system associated features. For instance, they express innate immune receptors, secrete chemokines and cytokines to alter the immune response, and even have neuro-protective functions in the CNS (Peferoen, Kipp, van der Valk, van Noort, & Amor, 2014).

The brain capillary endothelial cells form the BBB and are key sites of inflammatory cell migration into and out of the CNS. During homeostatic conditions, endothelial cells do not participate in inflammatory processes. However, in times of inflammation, they alter their permeability to leukocytes and allow entry of peripheral leukocytes in the CNS (Wu, Liu, & Zhou, 2017). This function indicates that the endothelial cells act as an inflammatory gateway that reacts to inflammatory signals such as chemokines and cytokines, playing

an important role in connecting the innate immune system of the CNS with systemic innate and adaptive immune systems (Schiller, Ben-Shaanan, & Rolls, 2021).

One of the barriers controlling movement of cells and molecules into the CNS is the blood-CSF barrier (BCSFB). BCSFB is housed within a specialized brain tissue that secretes CSF, the choroid plexus. The choroid plexus is located in each ventricle of the brain and is highly vascularized by fenestrated capillaries. These fenestrated endothelial cells are permeable to small molecules and water which enter the stromal space between the endothelium and the choroid plexus epithelium (Redzic & Segal, 2004). The choroid plexus epithelial cells are joined by tight junctions, forming the BCSFB, which has been shown to be an important selective gateway for immune cell entry into the brain (Schwartz & Baruch, 2014).

The choroid plexus stroma is highly populated by CD4<sup>+</sup> T cells that are distinct from CNS T cells in that they express receptors for CNS antigens and are effector-memory in nature (Baruch et al., 2013). A subset of these choroid stromal T cells has been shown to express a Th1 phenotype, secreting IFN- $\gamma$  that is involved in leukocyte trafficking through the BCSFB (Kunis et al., 2013). Thus, it has been proposed that the T cells constitutively populating the choroid plexus act as gatekeepers of the BCSFB.

The BCSFB is also regulated by the glymphatic system, which refers to the drainage and exchange of CSF and interstitial fluid (ISF) through canals in the CNS leading to deep cervical lymph nodes. In viral infections of the CNS, it has been proposed that the glymphatic acts centrally in priming the peripheral immune system for T cell responses (McGavern & Kang, 2011). It has also been shown that CNS injury can stimulate T cell proliferation and activation in deep cervical lymph nodes independent of MHCII signaling, suggesting a role for the glymphatic system in transporting soluble factors from the injury site to the peripheral immune system (Walsh et al., 2015). Upon peripheral immune activation in such cases, immune cells, particularly those involved in

inflammation resolution, utilize the BCSFB and the glymphatic system to traffic to the injury site.

The second and better understood barrier of the brain is the BBB. The BBB is a unique complex of capillaries that consists of specialized endothelial cells containing tight junctions that limit the movement of molecules, ions, and cells into the CNS. The BBB protects the CNS from toxins, pathogens, and regulates CNS homeostasis. For immune surveillance, in homeostatic conditions, only T cells can pass through the BBB and surveil the CNS. However, T cell infiltration is significantly slower into the CNS when compared to other parts of an organism. This delay is primarily due to a lack of P-selectin expression under homeostatic conditions, which limits the attraction of T cells towards the endothelial cells and requires chemokine secretion to be the primary driver of the process. During neuroinflammation, the BBB endothelial cells increase the rate of CD4<sup>+</sup> T cell infiltration into the CNS by expressing P-selectin and increasing expression of atypical chemokine receptor 1 (ACKR1). CD8<sup>+</sup> T cells also infiltrate the CNS during neuroinflammation; however, the changes at the BBB and the biochemical mechanisms involved are currently not well understood (Mapunda et al., 2022). To explore peripheral immune cell entry in the brain, especially during neuroinflammation, blood-derived monocytes provide a great example.

Blood-derived monocytes are functionally distinct from microglia but can also be characterized by the polar inflammatory M1/M2 paradigm, though they can be classified into many more subsets (Villani et al., 2017). These monocytes are excluded from brain tissue in homeostatic conditions but recruited after injury to facilitate resolution of inflammation induced by activated microglia (Shechter et al., 2009). They are vital to CNS repair in injury and disease, particularly by acquiring an M2 phenotype. Infiltration of circulating macrophages was previously attributed to mechanical fissure of the BBB in injuries such as stroke. However, it has been demonstrated in spinal cord injury in mice

that the M1 population of monocytes entered via the local spinal cord leptomeninges, while the cell population that differentiated to M2 macrophages trafficked into the brain through the BCSFB (Shechter et al., 2013).

In AD, inflammation has emerged as an important aspect of the pathophysiology of the disease. Damaged neurons, A $\beta$  plaques, and NFTs are all sources of stimuli for inflammation. A $\beta$  plaques have been specifically hypothesized to activate microglia which initially clear plaques via phagocytosis, but after long periods of the phagocytosis process, the microglia become enlarged and incapable of continuing phagocytosis (Bard et al., 2000; Hickman, Allison, & El Khoury, 2008). In addition to this primary issue associated with chronic inflammation in AD, the microglia continue releasing pro-inflammatory cytokines which damage neurons and recruit additional microglia leading to an increased immune response (Yates et al., 2000). Further, as the microglia lose the capability to clear A $\beta$  plaques, microglia start releasing cytokines to recruit peripheral macrophages that are likely to exacerbate the inflammation in the brain.

Three specific cytokines have been characterized in AD to have pro-inflammatory effects: TNF- $\alpha$ , IL-1 $\beta$ , and IL-6. TNF- $\alpha$  cytokine primarily induces the expression of adhesion molecules such as P-selectin which facilitates peripheral leukocyte entry into the CNS. TNF- $\alpha$  levels are higher in the brain and plasma of AD patients, and A $\beta$  has been shown to simulate TNF- $\alpha$  production via NF $\kappa$ B in microglia. Further, TNF- $\alpha$  could potentially be exacerbating AD pathology by upregulating the expression of  $\beta$ -secretase and in increasing  $\gamma$ -secretase activity which leads to increased production of amyloidogenic A $\beta$  (Kinney et al., 2018).

IL-1 $\beta$  cytokine controls the expression of other pro-inflammatory cytokines such as TNF- $\alpha$  and IL-6 in the CNS and coordinates the inflammatory response. In early stages of AD, IL-1 cytokine is upregulated and correlates with A $\beta$  plaque formation. Additionally, IL-1 $\beta$  appears to have polymorphic characteristics where specific forms are linked to

upregulation of IL-1 $\beta$  cytokine and a greater risk of developing AD. Further, IL-1 $\beta$  also increases activity of  $\gamma$ -secretase and protein kinase C, which again increases A $\beta$  presence in the CNS (Kinney et al., 2018).

IL-6 cytokine has both anti-inflammatory and pro-inflammatory functions depending on the context. Overproduction of IL-6 is linked to chronic neuroinflammation, and elevation of peripheral IL-6 correlates significantly with cognitive issues. IL-6 has been shown to co-localize with A $\beta$  plaques as well as with the hyperphosphorylated Tau AD patient brains. In essence IL-6 connects the three core pathologies associated with AD: A $\beta$ , hyperphosphorylated tau, and neuroinflammation (Kinney et al., 2018).

### **Toll-like receptors**

Like any system of an organism, the CNS must be able to respond to PAMPS (pathogen-associated molecular patterns) and DAMPS (damage-associated molecular patterns). These proteins, small molecules, and nucleic acids trigger the innate immune system by binding pattern recognition receptors (PRRs). Most innate immune functionality in the brain is derived from Toll-like receptor (TLR) signaling. Of the 11 TLR family members in humans, TLR1-9 have been implicated in the CNS. Most TLRs signal through the adaptive protein MyD88, leading to the production and release of inflammatory cytokines. The role of TLRs includes not only innate immune response, but they are also essential to the maturation of dendritic cells that initiate the antigen-specific response by the adaptive immune system (Nie, Cai, Shao, & Chen, 2018).

TLRs are a highly conserved and an ancient class of receptors. They are type I transmembrane proteins containing three structural domains. The extracellular domain consists of leucine-rich repeats motif (LRRs), a transmembrane domain, and an intracellular domain called Toll/IL-1 receptor (TIR) (Nie et al., 2018).

TLRs have a crucial role in innate immunity where they recognize microbial infection or damage indications and eventually activate the release of cytokines which

recruits immune cells, changes the local environment of the tissue under attack, and initiates many other features associated with innate immunity. For innate immune recognition, PAMPs are only produced by microbes and are essential to the survival of the microbe, thus are highly conserved. There are many examples of PAMPs that are recognized by TLRs, and some of the well-known ones are LPS, lipoprotein, peptidoglycans, and lipoteichoic acids (Medzhitov, 2001). Conversely, DAMPs are molecular patterns indicative of damage of the host itself that TLRs detect. A primary DAMP is hyaluronic acid (HA). HA is part of the extracellular matrix and in a typical homeostatic environment has a high molecular weight. However, in times of injury, HA can be broken down to low MW, and the low MW can be detected by specific TLRs (TLR2 and TLR4) and induce a signaling cascade that is different from the signaling cascade induced by PAMPs (Nie et al., 2018). In our experimental work, we utilized microbial ligands such as LPS (TLR4 ligand), a synthetic ligand PAM3CSK4 (TLR2 and TLR1 ligand), and HA (TLR2 and TLR4 ligand) to induce Siglec ligand expression.

In terms of signaling pathways, almost all TLRs use the MyD88-dependent response to initiate an intracellular signaling cascade. The signaling cascade involves multiple enzyme complexes and multiple signaling molecules that ultimately initiate activation of the transcription factor NF- $\kappa$ B. NF- $\kappa$ B translocates to the nucleus and initiates transcription of gene encoding inflammatory cytokines to respond to the pathogen or damage signals. The second well understood signaling pathway activated by TLRs is known as the TIR domain-containing adaptor-inducing IFN- $\beta$  TRIF-dependent pathway or also known as the MyD88-independent pathway. This pathway is only activated by a subset of TLRs unlike the MyD88-dependent pathways. For example, in mammals, only TLR3 and TLR4 activate this pathway. When the TRIF-dependent pathway is activated, various transcription factors can be activated including NF- $\kappa$ B, interferon regulatory factors, and activating protein-1. The transcription factors tend to collectively activate the

transcription of genes encoding pro-inflammatory cytokines and/or type I IFN (Nie et al., 2018).

### **The choroid plexus**

The choroid plexus (CP) is a plexus/network of cells that is present in each of the ventricles of the vertebrate brain, including the two lateral ventricles, third ventricle, cerebral aqueduct, and the fourth ventricle. The CP is mainly responsible for producing CSF that flows from the lateral ventricle to the third ventricle via the interventricular foramina, and then from the third ventricle to the fourth ventricle via the cerebral aqueduct. The path of CSF continues to the ependymal or central canal of the spinal cord, or it can enter the subarachnoid space between that arachnoid and pia mater of the meninges. In the subarachnoid space, microscopic arachnoid villi or macroscopic arachnoid granulations can reabsorb the CSF by classical lymphatics in sinonasal tissues that underlie the cribriform plate, or by the recently described meningeal-dural sinus lymphatics back into the systemic circulation or regional and cervical lymph nodes (Lun et al., 2015).

The structure of the CP follows its primary function of secreting CSF. The CP is made up of a single layer of cuboidal epithelial cells that surround a core of connective tissue and capillaries. The epithelial cells are connected on the lateral surface by desmosomes which aid in cell-to-cell adhesion and tight junctions that form the BCSFB. The tight junctions of the CP are not as restrictive as a typical epithelium, allowing for immune cells to surveil the central nervous system more effectively. However, the epithelium does pose a physical barrier to the passage of large molecules between the blood and CSF (Lun et al., 2015).

Our collaborators, the Lehtinen lab, have explored CP development in detail. The CP develops similarly in each of the ventricles and has four stages. In stage one, the CP epithelium appears pseudostratified with central nuclei and no villous presence. In stage two, the epithelial cells change to columnar epithelium with apical nuclei and some villous

presence. In stage three, the cuboidal epithelium is formed with cells demonstrating central or apical nuclei with significant increase in the presence of primary villi. In the final stage, stage four, nuclei are more basal, villi are more complex, and junctions and adhesion form via tight junctions, desmosomes, and adherens junction. At this stage, the CP epithelium is able to function as the blood-CSF barrier (Lun et al., 2015).

In recent studies, differences in the CP epithelium of the different ventricles have been explored and different gene expression is prominent. The third ventricle has been shown to show over-expression of *ins2*, which encodes for an insulin precursor, indicating that the third ventricle has a source of insulin that affects its development. Further, key differences in gene expression are present in the fourth ventricles where a “rostral-caudal gradient of gene expression along the medial core of the plexus” is present, while the rest of the fourth ventricle CP presents a subset of low scoring genes (Dani et al., 2021). In addition to the CP epithelial cells which are derived from neuroepithelium, the CP stroma is made up of cells with mesenchymal origins (Lehtinen et al., 2013). The mesenchymal cells are multipotent stem cells that differentiate into fibroblasts and mural cells in the stromal space of the CP. The mural cells include pericytes and smooth muscle actin-positive cells. While the pericytes and the rapidly multiplying mesenchymal cells are similar in all of the CP ventricles, the fibroblasts are present in much greater quantity in the lateral, third, and fourth ventricles (Dani et al., 2021). Overall, the cellular makeup of the CP is underexplored, but numerous strides utilizing new techniques are revealing the makeup of this secretory tissue that has important implications in health and disease.

The CP acts as a major gateway through which its own native immune cells and peripheral immune cells migrate to the CSF and eventually into the brain. At the CP, macrophages, dendritic cells, and Kolmer’s epiplexus cells are particularly abundant, however, the immune cell profile is continuously expanding as a result of new studies.

The CP macrophages and dendritic cells reside in the CP stroma, while the Kolmer's epiplexus cells reside along the apical/ventricular side of CP epithelium (Ransohoff & Engelhardt, 2012). In addition to these immune cells, recent studies have reported many more immune cell types residing at the CP, and these include basophils, mast cells, monocytes, and lymphocytes (Cui, Xu, & Lehtinen, 2021). The growing knowledge of the diversity of immune cells continues to support the proposed role of the CP as a major regulator of neuroinflammation that is triggered in diseases like AD, Parkinson's disease, and multiple sclerosis.

With the variety of immune cells at the CP, macrophages have been studied in great detail and provide insight into the general immune surveillance and inflammatory mechanisms at the CP. During homeostasis, mature CP macrophages have been shown to constantly monitor their surroundings via distal processes; however, there are major differences between the stromal macrophages and the epiplexus cells that reside along the apical/ventricular side. The stromal macrophages have been shown to have a relatively stationary cell body while having cellular processes that have high motility. The high motility processes allow these macrophages to monitor an expanded territory. The stromal macrophages also interact frequently with blood vessels, take up foreign material, and act in a very similar phagocytic nature like other brain resident macrophages. Alternatively, the epiplexus cells show significant mobility and movement which is not found in brain associated macrophages or microglia (Cui et al., 2021). These cells represent the homeostatic presence of resident macrophages at the CP. During an inflammatory response, there are key changes to the actions of the CP macrophages.

The resident macrophages of the CP experience a change in behavior when they come across environmental signals in the form of cytokines and chemokines. A key example of this change is presented by the increase in motility and in mobility of the embryonic CP macrophages in response to elevated CSF-CCL2 chemokine. When CSF-

CCL2 levels are elevated, stromal macrophages depart from their tilting pattern and come together at distinct 'hotspots' at the distal tips of fourth-ventricle CP villi. In a different model, where peripheral inflammation is modeled using LPS, adult stromal macrophages flatten along the periluminal region of vessels. In this model however, the epiplexus cells do not see any change which potentially depicts different roles of both macrophages depending on the type of inflammatory response needed. This variance in roles is further highlighted when the epiplexus class of macrophages act as a first responder during the time of a focal injury (Cui et al., 2021).

In addition to playing a role in inflammatory responses and immune surveillance through its resident immune cells, the CP serves as a gateway for pathogens such as coxsackievirus B3 (CVB3), haemophilus influenzae type B (HiB), and severe acute respiratory syndrome coronavirus 2 (SARS-CoV-2). In brain infections, a surge in CSF cytokines occurs which induces accumulation of immune cells in the CP and movement of immune cells into the brain via CP epithelial barrier. Additionally, the CP secretes its own cytokines and chemokines in response to the signals from the CSF. The CP secreted cytokines and chemokines further recruit immune cells from the periphery and alter the CP epithelial morphology to allow immune cells to take part in the inflammatory response. In various pathological conditions like AD, infections, autoimmune disorders, tumors, and age-related disorders, the CP has been shown to coordinate immune cell movement into the brain. Immune cell trafficking at the CP presents an opportunity to regulate neuroinflammation, especially in diseases with chronic neuroinflammation like AD. As of current, there have been studies indicating that either preventing monocyte infiltration of the brain or secretion of the cytokine IFN- $\gamma$  has improved cognitive function in AD mouse models (Cui et al., 2021). Although there is much more needed to be understood of specific immune cell actions and CP pathways, the current studies highlight the

importance of exploring the CP as a potential avenue for neurological therapies in the future.

### **The glymphatic system**

The glymphatic system refers to the network of vessels that remove waste from the central nervous system and also plays a role in distributing important compounds like glucose, lipids, and neurotransmitters across the brain. The glymphatic system functions by using a system of perivascular channels that allow CSF produced by the choroid plexus to move throughout the brain while simultaneously draining the interstitial fluid secreted by cells to remove waste products.

The process initiates with CP epithelium secreting CSF in each of the lateral ventricles. From here, the CSF flows into the third ventricle where more CSF is secreted, and the fluid moves toward the fourth ventricle. Here, the final addition of CSF is done by the CP epithelium before the fluid ultimately fills the subarachnoid space, surrounding the brain (Khasawneh, Garling, & Harris, 2018). The current evidence available suggests that the constant production of CSF by the CP leads to a pressure difference which directs the flow of the CSF through the ventricular system to the subarachnoid space. Additionally, it has been suggested that the flow of CSF is also driven by arterial pulsing, suggesting a reason for the influx of CSF occurring near pulsating arteries instead of cerebral veins (Jessen, Munk, Lundgaard, & Nedergaard, 2015). After filling the subarachnoid space, the CSF enters the brain parenchyma along small capillaries and the para-arterial space. This flow occurs because the CSF in the subarachnoid space runs adjacent with the arteries in the brain, and when the arteries transition into capillaries, the pressure of the CSF moves the fluid into the capillaries and eventually into the brain. After entering the brain, the CSF starts to mix with the interstitial fluid secreted by the cells, and this process is mediated by specialized aquaporin channels that reside on the ends of astrocytes. The CSF and interstitial fluid exchange continuously takes place, and the CSF influx drives the flux of

interstitial waste solutes to the paravenous space. From the paravenous space, the interstitial waste solutes can either be drained to the cervical lymph nodes or back to the CSF-dural sinus-meningeal lymphatic vessels (Natale et al., 2021).

The vital function of CSF circulation and waste clearances presented another captivating observation relating to the connection between sleep and glymphatic system activity. Although there are multiple theories describing the need for sleep which can be an extremely vulnerable state for an organism, there are few biological clues into the need for this process. With the glymphatic system, it was discovered that it is primarily active during sleep and demonstrates how sleep is necessary to clear neurotoxic waste from the brain. The currently proposed idea behind the greatly increased activity of the glymphatic system during sleep focused on the increase in volume of the interstitial space. This finding suggests that the increased volume capacity during sleep allows for the exchange between CSF and interstitial fluid to take place efficiently. In addition to the connection between sleep and the glymphatic system, studies on aging and disease (specifically AD) have provided evidence for the major changes that take place in the glymphatic system and its ability to clear waste like aggregated proteins from the brain.

With aging and neurodegenerative disorders like AD, the activity of the glymphatic system significantly decreases. In mice, it has been observed that in comparison to young mice, old mice experience a reduction of nearly 80-90% in glymphatic function (Jessen et al., 2015). This dramatic change is currently under investigation; however, a few hypotheses have emerged recently. One of the hypotheses discuss the dysregulation of the specialized aquaporin channels at the end of astrocytes which are essential for CSF and interstitial fluid exchange. The findings indicated that aging correlated with the loss of perivascular aquaporin polarization which directly impacts the glymphatic flow. Another major hypothesis proposed is focused on the reduction of CSF production with aging. With aging, CSF production declines significantly, and CSF pressure also sees a nearly 30%

decline. The decrease in CSF production by the CP, and the overall reduction in glymphatic activity, correlates well with increased chances of neurodegenerative diseases with increasing age (Jessen et al., 2015).

In AD, one of the primary drivers of neurodegeneration has been proposed to be aggregated proteins that become neurotoxic. In healthy young brains, the glymphatic system plays a vital role in clearing neurotoxic waste, including aggregated proteins, from the nervous system. However, as organisms age, the glymphatic activity decreases, and in AD the change is even more dramatic than typical aging. In AD, anatomic enlargement of the perivascular space is apparent which in turn can disrupt glymphatic flux. This can further accelerate the aggregation of proteins, especially A $\beta$ , further exacerbating AD pathology (Jessen et al., 2015). Given the recent establishment of the glymphatic system, much more research is needed regarding the changes in CNS fluid flow in disease models, but it offers an additional opportunity for therapeutic intervention.

### **Low-density lipoprotein receptor-related protein 1 (LRP1)**

LRP1 is a type I transmembrane protein consisting of a large extracellular  $\alpha$ -chain domain of 515 kDa and an 85 kDa intracellular  $\beta$ -chain. The  $\alpha$ -chain and  $\beta$ -chain are non-covalently attached across the plasma membrane (Auderset, Cullen, & Young, 2016; Li et al., 2000). LRP1 is also extensively glycosylated and contains 52 N-glycosylation sites on the  $\alpha$ -chain that can be modified differently depending on the tissue and cellular context (De Nardis et al., 2017). LRP1 functions as an endocytic receptor for over 40 ligands and is involved throughout the body in various biological processes and disease mechanisms (Lillis, Van Duyn, Murphy-Ullrich, & Strickland, 2008).

LRP1 is a widely expressed glycoprotein that has a significant presence in the liver, vascular smooth muscle cells, neurons, macrophages, and additional tissues where it plays a diverse and vital role, including in embryonic development. In experiments where *lrp1* was knocked out in mice, it led to embryonic lethality indicating that LRP1 is essential

for not just proper development but for life (Herz, Clouthier, & Hammer, 1992). Additionally, one of the best understood functions of LRP1 is the clearance of remnant lipoproteins in plasma by the liver. Liver expressed LRP1 assists with the clearance of lipoproteins by working with the low-density lipoprotein receptor (LDL) (Cooper, 1997). Additionally, if the LDL receptor is not present, LRP1 has an independent clearance mechanism where it recognizes APOE and clears lipoprotein remnants (Willnow, Armstrong, Hammer, & Herz, 1995). In a completely different tissue context of the vasculature, LRP1 plays a prominent role in maintaining vascular wall integrity and protecting from atherosclerosis (Boucher, Gotthardt, Li, Anderson, & Herz, 2003). In addition to these examples, there are many other roles of LRP1 that are essential to maintain homeostasis and linked to various disease mechanisms. However, in this review, we will elaborate on the function of this protein in the nervous system and the CP as well as its role in neuroinflammation and AD.

In the nervous system, LRP1 is highly expressed by neurons, activated astrocytes, and microglia. Studies have elucidated the vitality of LRP1 in the nervous system by selectively deleting LRP1 from differentiated neurons during mouse development, resulting in behavioral and motor defects, neurodegeneration, and neuroinflammation. The phenotype observed greatly resembled neurodegeneration associated with AD, and the study also points out that LRP1 regulates synaptic function at the post-synapse by regulating the turnover and recycling of proteins at the synapse (Auderset et al., 2016). With these important functions in a healthy state, LRP1 also contributes to mechanisms associated with modulating the pathological state of neuroinflammation.

Neuroinflammation is a major component of the pathophysiology in neuronal diseases such as head injuries, Parkinson's disease, and AD. As discussed above, the role of LRP1 is vast and neuroinflammation is another physiological process where this protein has been proposed to have an effect. Limited information is available regarding

the role of LRP1 in neuroinflammation; however, it has been observed that LRP1 can suppress microglial activation via modulation of NF- $\kappa$ B and JNK signaling pathways (Yang et al., 2016). Additionally, LRP1 expression was suppressed when microglia were exposed to pro-inflammatory cytokines, suggesting LRP1 expression could potentially regulate activation and suppression of microglia in the CNS (Yang et al., 2016). In addition to affecting neuroinflammation, LRP1 has been studied specifically in the context of AD and various interesting findings have arisen from that work as described below.

Currently, conflicting evidence regarding the role of LRP1 in AD pathology exists. Recently, the connection between tau uptake and LRP1 has emerged as a prominent mechanism of the tau pathology associated with AD and other forms of dementia. In human neuroglioma cells and induced pluripotent stem cell-derived neurons, it has been observed that by knocking out *Lrp1*, the uptake of tau significantly decreases. The *Lrp1* knockout also effectively blocked the uptake of full-length soluble monomeric tau, pathological mutant tau, and ptau which is relevant to AD pathology (Rauch et al., 2020).

In addition to the contribution to tau pathology, LRP1 has been implicated in amyloid pathology of AD. Although there are conflicting reports of the role of LRP1 in A $\beta$  production and clearance, most evidence points to LRP1 having a role in both. The production of amyloidogenic A $\beta$  is dependent upon the processing and cleavage of APP. LRP1 has been shown to co-localize with APP, and LRP1 and APP interact at both the extracellular and intracellular domains. LRP1 appears to promote APP cleavage by  $\beta$ -secretase, and when LRP1 endocytosis is impaired,  $\alpha$ -cleavage of APP increases (Van Gool et al., 2019). When it comes to A $\beta$  production, the essential idea is that LRP1 might be upregulating its formation by promoting cleavage of APP at the plasma membrane. In addition to affecting production of A $\beta$ , LRP1 has been categorized as a prominent A $\beta$  clearance receptor protein which works in conjunction with APOE and heparan sulfate (HS). The relationship between LRP1 and APOE is still controversial; however, current

studies have established that APOE plays a complex role in LRP1 mediated uptake of A $\beta$  where APOE may be facilitating or inhibiting the uptake of A $\beta$  (Kanekiyo & Bu, 2014). LRP1-HS mediated A $\beta$  clearance presents a much clearer mechanism. When LRP1 and HS colocalize, HS acts as a binding scaffold for A $\beta$ . In the cases where HS mediates the interaction between LRP1 and A $\beta$ , the presence of HS prevents uptake of A $\beta$ , indicating that LRP1-mediated uptake depends on the presence or absence of specific HS (Kanekiyo et al., 2011). Although the role of LRP1 in the CNS is incompletely understood, its relevance to AD pathology is undeniable.

### **Galectin-3 binding protein (Gal-3BP)**

Gal-3BP is a multifunctional and commonly secreted glycoprotein that is encoded by the gene *Igals3bp*. This glycoprotein is implicated in many tissues and disease states and thus has additional names including 90K tumor-associated antigen or Mac-2 binding protein. Gal-3BP was originally described by various research groups that were focused on characterizing secreted proteins from breast cancer cell lines and lung cancer (Iacobelli, Arno, D'Orazio, & Coletti, 1986; Iacobelli et al., 1993; Linsley et al., 1986). In addition to the context of cancer, Gal-3BP has been studied in viral infections, as a ligand for CD33-related Siglecs, and in AD. Gal-3BP acts as an inflammatory modulating glycoprotein in these different environments and can have both pro-inflammatory and anti-inflammatory effects as a part of the innate immune system.

Gal-3BP in its monomeric form is a 65.3 kD protein that consists of a six-stranded beta-sheet, an alpha-helix, and three intramolecular disulfide bonds (Loimaranta, Hepojoki, Laaksoaho, & Pulliainen, 2018). An interesting and vital feature of Gal-3BP is derived from its scavenger receptor cysteine-rich (SRCR) domain. This domain is highly conserved and is found in many soluble and membrane associated proteins of the innate immune system (Martinez, Moestrup, Holmskov, Mollenhauer, & Lozano, 2011). In addition to these features of Gal-3BP, the glycosylation of the protein contributes to its

structural features. Gal-3BP is heavily glycosylated and translates into a protein of 90-100 kD which is much greater than the monomeric weight of 65.3 kD of the peptide backbone. The structure of the Gal-3BP reveals seven glycosylation sites for N-linked glycans, and usually all seven sites are occupied. This extensive glycosylation plays an essential role in the secretion of the protein, and it has been shown that if the N-glycosylation sites are mutated or N-glycosylation is inhibited, very little Gal-3BP is secreted (Loimaranta et al., 2018).

Gal-3BP has an interesting inflammatory modulating role that changes significantly under different cellular contexts. It can have both immunosuppressive and pro-inflammatory effects by interacting with different receptors and affecting different pathways. For example, Gal-3BP has been shown to have a potential immunosuppressive role in asthma where a negative correlation is present between levels of Gal-3BP and eosinophils. Further, Gal-3BP has been shown to suppress dendritic cell maturation by interacting with dendritic cell-specific intracellular adhesion molecule (DC-SIGN) in a  $Ca^{2+}$ - and carbohydrate-dependent manner. In addition to suppressing dendritic cell maturation, the interaction of Gal-3BP with DC-SIGN can suppress the differentiation of monocyte-derived fibrocytes and can also induce immune tolerance for Gal-3BP-overexpressing colorectal cancer cells (Loimaranta et al., 2018).

With the multiple immunosuppressive activities of Gal-3BP, there are many pro-inflammatory mechanisms where Gal-3BP participation is significant. To highlight one of the earliest discovered examples: when peripheral blood mononuclear cells (PBMCs) were pre-conditioned with Gal-3BP, their cancer cell killing activity increased drastically. These studies showed that Gal-3BP treatment induced higher levels of pro-inflammatory molecules such as IL-1, IL-6, GM-CSF, and TNF- $\alpha$  (Powell et al., 1995). In addition to this example, there are various examples that highlight increased T-cell activation and other

pro-inflammatory molecules that demonstrate the dual role of Gal-3BP depending on the cellular context.

In viral infections, Gal-3BP has important functions in both chronic and acute infections though the mechanism of action is different. In chronic viral infections like human immunodeficiency virus (HIV) and hepatitis C virus (HCV), the Gal-3BP concentrations were significantly elevated. Multiple studies have proposed an antiviral role for Gal-3BP, and in HIV, it has been observed that Gal-3BP reduces the incorporation of HIV Gag proteins into the progeny virions. This function limits the amount of HIV progeny and thus limits the infectivity of the virus. In HCV, studies have shown an increase in serum concentrations of Gal-3BP during infection, indicating a role in the antiviral response. In acute viral infection, Gal-3BP upregulation was first seen when looking at the change in gene expression of muscle cells as a result of Dengue virus (DENV) infection. In another example, increased Gal-3BP levels were also found in an Epstein-Barr virus (EBV) infection. The studies highlight that there is a possibility that the Gal-3BP glycoprotein is secreted locally in acute viral infections in order to modulate the innate immune response (Loimaranta et al., 2018).

Another interesting role of Gal-3BP comes from its action as a CD33-related Siglec ligand and its inhibitory effect on neutrophils. A specific subset of Siglecs is known to act as immunosuppressants, and the study by Heinz Läubli et al. describes the interaction between Gal-3BP and Siglec-9 which suppresses neutrophil activation in a sialic acid- and Siglec-dependent manner (Laubli, Alisson-Silva, et al., 2014). This novel immunosuppressive role of Gal-3BP could play a role in cancer cells evading the immune system and continuing metastasis. This idea has interesting implications for disease contexts beyond cancer, including disease pathologies where inflammation plays an essential role.

In AD, A $\beta$  production and formation of amyloid plaques is associated with the pathology, where the A $\beta$ 's interaction with Gal-3BP supplements potential roles for this glycoprotein in the nervous system. For example, when GPI-anchored glycosylphosphatidylinositol specific phospholipase D1 (GPLD1) expression increases due to A $\beta$  production signaling, more Gal-3BP is secreted. This soluble Gal-3BP was found to suppress A $\beta$  production by inhibiting  $\beta$ -secretase that cleaves APP into the amyloid forming A $\beta$ . Additionally, Gal-3BP has been observed to colocalize with APP, which could open gateways into understanding how to modulate A $\beta$  production in AD patients (Seki et al., 2020).

## Research Gap

Currently, both diagnostics and therapeutics for AD are limited. Definitive diagnostic capabilities require post-mortem examination of affected tissues and may not differentiate between other forms of dementia or neuroinflammatory disease. Structural or functional scans, laboratory testing, CSF exams, and electroencephalograms similarly do not ensure a specific neurodegenerative diagnosis. For this reason, biomarker discovery should be prioritized in the AD field. Specifically, the utility of molecules that are differentially modified by glycosylation in the context of inflammation should be explored. To date, Siglec glycan ligands, their protein carriers, and their tissue specific expression patterns have not been thoroughly considered as predictive agents for neuroinflammation or neurodegeneration.

Most therapeutic approaches for AD involve management of symptoms but do not directly target disease mechanisms. Recently, an amyloid targeted antibody therapy, aducanumab, has acquired accelerated approval from the U.S. Food and Drug Administration as the first AD therapy approved since 2003. Unfortunately, aducanumab did not meet primary endpoint for all clinical trials, suggesting it may not reduce clinical decline in all patients. Thus, a significant vacancy exists in the field for treatment that alters mechanisms involved in AD pathogenesis. With substantial evidence for inflammatory processes contributing to neurodegeneration, we propose Siglec signaling as a therapeutic candidate. Resident and extravasating immune cells expressing Siglec receptors have demonstrated significant physiological consequences in traumatic brain injury and stroke models. Therefore, it is reasonable to consider the role of Siglecs in AD pathology. Regulating Siglec engagement and signaling presents a unique opportunity to modify both pro- and anti-inflammatory immune activity depending on the receptor expression, cell type expression, and counterreceptor expression in the tissue.

## Figures

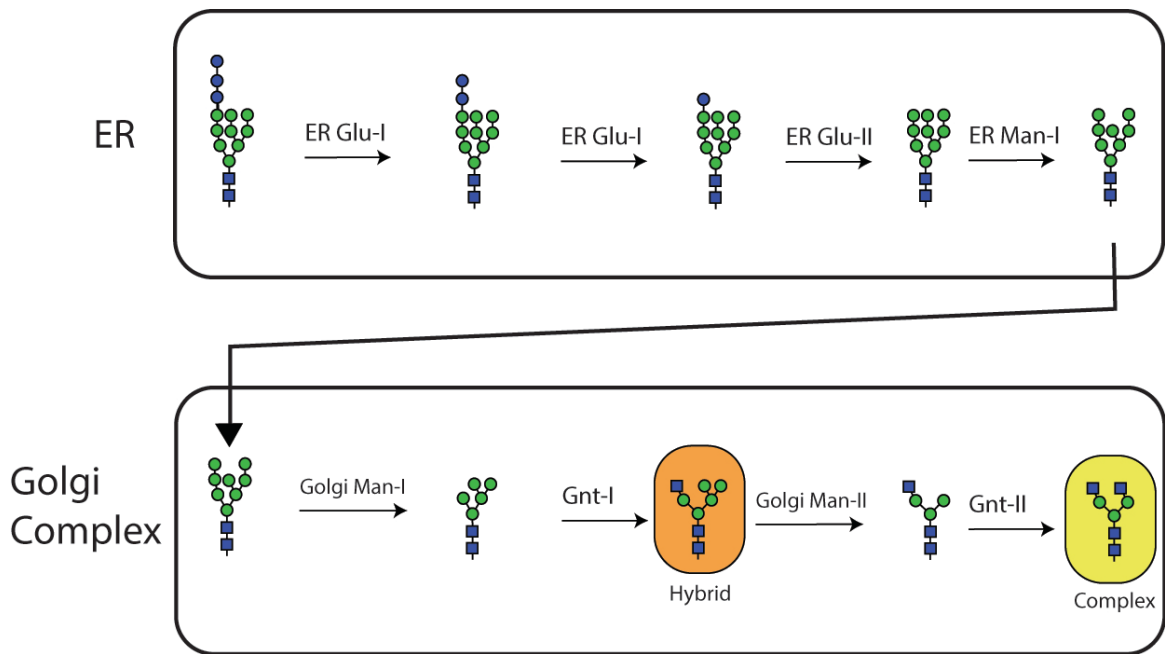


**Fig. 1.1. N-glycan biosynthesis occurs in multiple subcellular compartments**

Processing of N-glycans begins in the ER prior to protein folding. Glucosidase and mannosidase enzymes remove residues before transport to the Golgi where final processing happens. The destruction and re-building of the glycan can result in various oligomannose forms or elongated hybrid and complex structures.

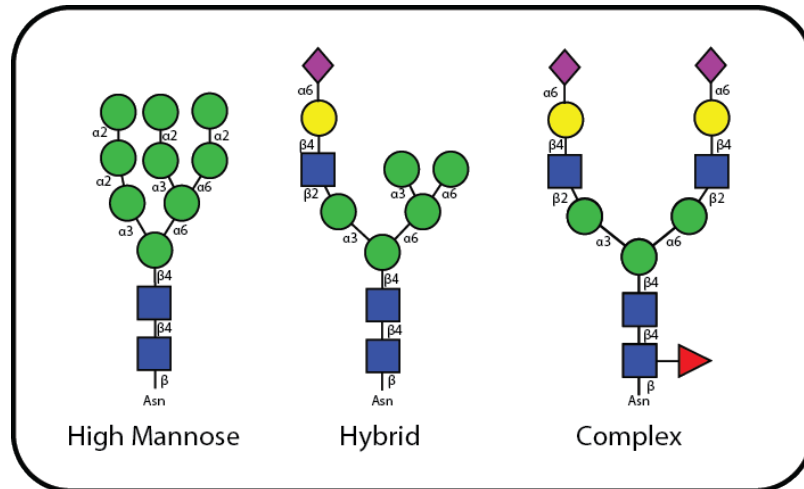


**Fig. 1.2. Structural diversity of mammalian N-glycans**

N-glycans can be broadly categorized into three main categories: high mannose, hybrid, or complex structures. High mannose structures are comprised of exclusively mannose residues at the reducing end, while complex structures can present several different monosaccharides and have greater heterogeneity.

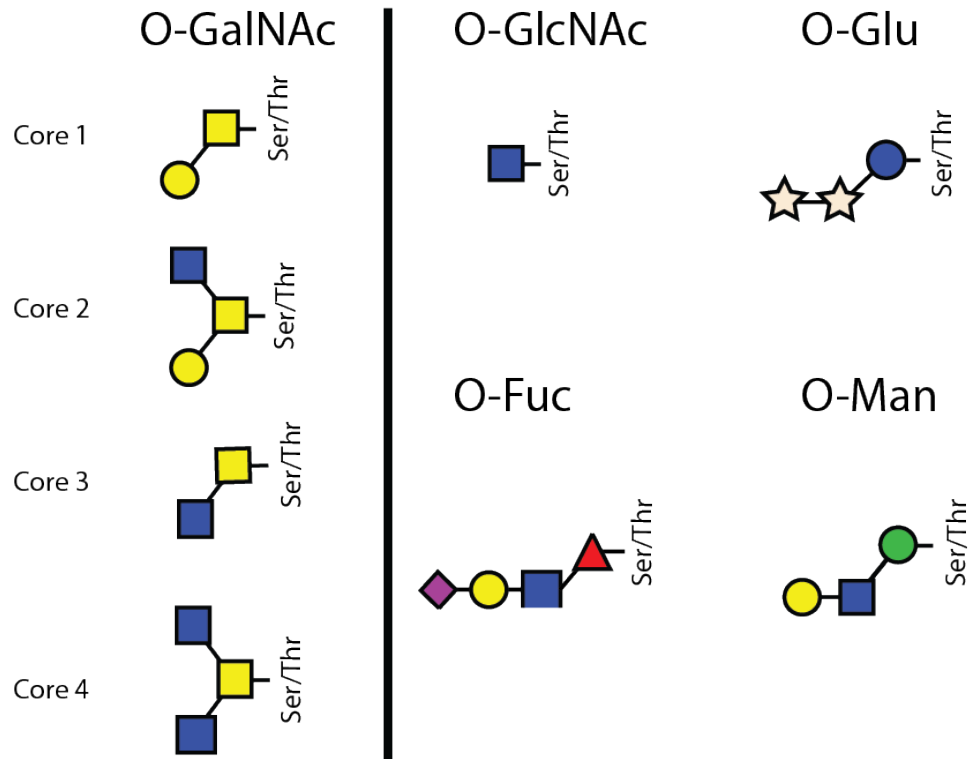


**Fig. 1.3. Structural diversity of mammalian O-glycans**

O-glycosylation can be initiated by five monosaccharides. O-GalNAc can be categorized by extension into four common cores and is the most common type of extracellular O-glycosylation. O-GlcNAc is typically not extended and found on intracellular proteins. O-glucose is commonly extended by two xylose residues and found on EGF repeats. O-fucose is often a tetrasaccharide and found along side glucose on EGF repeats. O-mannose can also be categorized by its extension and has an essential function in the extracellular matrix.

# Glycosphingolipids

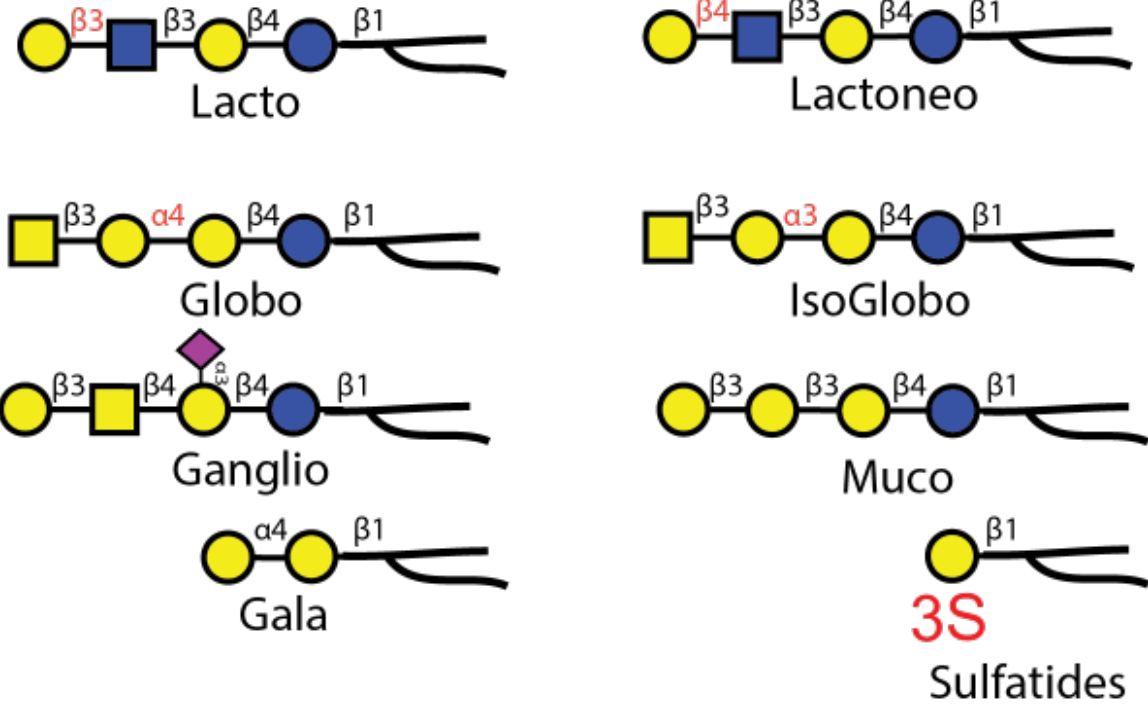


**Fig. 1.4. Structural diversity of mammalian GSLs**  
 Glycosphingolipids are categorized into eight categories based on two criteria: the extension of the reducing lactose and their linkages. Six of the categories are predominantly neutral, one is predominantly charged (the ganglio- series), and one is charged by the addition of sulfate (sulfatides).

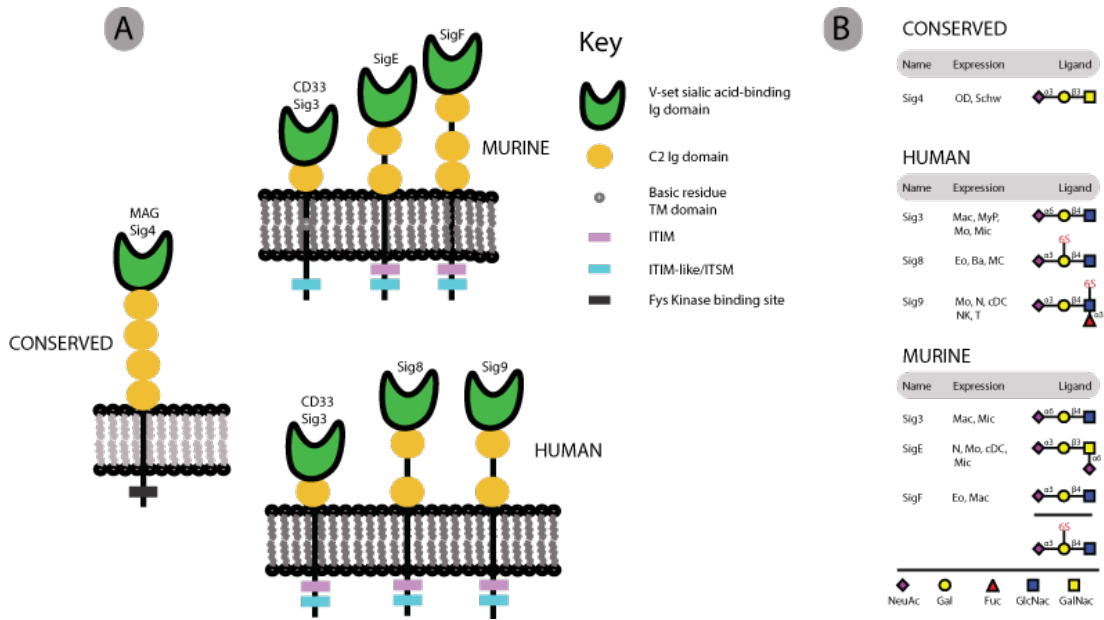


**Fig. 1.5. Siglecs are sialic acid receptors expressed by leukocytes**

Siglecs bind a broad range of glycans that are terminated in sialic acid, many of which require specific epitopes or modifications for binding (**B**). These lectins generally display immunoreceptor tyrosine-based inhibitory motifs (ITIM) on their intracellular domain, resulting in alterations to the immune response (**A**).

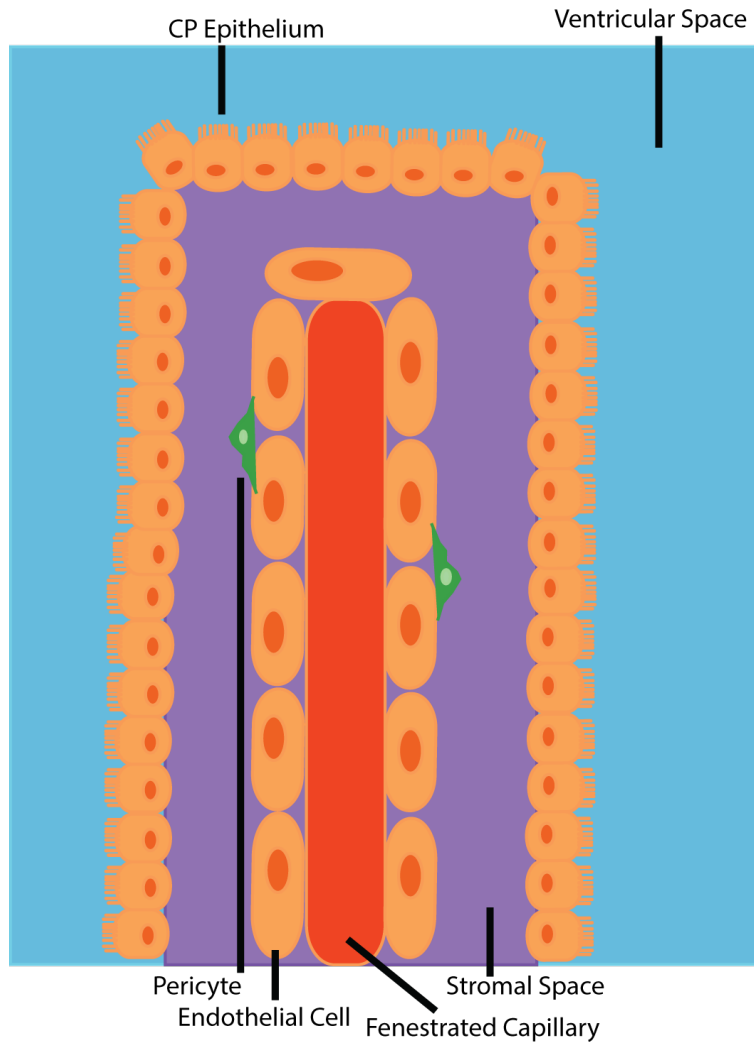


**Fig. 1.6. The choroid plexus is a highly specialized cell type located in the ventricles of the brain**

The CP is a modified form of ependyma that is found in the ventricular system of the CNS and secretes the CSF. The basal surface of the epithelium borders stromal tissue and highly fenestrated capillaries that allow immune cell extravasation and surveillance of the CNS. The apical surface is highly modified with non-motile cilia involved in signaling for growth and differentiation at the ependymal surface.

## References

- Alonso, A. C., Li, B., Grundke-Iqbal, I., & Iqbal, K. (2008). Mechanism of tau-induced neurodegeneration in Alzheimer disease and related tauopathies. *Curr Alzheimer Res*, 5(4), 375-384. doi:10.2174/156720508785132307
- Anderson, J. P., Chen, Y., Kim, K. S., & Robakis, N. K. (1992). An alternative secretase cleavage produces soluble Alzheimer amyloid precursor protein containing a potentially amyloidogenic sequence. *J Neurochem*, 59(6), 2328-2331. doi:10.1111/j.1471-4159.1992.tb10128.x
- Auderset, L., Cullen, C. L., & Young, K. M. (2016). Low Density Lipoprotein-Receptor Related Protein 1 Is Differentially Expressed by Neuronal and Glial Populations in the Developing and Mature Mouse Central Nervous System. *PLoS One*, 11(6), e0155878. doi:10.1371/journal.pone.0155878
- Bali, J., Gheinani, A. H., Zurbruggen, S., & Rajendran, L. (2012). Role of genes linked to sporadic Alzheimer's disease risk in the production of beta-amyloid peptides. *Proc Natl Acad Sci U S A*, 109(38), 15307-15311. doi:10.1073/pnas.1201632109
- Barber, R. C. (2012). The genetics of Alzheimer's disease. *Scientifica (Cairo)*, 2012, 246210. doi:10.6064/2012/246210
- Bard, F., Cannon, C., Barbour, R., Burke, R. L., Games, D., Grajeda, H., . . . Yednock, T. (2000). Peripherally administered antibodies against amyloid beta-peptide enter the central nervous system and reduce pathology in a mouse model of Alzheimer disease. *Nat Med*, 6(8), 916-919. doi:10.1038/78682
- Baruch, K., Ron-Harel, N., Gal, H., Deczkowska, A., Shifrut, E., Ndifon, W., . . . Schwartz, M. (2013). CNS-specific immunity at the choroid plexus shifts toward destructive Th2 inflammation in brain aging. *Proc Natl Acad Sci U S A*, 110(6), 2264-2269. doi:10.1073/pnas.1211270110

- Bhattacharjee, A., Rodrigues, E., Jung, J., Luzentales-Simpson, M., Enterina, J. R., Galleguillos, D., . . . Macauley, M. S. (2019). Repression of phagocytosis by human CD33 is not conserved with mouse CD33. *Commun Biol*, 2, 450. doi:10.1038/s42003-019-0698-6
- Boccuto, L., Aoki, K., Flanagan-Steet, H., Chen, C. F., Fan, X., Bartel, F., . . . Schwartz, C. E. (2014). A mutation in a ganglioside biosynthetic enzyme, ST3GAL5, results in salt & pepper syndrome, a neurocutaneous disorder with altered glycolipid and glycoprotein glycosylation. *Hum Mol Genet*, 23(2), 418-433. doi:10.1093/hmg/ddt434
- Bochner, B. S. (2009). Siglec-8 on human eosinophils and mast cells, and Siglec-F on murine eosinophils, are functionally related inhibitory receptors. *Clin Exp Allergy*, 39(3), 317-324. doi:10.1111/j.1365-2222.2008.03173.x
- Bochner, B. S., Alvarez, R. A., Mehta, P., Bovin, N. V., Blixt, O., White, J. R., & Schnaar, R. L. (2005). Glycan array screening reveals a candidate ligand for Siglec-8. *J Biol Chem*, 280(6), 4307-4312. doi:10.1074/jbc.M412378200
- Bond, M. R., & Hanover, J. A. (2015). A little sugar goes a long way: the cell biology of O-GlcNAc. *J Cell Biol*, 208(7), 869-880. doi:10.1083/jcb.201501101
- Boucher, P., Gotthardt, M., Li, W. P., Anderson, R. G., & Herz, J. (2003). LRP: role in vascular wall integrity and protection from atherosclerosis. *Science*, 300(5617), 329-332. doi:10.1126/science.1082095
- Brown, G. M., Huckerby, T. N., Morris, H. G., Abram, B. L., & Nieduszynski, I. A. (1994). Oligosaccharides derived from bovine articular cartilage keratan sulfates after keratanase II digestion: implications for keratan sulfate structural fingerprinting. *Biochemistry*, 33(16), 4836-4846. doi:10.1021/bi00182a012

- Brown, G. M., Huckerby, T. N., & Nieduszynski, I. A. (1994). Oligosaccharides derived by keratanase II digestion of bovine articular cartilage keratan sulphates. *Eur J Biochem*, 224(2), 281-308. doi:10.1111/j.1432-1033.1994.00281.x
- Burda, P., & Aebi, M. (1999). The dolichol pathway of N-linked glycosylation. *Biochim Biophys Acta*, 1426(2), 239-257. doi:10.1016/s0304-4165(98)00127-5
- Caterson, B., Christner, J. E., & Baker, J. R. (1983). Identification of a monoclonal antibody that specifically recognizes corneal and skeletal keratan sulfate. Monoclonal antibodies to cartilage proteoglycan. *J Biol Chem*, 258(14), 8848-8854. Retrieved from <https://www.ncbi.nlm.nih.gov/pubmed/6223038>
- Caterson, B., & Melrose, J. (2018). Keratan sulfate, a complex glycosaminoglycan with unique functional capability. *Glycobiology*, 28(4), 182-206. doi:10.1093/glycob/cwy003
- Cooper, A. D. (1997). Hepatic uptake of chylomicron remnants. *J Lipid Res*, 38(11), 2173-2192. Retrieved from <https://www.ncbi.nlm.nih.gov/pubmed/9392416>
- Crocker, P. R., & Varki, A. (2001). Siglecs, sialic acids and innate immunity. *Trends Immunol*, 22(6), 337-342. doi:10.1016/s1471-4906(01)01930-5
- Cui, J., Xu, H., & Lehtinen, M. K. (2021). Macrophages on the margin: choroid plexus immune responses. *Trends Neurosci*, 44(11), 864-875. doi:10.1016/j.tins.2021.07.002
- Dani, N., Herbst, R. H., McCabe, C., Green, G. S., Kaiser, K., Head, J. P., . . . Lehtinen, M. K. (2021). A cellular and spatial map of the choroid plexus across brain ventricles and ages. *Cell*, 184(11), 3056-3074 e3021. doi:10.1016/j.cell.2021.04.003
- De Nardis, C., Lossl, P., van den Biggelaar, M., Madoori, P. K., Leloup, N., Mertens, K., . . . Gros, P. (2017). Recombinant Expression of the Full-length Ectodomain of LDL Receptor-related Protein 1 (LRP1) Unravels pH-dependent Conformational

- Changes and the Stoichiometry of Binding with Receptor-associated Protein (RAP). *J Biol Chem*, 292(3), 912-924. doi:10.1074/jbc.M116.758862
- Delaveris, C. S., Chiu, S. H., Riley, N. M., & Bertozzi, C. R. (2021). Modulation of immune cell reactivity with cis-binding Siglec agonists. *Proc Natl Acad Sci U S A*, 118(3). doi:10.1073/pnas.2012408118
- Freeze, H. H., & Schachter, H. (2009). Genetic Disorders of Glycosylation. In nd, A. Varki, R. D. Cummings, J. D. Esko, H. H. Freeze, P. Stanley, C. R. Bertozzi, G. W. Hart, & M. E. Etzler (Eds.), *Essentials of Glycobiology*. Cold Spring Harbor (NY).
- Freire, M. O., & Van Dyke, T. E. (2013). Natural resolution of inflammation. *Periodontol* 2000, 63(1), 149-164. doi:10.1111/prd.12034
- Frolich, L., Blum-Degen, D., Bernstein, H. G., Engelsberger, S., Humrich, J., Laufer, S., . . . Riederer, P. (1998). Brain insulin and insulin receptors in aging and sporadic Alzheimer's disease. *J Neural Transm (Vienna)*, 105(4-5), 423-438. doi:10.1007/s007020050068
- Funderburgh, J. L. (2000). Keratan sulfate: structure, biosynthesis, and function. *Glycobiology*, 10(10), 951-958. doi:10.1093/glycob/10.10.951
- Gill, D. J., Clausen, H., & Bard, F. (2011). Location, location, location: new insights into O-GalNAc protein glycosylation. *Trends Cell Biol*, 21(3), 149-158. doi:10.1016/j.tcb.2010.11.004
- Ginhoux, F., Greter, M., Leboeuf, M., Nandi, S., See, P., Gokhan, S., . . . Merad, M. (2010). Fate mapping analysis reveals that adult microglia derive from primitive macrophages. *Science*, 330(6005), 841-845. doi:10.1126/science.1194637
- Gonzalez-Gil, A., Li, T. A., Porell, R. N., Fernandes, S. M., Tarbox, H. E., Lee, H. S., . . . Schnaar, R. L. (2021). Isolation, identification, and characterization of the human

- airway ligand for the eosinophil and mast cell immunoinhibitory receptor Siglec-8. *J Allergy Clin Immunol*, 147(4), 1442-1452. doi:10.1016/j.jaci.2020.08.001
- Gonzalez-Gil, A., Porell, R. N., Fernandes, S. M., Wei, Y., Yu, H., Carroll, D. J., . . . Schnaar, R. L. (2018). Sialylated keratan sulfate proteoglycans are Siglec-8 ligands in human airways. *Glycobiology*, 28(10), 786-801. doi:10.1093/glycob/cwy057
- Guillozet, A. L., Weintraub, S., Mash, D. C., & Mesulam, M. M. (2003). Neurofibrillary tangles, amyloid, and memory in aging and mild cognitive impairment. *Arch Neurol*, 60(5), 729-736. doi:10.1001/archneur.60.5.729
- Hardy, J., & Selkoe, D. J. (2002). The amyloid hypothesis of Alzheimer's disease: progress and problems on the road to therapeutics. *Science*, 297(5580), 353-356. doi:10.1126/science.1072994
- Hardy, J. A., & Higgins, G. A. (1992). Alzheimer's disease: the amyloid cascade hypothesis. *Science*, 256(5054), 184-185. doi:10.1126/science.1566067
- Hebert, L. E., Weuve, J., Scherr, P. A., & Evans, D. A. (2013). Alzheimer disease in the United States (2010-2050) estimated using the 2010 census. *Neurology*, 80(19), 1778-1783. doi:10.1212/WNL.0b013e31828726f5
- Helenius, A., & Aebi, M. (2004). Roles of N-linked glycans in the endoplasmic reticulum. *Annu Rev Biochem*, 73, 1019-1049. doi:10.1146/annurev.biochem.73.011303.073752
- Herz, J., Clouthier, D. E., & Hammer, R. E. (1992). LDL receptor-related protein internalizes and degrades uPA-PAI-1 complexes and is essential for embryo implantation. *Cell*, 71(3), 411-421. doi:10.1016/0092-8674(92)90511-a
- Hickman, S. E., Allison, E. K., & El Khoury, J. (2008). Microglial dysfunction and defective beta-amyloid clearance pathways in aging Alzheimer's disease mice. *J Neurosci*, 28(33), 8354-8360. doi:10.1523/JNEUROSCI.0616-08.2008

- Hollingworth, P., Harold, D., Sims, R., Gerrish, A., Lambert, J. C., Carrasquillo, M. M., . . . Williams, J. (2011). Common variants at ABCA7, MS4A6A/MS4A4E, EPHA1, CD33 and CD2AP are associated with Alzheimer's disease. *Nat Genet*, *43*(5), 429-435. doi:10.1038/ng.803
- Iacobelli, S., Arno, E., D'Orazio, A., & Coletti, G. (1986). Detection of antigens recognized by a novel monoclonal antibody in tissue and serum from patients with breast cancer. *Cancer Res*, *46*(6), 3005-3010. Retrieved from <https://www.ncbi.nlm.nih.gov/pubmed/3516389>
- Iacobelli, S., Bucci, I., D'Egidio, M., Giuliani, C., Natoli, C., Tinari, N., . . . Schlessinger, J. (1993). Purification and characterization of a 90 kDa protein released from human tumors and tumor cell lines. *FEBS Lett*, *319*(1-2), 59-65. doi:10.1016/0014-5793(93)80037-u
- Iqbal, K., Alonso Adel, C., Chen, S., Chohan, M. O., El-Akkad, E., Gong, C. X., . . . Grundke-Iqbal, I. (2005). Tau pathology in Alzheimer disease and other tauopathies. *Biochim Biophys Acta*, *1739*(2-3), 198-210. doi:10.1016/j.bbadis.2004.09.008
- Jessen, N. A., Munk, A. S., Lundgaard, I., & Nedergaard, M. (2015). The Glymphatic System: A Beginner's Guide. *Neurochem Res*, *40*(12), 2583-2599. doi:10.1007/s11064-015-1581-6
- Kanekiyo, T., & Bu, G. (2014). The low-density lipoprotein receptor-related protein 1 and amyloid-beta clearance in Alzheimer's disease. *Front Aging Neurosci*, *6*, 93. doi:10.3389/fnagi.2014.00093
- Kanekiyo, T., Zhang, J., Liu, Q., Liu, C. C., Zhang, L., & Bu, G. (2011). Heparan sulphate proteoglycan and the low-density lipoprotein receptor-related protein 1 constitute major pathways for neuronal amyloid-beta uptake. *J Neurosci*, *31*(5), 1644-1651. doi:10.1523/JNEUROSCI.5491-10.2011

- Kelm, S., Pelz, A., Schauer, R., Filbin, M. T., Tang, S., de Bellard, M. E., . . . et al. (1994). Sialoadhesin, myelin-associated glycoprotein and CD22 define a new family of sialic acid-dependent adhesion molecules of the immunoglobulin superfamily. *Curr Biol*, 4(11), 965-972. doi:10.1016/s0960-9822(00)00220-7
- Keshavan, A., Heslegrave, A., Zetterberg, H., & Schott, J. M. (2017). Blood Biomarkers for Alzheimer's Disease: Much Promise, Cautious Progress. *Mol Diagn Ther*, 21(1), 13-22. doi:10.1007/s40291-016-0241-0
- Khasawneh, A. H., Garling, R. J., & Harris, C. A. (2018). Cerebrospinal fluid circulation: What do we know and how do we know it? *Brain Circ*, 4(1), 14-18. doi:10.4103/bc.bc\_3\_18
- Khlistunova, I., Biernat, J., Wang, Y., Pickhardt, M., von Bergen, M., Gazova, Z., . . . Mandelkow, E. M. (2006). Inducible expression of Tau repeat domain in cell models of tauopathy: aggregation is toxic to cells but can be reversed by inhibitor drugs. *J Biol Chem*, 281(2), 1205-1214. doi:10.1074/jbc.M507753200
- Kinney, J. W., Bemiller, S. M., Murtishaw, A. S., Leisgang, A. M., Salazar, A. M., & Lamb, B. T. (2018). Inflammation as a central mechanism in Alzheimer's disease. *Alzheimers Dement (N Y)*, 4, 575-590. doi:10.1016/j.trci.2018.06.014
- Kiwamoto, T., Katoh, T., Evans, C. M., Janssen, W. J., Brummet, M. E., Hudson, S. A., . . . Bochner, B. S. (2015). Endogenous airway mucins carry glycans that bind Siglec-F and induce eosinophil apoptosis. *J Allergy Clin Immunol*, 135(5), 1329-1340 e1329. doi:10.1016/j.jaci.2014.10.027
- Kopan, R., & Goate, A. (2000). A common enzyme connects notch signaling and Alzheimer's disease. *Genes Dev*, 14(22), 2799-2806. doi:10.1101/gad.836900
- Kunis, G., Baruch, K., Rosenzweig, N., Kertser, A., Miller, O., Berkutzki, T., & Schwartz, M. (2013). IFN-gamma-dependent activation of the brain's choroid plexus for

- CNS immune surveillance and repair. *Brain*, 136(Pt 11), 3427-3440.  
doi:10.1093/brain/awt259
- Laubli, H., Alisson-Silva, F., Stanczak, M. A., Siddiqui, S. S., Deng, L., Verhagen, A., . . . Varki, A. (2014). Lectin galactoside-binding soluble 3 binding protein (LGALS3BP) is a tumor-associated immunomodulatory ligand for CD33-related Siglecs. *J Biol Chem*, 289(48), 33481-33491. doi:10.1074/jbc.M114.593129
- Laubli, H., Pearce, O. M., Schwarz, F., Siddiqui, S. S., Deng, L., Stanczak, M. A., . . . Varki, A. (2014). Engagement of myelomonocytic Siglecs by tumor-associated ligands modulates the innate immune response to cancer. *Proc Natl Acad Sci U S A*, 111(39), 14211-14216. doi:10.1073/pnas.1409580111
- Lee, B. E., Suh, P. G., & Kim, J. I. (2021). O-GlcNAcylation in health and neurodegenerative diseases. *Exp Mol Med*, 53(11), 1674-1682.  
doi:10.1038/s12276-021-00709-5
- Lehtinen, M. K., Bjornsson, C. S., Dymecki, S. M., Gilbertson, R. J., Holtzman, D. M., & Monuki, E. S. (2013). The choroid plexus and cerebrospinal fluid: emerging roles in development, disease, and therapy. *J Neurosci*, 33(45), 17553-17559.  
doi:10.1523/JNEUROSCI.3258-13.2013
- Li, Y. M., Xu, M., Lai, M. T., Huang, Q., Castro, J. L., DiMuzio-Mower, J., . . . Gardell, S. J. (2000). Photoactivated gamma-secretase inhibitors directed to the active site covalently label presenilin 1. *Nature*, 405(6787), 689-694. doi:10.1038/35015085
- Lillis, A. P., Van Duyn, L. B., Murphy-Ullrich, J. E., & Strickland, D. K. (2008). LDL receptor-related protein 1: unique tissue-specific functions revealed by selective gene knockout studies. *Physiol Rev*, 88(3), 887-918.  
doi:10.1152/physrev.00033.2007
- Lindahl, U., Couchman, J., Kimata, K., & Esko, J. D. (2015). Proteoglycans and Sulfated Glycosaminoglycans. In rd, A. Varki, R. D. Cummings, J. D. Esko, P. Stanley, G.

- W. Hart, M. Aebi, A. G. Darvill, T. Kinoshita, N. H. Packer, J. H. Prestegard, R. L. Schnaar, & P. H. Seeberger (Eds.), *Essentials of Glycobiology* (pp. 207-221). Cold Spring Harbor (NY).
- Linden, S. K., Sutton, P., Karlsson, N. G., Korolik, V., & McGuckin, M. A. (2008). Mucins in the mucosal barrier to infection. *Mucosal Immunol*, *1*(3), 183-197.  
doi:10.1038/mi.2008.5
- Ling, E. A. (1979). Transformation of monocytes into amoeboid microglia in the corpus callosum of postnatal rats, as shown by labelling monocytes by carbon particles. *J Anat*, *128*(Pt 4), 847-858. Retrieved from  
<https://www.ncbi.nlm.nih.gov/pubmed/489472>
- Linsley, P. S., Horn, D., Marquardt, H., Brown, J. P., Hellstrom, I., Hellstrom, K. E., . . . Tolentino, E. (1986). Identification of a novel serum protein secreted by lung carcinoma cells. *Biochemistry*, *25*(10), 2978-2986. doi:10.1021/bi00358a037
- Liu, H., Zheng, Y., Zhang, Y., Li, J., Fernandes, S. M., Zeng, D., . . . Jia, Y. (2020). Immunosuppressive Siglec-E ligands on mouse aorta are up-regulated by LPS via NF-kappaB pathway. *Biomed Pharmacother*, *122*, 109760.  
doi:10.1016/j.biopha.2019.109760
- Loimaranta, V., Hepojoki, J., Laaksoaho, O., & Pulliainen, A. T. (2018). Galectin-3-binding protein: A multitask glycoprotein with innate immunity functions in viral and bacterial infections. *J Leukoc Biol*, *104*(4), 777-786.  
doi:10.1002/JLB.3VMR0118-036R
- Macauley, M. S., Crocker, P. R., & Paulson, J. C. (2014). Siglec-mediated regulation of immune cell function in disease. *Nat Rev Immunol*, *14*(10), 653-666.  
doi:10.1038/nri3737

- Mapunda, J. A., Tibar, H., Regragui, W., & Engelhardt, B. (2022). How Does the Immune System Enter the Brain? *Front Immunol*, *13*, 805657.  
doi:10.3389/fimmu.2022.805657
- Martinez, V. G., Moestrup, S. K., Holmskov, U., Mollenhauer, J., & Lozano, F. (2011). The conserved scavenger receptor cysteine-rich superfamily in therapy and diagnosis. *Pharmacol Rev*, *63*(4), 967-1000. doi:10.1124/pr.111.004523
- McGavern, D. B., & Kang, S. S. (2011). Illuminating viral infections in the nervous system. *Nat Rev Immunol*, *11*(5), 318-329. doi:10.1038/nri2971
- Medzhitov, R. (2001). Toll-like receptors and innate immunity. *Nat Rev Immunol*, *1*(2), 135-145. doi:10.1038/35100529
- Moremen, K. W., & Molinari, M. (2006). N-linked glycan recognition and processing: the molecular basis of endoplasmic reticulum quality control. *Curr Opin Struct Biol*, *16*(5), 592-599. doi:10.1016/j.sbi.2006.08.005
- Moremen, K. W., Tiemeyer, M., & Nairn, A. V. (2012). Vertebrate protein glycosylation: diversity, synthesis and function. *Nat Rev Mol Cell Biol*, *13*(7), 448-462.  
doi:10.1038/nrm3383
- Muller, J., Obermeier, I., Wohner, M., Brandl, C., Mrotzek, S., Angermuller, S., . . . Nitschke, L. (2013). CD22 ligand-binding and signaling domains reciprocally regulate B-cell Ca<sup>2+</sup> signaling. *Proc Natl Acad Sci U S A*, *110*(30), 12402-12407.  
doi:10.1073/pnas.1304888110
- Murphy, M. P., & LeVine, H., 3rd. (2010). Alzheimer's disease and the amyloid-beta peptide. *J Alzheimers Dis*, *19*(1), 311-323. doi:10.3233/JAD-2010-1221
- Natale, G., Limanaqi, F., Busceti, C. L., Mastroiacovo, F., Nicoletti, F., Puglisi-Allegra, S., & Fornai, F. (2021). Glymphatic System as a Gateway to Connect Neurodegeneration From Periphery to CNS. *Front Neurosci*, *15*, 639140.  
doi:10.3389/fnins.2021.639140

- Nie, L., Cai, S. Y., Shao, J. Z., & Chen, J. (2018). Toll-Like Receptors, Associated Biological Roles, and Signaling Networks in Non-Mammals. *Front Immunol*, *9*, 1523. doi:10.3389/fimmu.2018.01523
- Peferoen, L., Kipp, M., van der Valk, P., van Noort, J. M., & Amor, S. (2014). Oligodendrocyte-microglia cross-talk in the central nervous system. *Immunology*, *141*(3), 302-313. doi:10.1111/imm.12163
- Pless, D. D., & Lennarz, W. J. (1977). Enzymatic conversion of proteins to glycoproteins. *Proc Natl Acad Sci U S A*, *74*(1), 134-138. doi:10.1073/pnas.74.1.134
- Powell, T. J., Schreck, R., McCall, M., Hui, T., Rice, A., App, H., . . . Shawver, L. K. (1995). A tumor-derived protein which provides T-cell costimulation through accessory cell activation. *J Immunother Emphasis Tumor Immunol*, *17*(4), 209-221. doi:10.1097/00002371-199505000-00003
- Praissman, J. L., & Wells, L. (2014). Mammalian O-mannosylation pathway: glycan structures, enzymes, and protein substrates. *Biochemistry*, *53*(19), 3066-3078. doi:10.1021/bi500153y
- Priego, N., & Valiente, M. (2019). The Potential of Astrocytes as Immune Modulators in Brain Tumors. *Front Immunol*, *10*, 1314. doi:10.3389/fimmu.2019.01314
- Ransohoff, R. M. (2016). A polarizing question: do M1 and M2 microglia exist? *Nat Neurosci*, *19*(8), 987-991. doi:10.1038/nn.4338
- Ransohoff, R. M., & Engelhardt, B. (2012). The anatomical and cellular basis of immune surveillance in the central nervous system. *Nat Rev Immunol*, *12*(9), 623-635. doi:10.1038/nri3265
- Rashmi, R., Bode, B. P., Panesar, N., King, S. B., Rudloff, J. R., Gartner, M. R., & Koenig, J. M. (2009). Siglec-9 and SHP-1 are differentially expressed in neonatal and adult neutrophils. *Pediatr Res*, *66*(3), 266-271. doi:10.1203/PDR.0b013e3181b1bc19

- Rauch, J. N., Luna, G., Guzman, E., Audouard, M., Challis, C., Sibih, Y. E., . . . Kosik, K. S. (2020). LRP1 is a master regulator of tau uptake and spread. *Nature*, *580*(7803), 381-385. doi:10.1038/s41586-020-2156-5
- Redzic, Z. B., & Segal, M. B. (2004). The structure of the choroid plexus and the physiology of the choroid plexus epithelium. *Adv Drug Deliv Rev*, *56*(12), 1695-1716. doi:10.1016/j.addr.2004.07.005
- Schiller, M., Ben-Shaan, T. L., & Rolls, A. (2021). Neuronal regulation of immunity: why, how and where? *Nat Rev Immunol*, *21*(1), 20-36. doi:10.1038/s41577-020-0387-1
- Schnaar, R. L., & Kinoshita, T. (2015). Glycosphingolipids. In rd, A. Varki, R. D. Cummings, J. D. Esko, P. Stanley, G. W. Hart, M. Aebi, A. G. Darvill, T. Kinoshita, N. H. Packer, J. H. Prestegard, R. L. Schnaar, & P. H. Seeberger (Eds.), *Essentials of Glycobiology* (pp. 125-135). Cold Spring Harbor (NY).
- Schwartz, M., & Baruch, K. (2014). The resolution of neuroinflammation in neurodegeneration: leukocyte recruitment via the choroid plexus. *EMBO J*, *33*(1), 7-22. doi:10.1002/emj.201386609
- Seki, T., Kanagawa, M., Kobayashi, K., Kowa, H., Yahata, N., Maruyama, K., . . . Toda, T. (2020). Galectin 3-binding protein suppresses amyloid-beta production by modulating beta-cleavage of amyloid precursor protein. *J Biol Chem*, *295*(11), 3678-3691. doi:10.1074/jbc.RA119.008703
- Shechter, R., London, A., Varol, C., Raposo, C., Cusimano, M., Yovel, G., . . . Schwartz, M. (2009). Infiltrating blood-derived macrophages are vital cells playing an anti-inflammatory role in recovery from spinal cord injury in mice. *PLoS Med*, *6*(7), e1000113. doi:10.1371/journal.pmed.1000113
- Shechter, R., Miller, O., Yovel, G., Rosenzweig, N., London, A., Ruckh, J., . . . Schwartz, M. (2013). Recruitment of beneficial M2 macrophages to injured spinal cord is

- orchestrated by remote brain choroid plexus. *Immunity*, 38(3), 555-569.  
doi:10.1016/j.immuni.2013.02.012
- Siddiqui, S. S., Matar, R., Merheb, M., Hodeify, R., Vazhappilly, C. G., Marton, J., . . . Al Zouabi, H. (2019). Siglecs in Brain Function and Neurological Disorders. *Cells*, 8(10). doi:10.3390/cells8101125
- Siddiqui, S. S., Springer, S. A., Verhagen, A., Sundaramurthy, V., Alisson-Silva, F., Jiang, W., . . . Varki, A. (2017). The Alzheimer's disease-protective CD33 splice variant mediates adaptive loss of function via diversion to an intracellular pool. *J Biol Chem*, 292(37), 15312-15320. doi:10.1074/jbc.M117.799346
- Siracusa, R., Fusco, R., & Cuzzocrea, S. (2019). Astrocytes: Role and Functions in Brain Pathologies. *Front Pharmacol*, 10, 1114. doi:10.3389/fphar.2019.01114
- Soulet, D., & Rivest, S. (2008). Bone-marrow-derived microglia: myth or reality? *Curr Opin Pharmacol*, 8(4), 508-518. doi:10.1016/j.coph.2008.04.002
- Stanley, P., Taniguchi, N., & Aebi, M. (2015). N-Glycans. In rd, A. Varki, R. D. Cummings, J. D. Esko, P. Stanley, G. W. Hart, M. Aebi, A. G. Darvill, T. Kinoshita, N. H. Packer, J. H. Prestegard, R. L. Schnaar, & P. H. Seeberger (Eds.), *Essentials of Glycobiology* (pp. 99-111). Cold Spring Harbor (NY).
- Sun, J., Shaper, N. L., Itonori, S., Heffer-Lauc, M., Sheikh, K. A., & Schnaar, R. L. (2004). Myelin-associated glycoprotein (Siglec-4) expression is progressively and selectively decreased in the brains of mice lacking complex gangliosides. *Glycobiology*, 14(9), 851-857. doi:10.1093/glycob/cwh107
- Tateno, H., Li, H., Schur, M. J., Bovin, N., Crocker, P. R., Wakarchuk, W. W., & Paulson, J. C. (2007). Distinct endocytic mechanisms of CD22 (Siglec-2) and Siglec-F reflect roles in cell signaling and innate immunity. *Mol Cell Biol*, 27(16), 5699-5710. doi:10.1128/MCB.00383-07

- Van Gool, B., Storck, S. E., Reekmans, S. M., Lechat, B., Gordts, P., Pradier, L., . . .  
 Roebroek, A. J. M. (2019). LRP1 Has a Predominant Role in Production over  
 Clearance of Abeta in a Mouse Model of Alzheimer's Disease. *Mol Neurobiol*,  
 56(10), 7234-7245. doi:10.1007/s12035-019-1594-2
- Varki, A., & Kornfeld, S. (2015). Historical Background and Overview. In rd, A. Varki, R.  
 D. Cummings, J. D. Esko, P. Stanley, G. W. Hart, M. Aebi, A. G. Darvill, T.  
 Kinoshita, N. H. Packer, J. H. Prestegard, R. L. Schnaar, & P. H. Seeberger  
 (Eds.), *Essentials of Glycobiology* (pp. 1-18). Cold Spring Harbor (NY).
- Varki, A., Schnaar, R. L., & Crocker, P. R. (2015). I-Type Lectins. In rd, A. Varki, R. D.  
 Cummings, J. D. Esko, P. Stanley, G. W. Hart, M. Aebi, A. G. Darvill, T.  
 Kinoshita, N. H. Packer, J. H. Prestegard, R. L. Schnaar, & P. H. Seeberger  
 (Eds.), *Essentials of Glycobiology* (pp. 453-467). Cold Spring Harbor (NY).
- Vavasseur, F., Yang, J. M., Dole, K., Paulsen, H., & Brockhausen, I. (1995). Synthesis of  
 O-glycan core 3: characterization of UDP-GlcNAc: GalNAc-R beta 3-N-acetyl-  
 glucosaminyltransferase activity from colonic mucosal tissues and lack of the  
 activity in human cancer cell lines. *Glycobiology*, 5(3), 351-357.  
 doi:10.1093/glycob/5.3.351
- Villani, A. C., Satija, R., Reynolds, G., Sarkizova, S., Shekhar, K., Fletcher, J., . . .  
 Hacohen, N. (2017). Single-cell RNA-seq reveals new types of human blood  
 dendritic cells, monocytes, and progenitors. *Science*, 356(6335).  
 doi:10.1126/science.aah4573
- Walsh, J. T., Hendrix, S., Boato, F., Smirnov, I., Zheng, J., Lukens, J. R., . . . Kipnis, J.  
 (2015). MHCII-independent CD4+ T cells protect injured CNS neurons via IL-4. *J*  
*Clin Invest*, 125(6), 2547. doi:10.1172/JCI82458

- Wang, X., Su, B., Lee, H. G., Li, X., Perry, G., Smith, M. A., & Zhu, X. (2009). Impaired balance of mitochondrial fission and fusion in Alzheimer's disease. *J Neurosci*, 29(28), 9090-9103. doi:10.1523/JNEUROSCI.1357-09.2009
- Willnow, T. E., Armstrong, S. A., Hammer, R. E., & Herz, J. (1995). Functional expression of low density lipoprotein receptor-related protein is controlled by receptor-associated protein in vivo. *Proc Natl Acad Sci U S A*, 92(10), 4537-4541. doi:10.1073/pnas.92.10.4537
- Wu, F., Liu, L., & Zhou, H. (2017). Endothelial cell activation in central nervous system inflammation. *J Leukoc Biol*, 101(5), 1119-1132. doi:10.1189/jlb.3RU0816-352RR
- Yang, L., Liu, C. C., Zheng, H., Kanekiyo, T., Atagi, Y., Jia, L., . . . Bu, G. (2016). LRP1 modulates the microglial immune response via regulation of JNK and NF-kappaB signaling pathways. *J Neuroinflammation*, 13(1), 304. doi:10.1186/s12974-016-0772-7
- Yates, S. L., Burgess, L. H., Kocsis-Angle, J., Antal, J. M., Dority, M. D., Embury, P. B., . . . Brunden, K. R. (2000). Amyloid beta and amylin fibrils induce increases in proinflammatory cytokine and chemokine production by THP-1 cells and murine microglia. *J Neurochem*, 74(3), 1017-1025. doi:10.1046/j.1471-4159.2000.0741017.x
- Yu, H., Gonzalez-Gil, A., Wei, Y., Fernandes, S. M., Porell, R. N., Vajn, K., . . . Schnaar, R. L. (2017). Siglec-8 and Siglec-9 binding specificities and endogenous airway ligand distributions and properties. *Glycobiology*, 27(7), 657-668. doi:10.1093/glycob/cwx026
- Zachara, N., Akimoto, Y., & Hart, G. W. (2015). The O-GlcNAc Modification. In rd, A. Varki, R. D. Cummings, J. D. Esko, P. Stanley, G. W. Hart, M. Aebi, A. G. Darvill, T. Kinoshita, N. H. Packer, J. H. Prestegard, R. L. Schnaar, & P. H. Seeberger (Eds.), *Essentials of Glycobiology* (pp. 239-251). Cold Spring Harbor (NY).

- Zachara, N. E. (2018). Critical observations that shaped our understanding of the function(s) of intracellular glycosylation (O-GlcNAc). *FEBS Lett*, 592(23), 3950-3975. doi:10.1002/1873-3468.13286
- Zhang, M., Angata, T., Cho, J. Y., Miller, M., Broide, D. H., & Varki, A. (2007). Defining the in vivo function of Siglec-F, a CD33-related Siglec expressed on mouse eosinophils. *Blood*, 109(10), 4280-4287. doi:10.1182/blood-2006-08-039255
- Zhang, Y., Zheng, Y., Li, J., Nie, L., Hu, Y., Wang, F., . . . Jia, Y. (2019). Immunoregulatory Siglec ligands are abundant in human and mouse aorta and are up-regulated by high glucose. *Life Sci*, 216, 189-199. doi:10.1016/j.lfs.2018.11.049

CHAPTER TWO  
STEM CELL MODELING OF THE ALZHEIMER'S DISEASE GLYCOME

---

Adapted from:

**Rosenbalm KE**, Nix DB, Tiemeyer M. Cortical brain glycomics of Alzheimer's disease (2022) To be submitted to *Glycobiology*

## Abstract

Induced pluripotent stem cells (iPSCs) and their derivatives are a powerful and popular tool for disease modeling, particularly for neurological and neurodegenerative diseases using neural induction (NI) differentiations. To date, little research has demonstrated how glycosylation is affected by differentiation of iPSCs (iPSC vs. NI) or how cortical neuron glycosylation is affected by Alzheimer's disease pathology (NDC vs. APP<sup>DP2</sup>). Here, we illustrate glycome alterations induced by developmental changes as well as pathological changes using an *in vitro* model analyzing N- and O-linked glycoprotein glycans and glycosphingolipids (GSLs). Upon NI differentiation, N-glycans shift towards higher complexity in contrast to majority high mannose structures seen in iPSCs. AD NI cultures also had a significant increase in bisected N-glycans over control NI cultures, which have been proposed as a possible biomarker for AD diagnosis. Control NI O-glycans demonstrated several significant variations relative to pluripotency, where GSLs were broadly affected for both genotypes. Glycome characterization expands diagnostic and therapeutic potential for AD by unveiling possible biomarkers and functional glycan epitopes such as Siglec ligands.

### Key words

mass spectrometry, glycomics, disease modeling, stem cells, Alzheimer's disease, secretory pathway

## Introduction

The majority of brain proteins, approximately 75%, are glycosylated. Likewise, the mammalian brain also contains up to 400 species of GSLs. Despite the wide array of neurological diseases, few studies have comprehensively analyzed CNS glycans through development, in disease, and how human glycosylation compares to a rodent

model. Here, we have demonstrated changes in glycosylation in Alzheimer's disease using a patient-derived stem cell-based disease model.

Many preceding studies of brain glycomes have utilized technologies with inadequacies in particular areas. For example, lectin array assays can be automated for high throughput capacities, but they usually offer limited information about glycan type or composition. Matrix-assisted laser desorption/ionization (MALDI) mass spectrometry is able to provide compositional information but does not support isomer separation or detailed structural information. Liquid chromatography coupled with multistage accurate mass spectrometry (LC-MSn) can separate glycan isomers and provide detailed structural data including linkage information using certain adducts but requires characterized input standards and a great deal of optimization (Kurz, Sheikh, Lu, Wells, & Tiemeyer, 2021).

That said, glycomic and glycoproteomic analysis of neurological disease patients and model systems is an active field of research. It has been noted that N-glycans in the CNS tend to differ from serum N-glycans by the presence of bisecting GlcNAc. Core fucosylated bisecting GlcNAc N-glycan structures ("brain type" N-glycans) are prevalent in brain tissues, and their glycan density is associated with proper brain development. Bisecting GlcNAc on N-glycans is catalyzed by the enzyme  $\beta$ 1,4-N-acetylglucosaminyltransferase III (GnT-III). In brain tissue from AD diagnosed patients, mRNA levels of *Gnt-III* were significantly increased, which has been postulated to be an adaptive response to A $\beta$  secretion (Akasaka-Manya et al., 2010). GnT-III modified N-glycans also serve a regulatory function in N-glycan biosynthesis, as bisected structures are less likely to undergo branching initiated by other GlcNAc transferases (Stanley, Schachter, & Taniguchi, 2009). Similarly, N-glycomic analysis has been completed on CSF provided by sporadic Alzheimer's affected patients, which showed high variability

among age-matched controls and AD patients though the abundance of these brain type N-glycans was noted in the AD patients (Palmigiano et al., 2016).

Using a glycoblotting method, Gizaw et al. analyzed major N- and GSL-glycans in AD postmortem human brain tissue as well as serum and CSF. Paradoxically, brain type N-glycans were found to be decreased in AD patient brain tissues. Serum N-glycans were significantly increased in AD patients, and specifically the brain type N-glycan structures were found to be elevated in patient serum. A similar result was observed for patient CSF. GSL-glycans derived from ozonolysis release demonstrated reduced ganglioside expression levels in the cortices of patients compared to healthy controls (Gizaw, Ohashi, Tanaka, Hinou, & Nishimura, 2016).

Lee et al. characterized human and mouse brain N-glycomes by age and by brain region using LC-MSn. The prefrontal cortex region (PFC) was of particular interest to the authors because is associated with functional changes during development. Temporal related changes in the PFC were found to be in glycans containing fucosylated sialylated LacdiNAc epitopes (J. Lee et al., 2020).

Recently, Williams et al. assessed brain protein glycosylation in adult mice with regional specificity including cortex, hippocampus, striatum, and cerebellum using MALDI-TOF MS, lectin blotting, and RNA sequencing. They annotated 95 N-linked structures, where the majority of N-glycans were high-mannose structures. Bisected structures comprised ~30% of glycans, while only <3% of N-glycans were sialylated. The second highest abundance structure was found to be a core fucosylated, bisecting GlcNAc structure. The majority of O-glycans detected were O-GalNAc mucin type, where the proportion of O-mannose structures varied significantly among brain regions (S. E. Williams et al., 2022).

In AD studies exploring diagnostics or contributions to neuropathology, the glycosylation of tau has also been of particular interest. Tau N-glycosylation appears to

contribute to tau phosphorylation and hyperphosphorylation (F. Liu et al., 2002). Granulovacuolar degenerations, a site for tau phosphorylation, neurofibrillary tangles, and senile plaque dystrophic neurites exhibited co-localization with Neu5Ac antibodies. Hypersialylation of these structures was found to be highly specific to AD when several other neuropathologies were examined (Nagamine et al., 2016).

Glycoproteomic studies of AD have been completed, and network analysis has alluded to alterations in modules associated with N-glycosylation unique to AD pathology. For example, <sup>18</sup>O-labelling of N-glycosylation sites in human control and AD patient brains revealed aberrations of the N-glycan pathway involved in AD pathogenesis, including ECM dysfunction, neuroinflammatory processes, and dysregulation of endocytic trafficking (Q. Zhang, Ma, Chin, & Li, 2020). Several studies have analyzed additional -omic-based changes in AD. Recently, a large-scale proteomic study using tandem mass tag MS described a protein module for glycosylation and ER trafficking that was not preserved in the RNA network, meaning glycosylation changes in AD were not observed in the transcriptomic data (Johnson et al., 2022).

In this study, we utilize AD patient-derived iPSCs established by the Goldstein lab and maintained in biobank by Coriell Institute for Medical Research. Patient APP<sup>DP2</sup> is a female with a genome duplication of *app* without mental retardation. *App* duplications account for approximately half of familial cases derived from *app* mutations (McNaughton et al., 2012; Sleegers et al., 2006). The patient described in this study experienced familial AD onset at 53 years of age with an APOE genotype 3/3, the most common APOE genotype that does not appear protective nor contributory to development of AD.

Here, we demonstrate changes to global glycosylation processes as iPSCs are differentiated to neuronal populations. We also observe effects of a genetic variant of

familial Alzheimer's disease on glycosylation in iPSCs and neuronal cultures as compared to non-demented control (NDC) cultures.

## **Experimental Procedures**

### **Reagents**

All antibodies and blocking buffer [4% (w/v) BSA, 10% (v/v) goat serum in PBS-T] were filtered through 0.2 µm SFCA filters (Corning) prior to immunofluorescence. Antibodies used in this study were as follows: Oct-3/4 (Santa Cruz Biotechnology), SSEA4 (Santa Cruz Biotechnology), Sox2 (Santa Cruz Biotechnology), Pax6 (DSHB), Map2 (Abcam), TuJ-1 (R&D Systems), GM130 (Santa Cruz Biotechnology), and EEA1 (Santa Cruz Biotechnology).

### **iPSC culture**

Induced pluripotent stem cells were cultured as previously described (Michelle Dookwah, 2021). K3 NCD iPSCs (Si-Tayeb et al., 2010) and APP<sup>DP2</sup> iPSCs (Israel et al., 2012) (Coriell GM24675) were cultured in HAIF-based media (Menendez et al., 2013). APP<sup>DP2</sup> iPSCs were transitioned from MEF feeder layer to Geltrex (ThermoFisher) matrix as well as from mTeSR media (Stem Cell Technologies) to HAIF in quarter ratio increments. Pluripotency was assessed by immunofluorescence of selected markers.

### **Neural induction**

Cortical neural induction was carried out as previously described (Shi, Kirwan, & Livesey, 2012). Dual SMAD inhibition with Dorsomorphin (StemRD) and SB431542 (Tocris) in conjunction with vitamin A is required for differentiation. Neural progenitors are achieved after 12 DIV from confluent iPSC culture in N2/B27-containing (ThermoFisher) neural maintenance media with SMAD inhibitors. The neuroepithelial sheet was disrupted with Dispase (Stem Cell Technologies), and aggregates were plated on 2X Geltrex-coated dishes in neural maintenance media. Rosettes were

expanded with FGF2 (R&D Systems). Upon emergence of neurons, cultures were passaged to single cell with Accutase (Innovative Cell Technologies). Successful differentiation was assessed by cell morphology and immunofluorescence of selected markers. While functional chemical synapses were formed after 45 DIV, where cultures were harvested by cell scraping around 40 DIV for glycomic analysis. Collected cells were rinsed with PBS, centrifuged to a pellet and aspirated, and stored at -20°C.

### **Immunofluorescence**

Cells were grown on round glass coverslips (Fisher Scientific, 12-545) in a 12 well plate to desired confluency. Cells were washed with PBS and fixed for 20 minutes at room temperature with 4% paraformaldehyde. After washing with PBS, cells were blocked with 4% BSA (w/v), 10% serum (v/v) in PBS-0.1% Triton X-100 (v/v). Prolong Diamond mounting medium (Invitrogen, P36970) cured overnight before coverslips were sealed. Images were obtained using Olympus FV1200 confocal microscope, and images were normalized and prepared in Slidebook 5.0 x64 software.

### **Glycan analysis**

Cell pellets were collected by scraping for glycan analysis and rinsed with PBS. Cells were thoroughly homogenized in 50% MeOH and transferred to a glass tube where final concentration was adjusted to 4:8:3 water:chloroform:methanol (v/v/v). Lipid components were extracted twice, and proteins were precipitated with ice cold acetone.

N-linked glycan analysis was completed as previously described (Aoki et al., 2007). Glycopeptides were generated with overnight trypsin (Sigma-Aldrich T8003) and chymotrypsin (Sigma-Aldrich C4129) digests which were enriched with Sep-Pak C18 cartridge chromatography (Waters, WAT023590). Oligosaccharides were released with PNGase F treatment for 18 hr at 37°C. Released oligosaccharides were separated from residual peptides with C18 cartridge cleanup and permethylated prior to mass spectrometry analysis.

O-linked glycan analysis was completed as previously described (Aoki et al., 2008). O-glycans were released by reductive  $\beta$ -elimination, desalted with AG-50W-X8 H<sup>+</sup> resin, and enriched with Sep-Pak C18 cartridge chromatography. Prior to permethylation, graphitized carbon column cleanup was included (Alltech, 210142) (Kurz et al., 2015). The water fraction from permethylation containing sulfated O-glycans was purified with C18 and analyzed by NSI-MS in positive and negative ion modes.

Glycosphingolipid analysis was completed as previously described (Boccutto et al., 2014). Dried GSLs were subjected to saponification and desalting with Sep-Pak tC18 cartridge (Waters, WAT036805) chromatography. Free fatty acids were removed with hexanes, and GLSs were visualized with HPTLC prior to permethylation and mass spectrometry.

Permethyated N-glycans, O-glycans, and GSLs were analyzed by nano-electrospray ionization mass spectrometry using an ion-trap instrument (NSI-LTQ Orbitrap Discovery, ThermoFisher). Protein-derived glycans were dissolved in 1 mM NaOH in 50% aqueous methanol (v/v) for direct infusion, while GSLs were prepared in 1 mM NaOH in 16:3:3 methanol:2-propanol:1-propanol (v/v/v). A syringe flow rate of 0.4-0.6  $\mu$ L/min. For MS<sup>n</sup> analysis with collision induced dissociation (CID), 40-45% collision energy was utilized. Total ion mapping functionality of Xcalibur software (version 2.0) was used to detect individual glycan compositions. Prevalence of glycans was calculated based on full MS intensities with all charge states detected accounted for. Quantification was performed relative to known quantities of external standards which were heavy permethylated with methyl iodide (Mehta et al., 2016).

## Results

Our iPSC cultures were positive for appropriate pluripotency markers including transcription factors Oct4, Sox2, and Nanog as well as cell surface epitope SSEA4 (**Fig.**

**2.1A**). With the potential to alter cell fate confirmed, we utilized dual SMAD inhibition in the presence of retinoids to achieve neural induction (NI) in approximately 40 DIV (**Fig. 2.1B**) (Chambers et al., 2009). Of note, the differentiation protocol used here generates a heterogeneous cortical network. These assemblies include forebrain progenitors, deep and upper layer glutamatergic cortical neurons, and eventually functional astrocytes (Kirwan et al., 2015). The formation of neural networks mimics the higher-order organization of brain tissue, an important distinction as it allows us to compare the glycome of human or rodent cortex. NI cultures were positive for neuroepithelial markers including transcription factor Pax6 and intracellular structural proteins Map2 and TuJ-1 (**Fig. 2.1B**).

Though NI was successfully achieved with AD line APP<sup>DP2</sup>, efficiency of the induction and morphological anomalies were noted compared to the NDC line K3. These phenotypes were similarly observed during establishment of the APP<sup>DP2</sup> line and its differentiation to ectodermal tissue (Israel et al., 2012). We observed that the cells displayed inappropriate vesicular trafficking and secretory dysfunction, as demonstrated by an accumulation of endosomal compartments as well as disperse and fragmented cis-Golgi complex (**Fig. 2.1C**).

Seventy-five N-linked structures were assessed for relative abundance in iPSCs and NI cultures for NDC and AD cell lines. iPSC cultures were comprised of primarily high mannose glycans (**Fig. 2.2A**), while neural differentiation altered the glycome towards a greater complexity (**Fig. 2.2B**). AD neural cultures contained significantly more complex and bisected N-glycans than NDC. A statistically significant change in protein sialylation was not detected; however, we observed considerably greater sialylation than was detected in mouse brain (Sarah E. Williams et al., 2020). Upon differentiation to neural fate, AD cultures demonstrated an increase in bisected N-glycans, while NDC did not (**Fig. 2.2C**). Through differentiation, both genotypes

displayed changes in the same classes of N-glycans (**Fig. 2.2D**). In the future, Endo H sensitivity should be considered for enhanced structural characterization between hybrid and complex glycans.

Forty-nine O-linked structures were also assessed for relative abundance and summarized based on their structural features. The majority of O-glycans in iPSC and neural cultures were mucin-type O-GalNAc glycans, where no significant differences were found between NCD and AD iPSC O-glycans (**Fig. 2.3A**). Neural cultures demonstrated a greater disparity between core 1 and core 2 O-glycans than was seen in iPSC cultures (**Fig. 2.3B**). Approximately 10% of neural O-glycans were O-mannose species, while spatial mouse brain analysis found up to 25% of glycans to be O-mannosylated (Sarah E. Williams et al., 2020). Mouse brain O-glycan analysis also found ~10% fucosylated but ~90% sialylated O-glycans, while our analysis found ~10% fucosylated but only ~30% of neural culture O-glycans to be sialylated (**Fig. 2.3B**) which is slightly increased relative to iPSC cultures (**Fig. 2.3C**). While differentiation stimulated changes in several subtypes of NDC O-glycans, AD glycan classes did not reflect any significant differences compared to their iPSC profile (**Fig. 2.3D**).

We also analyzed O-glycans in negative mode to address possible sulfated structures. For several carbohydrate sulfotransferases, overexpression has been shown to increase Siglec binding (Jung et al., 2021). These immunomodulatory lectins are of particular interest in AD pathology and have been shown to bind to sulfated ligands *in vivo* (Gonzalez-Gil et al., 2018). We observed many more sulfated O-glycans in AD NI cultures compared to NDC (**Fig. 2.4A**). Some of the glycans detected contained epitopes that were compatible as ligands for our Siglecs of interest (**Fig. 2.4B**).

Furthermore, eighteen glycan epitopes were assessed for relative abundance on a variety of lipid chain lengths. GSL profiles have been previously described for iPSC cultures (Saljo et al., 2017) as well as in Alzheimer's disease. Monosialoganglioside

GM1 has been implicated in AD pathogenesis through its ability to seed the aggregation of A $\beta$  and contribute to plaque formation (Cebecauer, Hof, & Amaro, 2017; S. Hong et al., 2014; Yanagisawa & Ihara, 1998). Some groups have reported not an alteration in the density of gangliosides in AD brains but rather disordered localization (Hirano-Sakamaki et al., 2015). Surprisingly, for both iPSC (**Fig. 2.5A**) and neural cultures (**Fig. 2.5B**), NDC control line expressed greater percentage of the profile as gangliosides. Comparing the ratio of gangliosides to neutral GSLs over differentiation did demonstrate a statistically significant increase in ganglio-series species in AD compared to NDC (**Fig. 2.5C**).

AD signaling analysis has revealed a role for ceramide and its interplay with Siglecs in the pathogenesis of AD (Mizuno et al., 2016). Lactosylceramide was increased in AD cultures for both iPSC (**Fig. 2.5A**) and neural cultures (**Fig. 2.5B**), which we also observed in cortical tissue from 5xFAD mouse brain and has been observed in other cellular AD models (Noel, Ingrand, & Barrier, 2017). Interestingly, ceramide accumulation has been noted in some inflammatory conditions as an initiation factor for aberrant autophagy and apoptosis (Bodas, Min, & Vij, 2015).

## Discussion

This study has explored how cell type specialization impacts glycosylation as well as the effects of a genetic neurodegenerative phenotype on the glycome of human stem cells and neural differentiated cultures. Broadly, differentiation from pluripotent stem cell lineage to a specialized cell population as well as familial AD genetics have effects on the glycome. However, there is still substantial opportunity to increase our understanding of these facets. We must acknowledge that despite billions of dollars of federally funded research annually, the AD field is significantly lacking in both diagnostics and effective

therapies. Further appreciation for the role of glycosylation may aid in clinical utility for each of these avenues.

Glycoproteomics of CSF and serum may facilitate biomarker discovery and diagnosis of AD. Glycomics profiles and proteomics profiles have been attempted in the past, but comprehensive site-specific glycoproteomics is just beginning to be attempted (Z. Chen et al., 2021; Gaunitz, Tjernberg, & Schedin-Weiss, 2021). Glycoproteomics, particularly N-glycoproteomics, may offer a promising opportunity for biomarker discovery as many AD-related pathogenic proteins are glycosylated in some capacity. It may be interesting to incorporate sex differences in these studies with many more patient cells lines, as APP<sup>DP2</sup> are derived from a female patient.

This study did not characterize O-GlcNAcylation of tau, which has been implicated in reduction of neurofibrillary tangle (NFT) assembly (Yuzwa et al., 2012). ELISA analysis of brain tissue has demonstrated increased levels of O-GlcNAc in the brains of AD patients, though glycoproteomics studies can aid in characterizing sites of tau modification (Frenkel-Pinter et al., 2017). Engineering tau modifications to prevent NFT formation, which has been correlated with neuron apoptosis and inflammatory signaling cascades, may serve as a potential prophylactic treatment for AD.

With our current model system, glycome discovery could be supplemented with mass spectrometry imaging or staining approaches (McDowell et al., 2021). Our present culture system does not account for cortical spatial heterogeneity. Co-culture systems including neuronal populations with glial and endothelial cells could contribute to our understanding of spatial differences. For a snapshot of the glycome in these co-cultures, global glycosylation detection for preliminary analysis can be completed with periodic acid-Schiff staining (Frenkel-Pinter et al., 2017). For dynamic interactions in co-cultures, sialic acid remodeling can be monitored with isotopic detection of animosugars with

glutamine (iDAWG) *in vitro* (Orlando et al., 2009) or with liposome-assisted biorthogonal reporter (LABOR) *in vivo* (Xie et al., 2016).

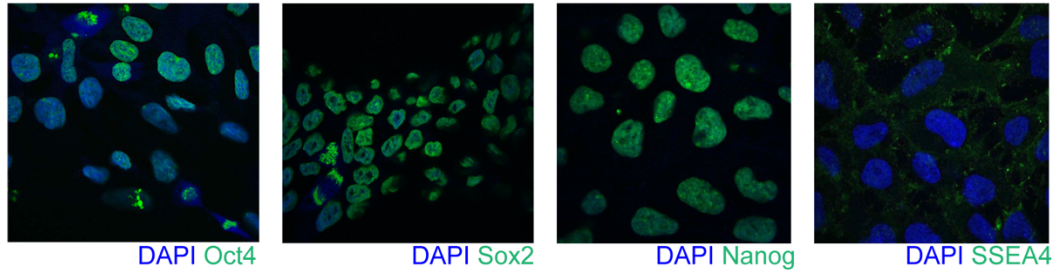
Our AD model systems have independently shown accumulation of simple glyco-ceramide precursor GSLs. Postmortem AD brain tissue has also shown perturbations in several lipid pathways through extensive quantitative lipidomics (Akyol et al., 2021). Given our observation of increased ceramide quantities relative to control, in depth lipid profiling in our model systems may reveal lipid species as putative biomarkers. Ion mobility coupled to mass spectrometry allows for separation and detection of hippocampal ganglioside species by charge state, m/z ratio, carbohydrate chain length, and degree of sialylation. Using this approach with CID MS/MS allowed researchers to discover a novel (d18:1/24:1) ceramide structure forming GD1 ganglioside species (Sarbu, Vukelic, Clemmer, & Zamfir, 2018). In-depth IM-MS analysis of glycosphingolipids from other sample origins could contribute to the currently annotated ceramide library.

To profile specific glycan binding protein interactions, glycan microarrays can be a useful tool. A chemoenzymatic method using lectin-resistant Chinese hamster ovary (CHO) cell mutant Lec2 has been used to install chemically defined glycan epitopes at the cell surface (Briard, Jiang, Moremen, Macauley, & Wu, 2018). If epitopes of interest are discovered in patient samples, they can be engineered into CHO cells to assess their affinity and engagement with physiologically relevant lectins of interest such as Siglecs. To further explore the expression of Siglec ligand epitopes, sulfated N-glycans should be characterized as well as N- and O-glycans carrying sialylated keratan sulfate (J. R. Wang et al., 2017). Keratan sulfate analysis could be completed in conjunction with proteoglycan and glycosaminoglycan characterization, as their glycosylation has been altered in affected cortical areas of neurodegenerative disorders such as Parkinson's disease (Raghunathan, Hogan, Labadorf, Myers, & Zaia, 2020). The

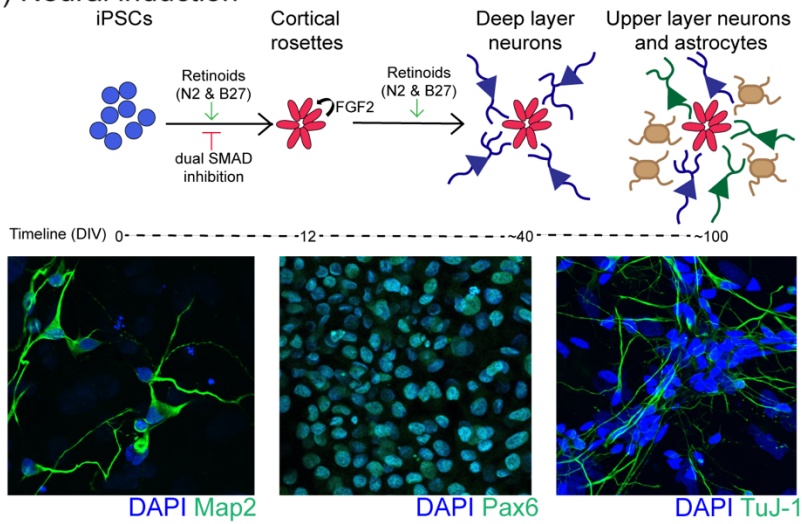
functionality and potential clinical utility of such glycan epitopes are explored in the next chapter.

## Figures

### (A) iPSCs



### (B) Neural induction



### (C) Neural induction

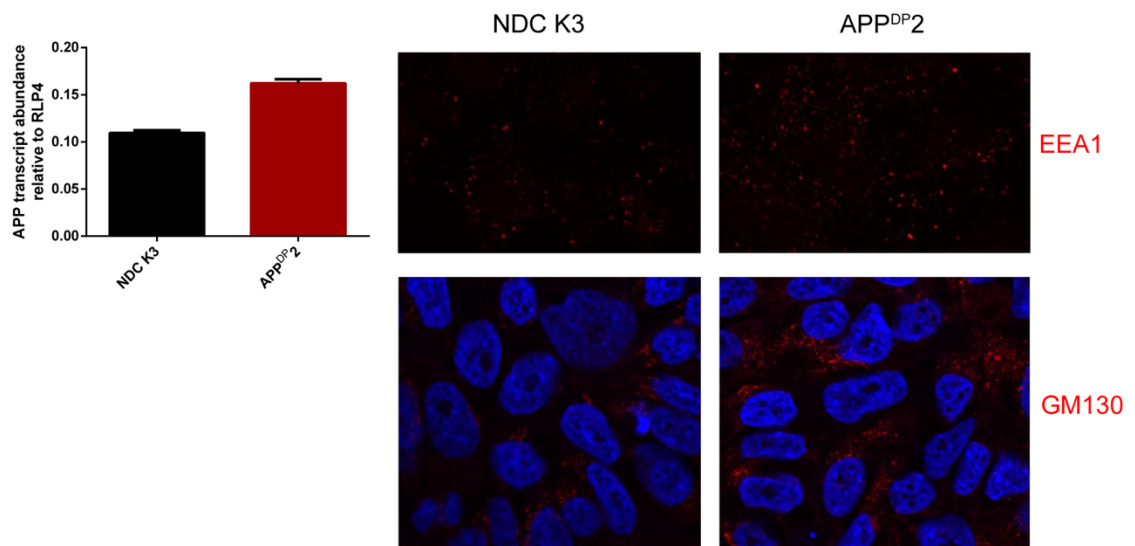
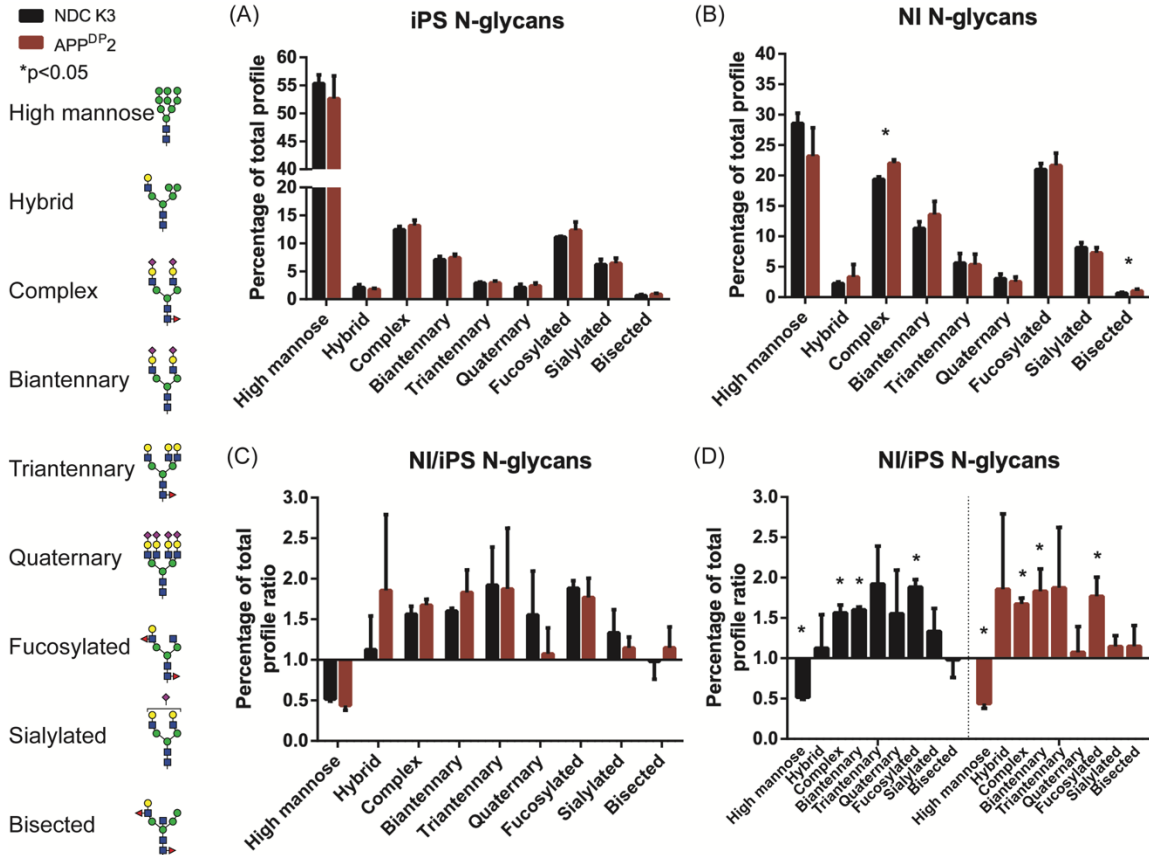


Fig. 2.1. AD patient-derived stem cells can be differentiated to cortical tissue

Patient derived iPSCs were reprogrammed retrovirally and expressed appropriate pluripotent markers (transcription factors Oct4, Sox2, Nanog and cell surface epitope SSEA4) **(A)**. Neural induction is achieved with dual SMAD inhibition using small molecules, where cortical neurons were harvested at 40 DIV and expressed neuronal markers (cytoskeletal proteins Map2, TuJ-1 and transcription factor Pax6) **(B)**. Neural cultures maintained elevated APP expression through differentiation as previously demonstrated (Israel et al., 2012) **(C)**. AD differentiated cultures also displayed interruptions in the secretory pathway with an accumulation of early endosome antigen 1 (EEA1) compartments and fragmented Golgi matrix protein 130 (GM130) which localizes with the cis-Golgi compartment **(D)**.



**Fig. 2.2. Summarized N-glycome of iPSCs and NI cultures detects differences in glycan classes upon differentiation**

Mass spectra were obtained by NSI-MS (n=3 biological replicates for each genotype and differentiation), annotated manually, and summarized based on structural features (left). iPSCs were comprised of majority high mannose structures (A), while AD NI cultures contained significantly more complex and bisected N-glycans than NDC cultures (B). No significant changes were detected by comparing NI cultures to iPSCs by genotype (C), but significant (p<0.05) changes were induced by differentiation for each sample (D).

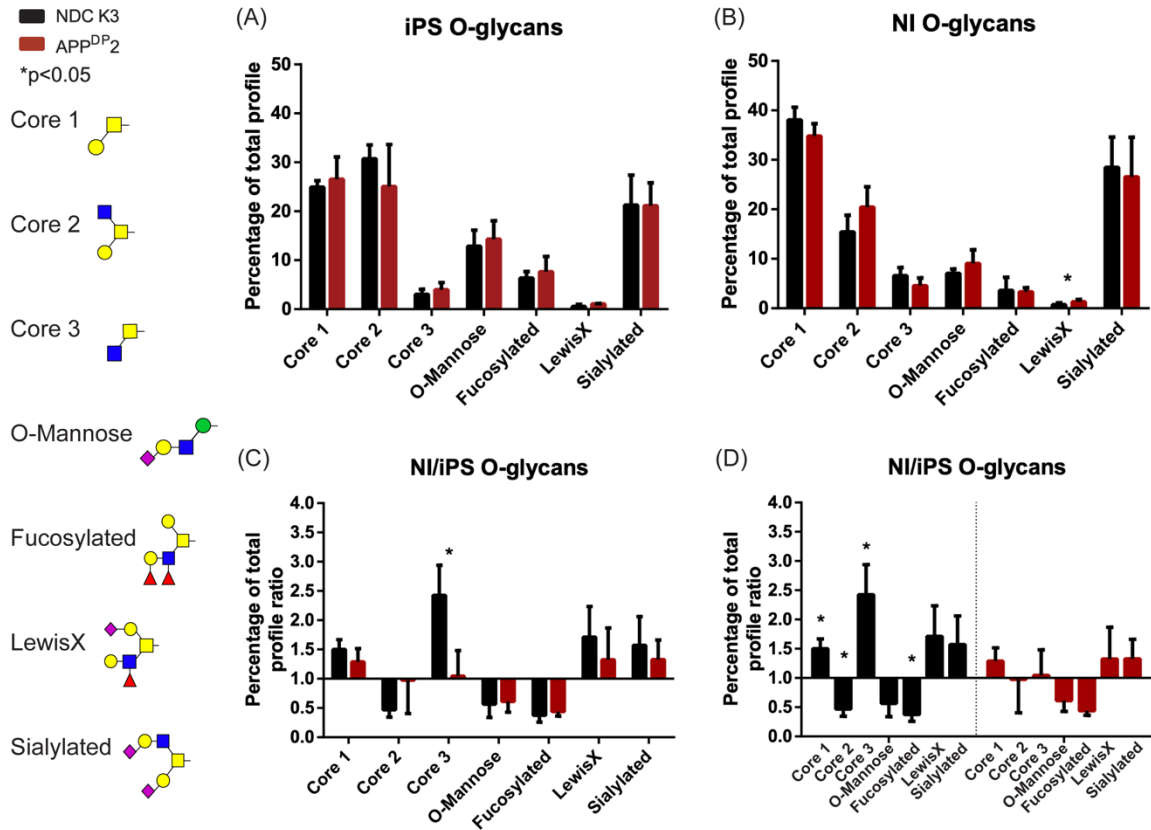


**Fig. 2.3. Summarized O-glycome of iPSC and NI cultures reveals no significant changes in AD glycans through differentiation**

Mass spectra were obtained by NSI-MS (n=3 biological replicates for each genotype and differentiation), annotated manually, and summarized based on structural features (left). iPSCs were comprised of majority Core 1 structures (A), while AD NI cultures contained significantly more LewisX O-glycans than NDC cultures (B). Comparing NI cultures to iPSCs by genotype revealed an increase (p<0.05) in Core 3 structures in NDC vs. AD (C), where differentiation to neural fate generated several significant changes in NDC cultures but not in AD (D).

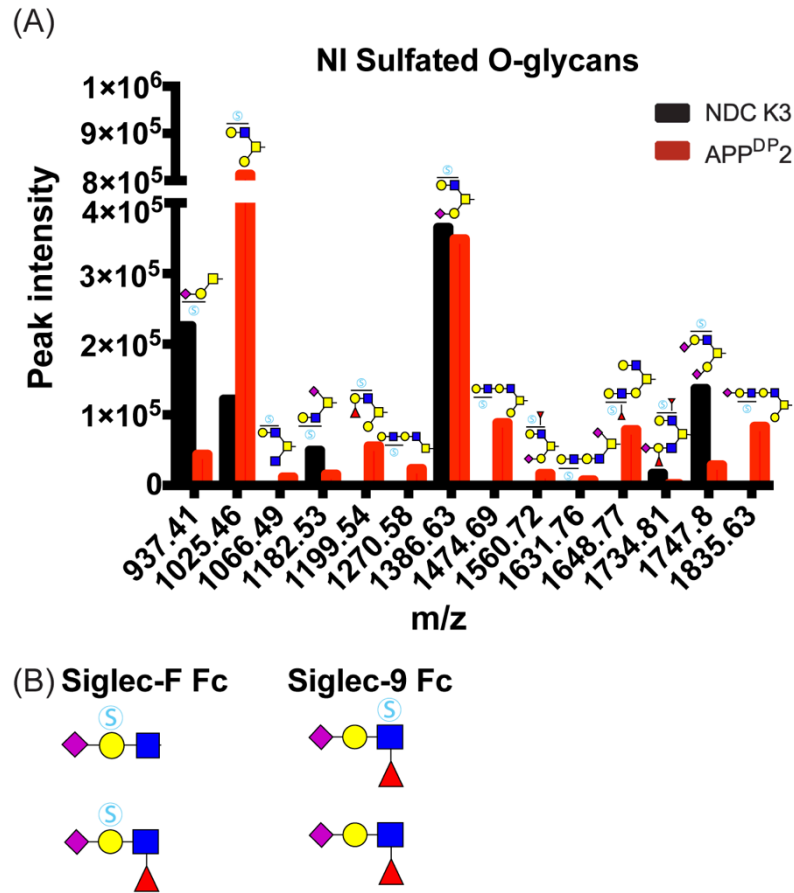


**Fig. 2.4. AD NI cultures incorporated greater diversity of sulfated O-glycan structures**

Mass spectra were obtained by negative ion mode of NSI-MS and annotated manually. Several additional sulfated structures were detected in AD NI cultures relative to NDC (A). Binding of human Fc chimeras of Siglec-F and -9 to the Consortium for Functional Glycomics array derived from (Yu et al., 2017). Siglec Fc recombinant proteins were overlaid on microarray v5.1 containing 610 glycans and epitopes. Binding was detected with fluorescently labeled secondary antibody. Preferential epitopes (>60% binding) are illustrated here (B).

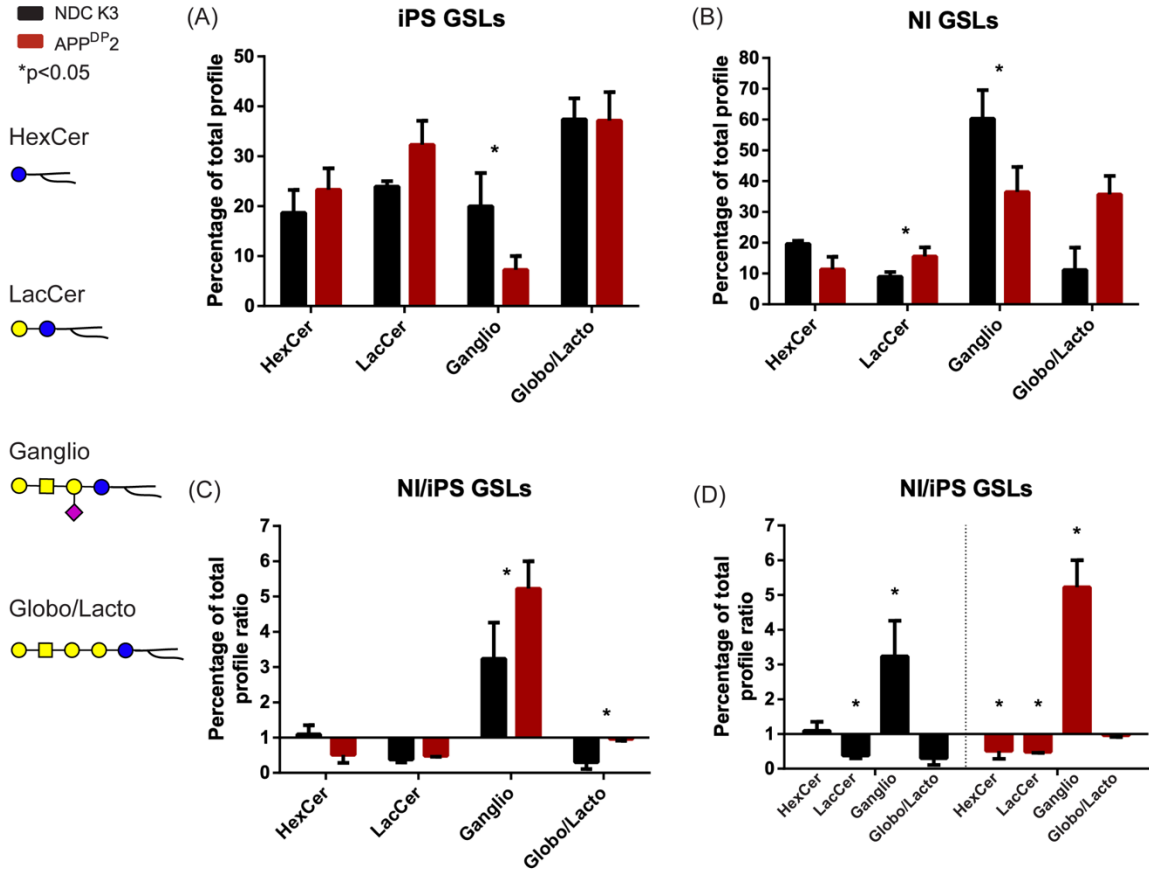


**Fig. 2.5. Summarized GSL profiles of iPSCs and NI cultures detects subtle differences in GSL biosynthesis**

Mass spectra were obtained by NSI-MS (n=3 biological replicates for each genotype and differentiation), annotated manually, and summarized based on structural features of their glycan epitopes (left). Ceramide compositions are not depicted here. NI cultures shifted to majority ganglioside composition (B), where both genotypes had a significant (p<0.05) increase in the ratio of gangliosides present in iPSCs vs. NI cultures (D). AD NI cultures demonstrated a greater increase than NDC (C).

## References

- Akasaka-Manyá, K., Manyá, H., Sakurai, Y., Wojczyk, B. S., Kozutsumi, Y., Saito, Y., . . . Endo, T. (2010). Protective effect of N-glycan bisecting GlcNAc residues on beta-amyloid production in Alzheimer's disease. *Glycobiology*, *20*(1), 99-106.  
doi:10.1093/glycob/cwp152
- Akyol, S., Ugur, Z., Yilmaz, A., Ustun, I., Gorti, S. K. K., Oh, K., . . . Graham, S. F. (2021). Lipid Profiling of Alzheimer's Disease Brain Highlights Enrichment in Glycerol(phospho)lipid, and Sphingolipid Metabolism. *Cells*, *10*(10).  
doi:10.3390/cells10102591
- Aoki, K., Perlman, M., Lim, J. M., Cantu, R., Wells, L., & Tiemeyer, M. (2007). Dynamic developmental elaboration of N-linked glycan complexity in the *Drosophila melanogaster* embryo. *J Biol Chem*, *282*(12), 9127-9142.  
doi:10.1074/jbc.M606711200
- Aoki, K., Porterfield, M., Lee, S. S., Dong, B., Nguyen, K., McGlamry, K. H., & Tiemeyer, M. (2008). The diversity of O-linked glycans expressed during *Drosophila melanogaster* development reflects stage- and tissue-specific requirements for cell signaling. *J Biol Chem*, *283*(44), 30385-30400. doi:10.1074/jbc.M804925200
- Boccuto, L., Aoki, K., Flanagan-Steet, H., Chen, C. F., Fan, X., Bartel, F., . . . Schwartz, C. E. (2014). A mutation in a ganglioside biosynthetic enzyme, ST3GAL5, results in salt & pepper syndrome, a neurocutaneous disorder with altered glycolipid and glycoprotein glycosylation. *Hum Mol Genet*, *23*(2), 418-433.  
doi:10.1093/hmg/ddt434
- Bodas, M., Min, T., & Vij, N. (2015). Lactosylceramide-accumulation in lipid-rafts mediate aberrant-autophagy, inflammation and apoptosis in cigarette smoke induced emphysema. *Apoptosis*, *20*(5), 725-739. doi:10.1007/s10495-015-1098-0

- Briard, J. G., Jiang, H., Moremen, K. W., Macauley, M. S., & Wu, P. (2018). Cell-based glycan arrays for probing glycan-glycan binding protein interactions. *Nat Commun*, 9(1), 880. doi:10.1038/s41467-018-03245-5
- Cebecauer, M., Hof, M., & Amaro, M. (2017). Impact of GM1 on Membrane-Mediated Aggregation/Oligomerization of beta-Amyloid: Unifying View. *Biophys J*, 113(6), 1194-1199. doi:10.1016/j.bpj.2017.03.009
- Chambers, S. M., Fasano, C. A., Papapetrou, E. P., Tomishima, M., Sadelain, M., & Studer, L. (2009). Highly efficient neural conversion of human ES and iPS cells by dual inhibition of SMAD signaling. *Nat Biotechnol*, 27(3), 275-280. doi:10.1038/nbt.1529
- Chen, Z., Yu, Q., Yu, Q., Johnson, J., Shipman, R., Zhong, X., . . . Li, L. (2021). In-depth Site-specific Analysis of N-glycoproteome in Human Cerebrospinal Fluid and Glycosylation Landscape Changes in Alzheimer's Disease. *Mol Cell Proteomics*, 20, 100081. doi:10.1016/j.mcpro.2021.100081
- Frenkel-Pinter, M., Shmueli, M. D., Raz, C., Yanku, M., Zilberzwige, S., Gazit, E., & Segal, D. (2017). Interplay between protein glycosylation pathways in Alzheimer's disease. *Sci Adv*, 3(9), e1601576. doi:10.1126/sciadv.1601576
- Gaunitz, S., Tjernberg, L. O., & Schedin-Weiss, S. (2021). What Can N-glycomics and N-glycoproteomics of Cerebrospinal Fluid Tell Us about Alzheimer Disease? *Biomolecules*, 11(6). doi:10.3390/biom11060858
- Gizaw, S. T., Ohashi, T., Tanaka, M., Hinou, H., & Nishimura, S. (2016). Glycoblotting method allows for rapid and efficient glycome profiling of human Alzheimer's disease brain, serum and cerebrospinal fluid towards potential biomarker discovery. *Biochim Biophys Acta*, 1860(8), 1716-1727. doi:10.1016/j.bbagen.2016.03.009

- Gonzalez-Gil, A., Porell, R. N., Fernandes, S. M., Wei, Y., Yu, H., Carroll, D. J., . . . Schnaar, R. L. (2018). Sialylated keratan sulfate proteoglycans are Siglec-8 ligands in human airways. *Glycobiology*, *28*(10), 786-801. doi:10.1093/glycob/cwy057
- Hirano-Sakamaki, W., Sugiyama, E., Hayasaka, T., Ravid, R., Setou, M., & Taki, T. (2015). Alzheimer's disease is associated with disordered localization of ganglioside GM1 molecular species in the human dentate gyrus. *FEBS Lett*, *589*(23), 3611-3616. doi:10.1016/j.febslet.2015.09.033
- Hong, S., Ostaszewski, B. L., Yang, T., O'Malley, T. T., Jin, M., Yanagisawa, K., . . . Selkoe, D. J. (2014). Soluble Abeta oligomers are rapidly sequestered from brain ISF in vivo and bind GM1 ganglioside on cellular membranes. *Neuron*, *82*(2), 308-319. doi:10.1016/j.neuron.2014.02.027
- Israel, M. A., Yuan, S. H., Bardy, C., Reyna, S. M., Mu, Y., Herrera, C., . . . Goldstein, L. S. (2012). Probing sporadic and familial Alzheimer's disease using induced pluripotent stem cells. *Nature*, *482*(7384), 216-220. doi:10.1038/nature10821
- Johnson, E. C. B., Carter, E. K., Dammer, E. B., Duong, D. M., Gerasimov, E. S., Liu, Y., . . . Seyfried, N. T. (2022). Large-scale deep multi-layer analysis of Alzheimer's disease brain reveals strong proteomic disease-related changes not observed at the RNA level. *Nat Neurosci*, *25*(2), 213-225. doi:10.1038/s41593-021-00999-y
- Jung, J., Enterina, J. R., Bui, D. T., Mozaneh, F., Lin, P. H., Nitin, . . . Macauley, M. S. (2021). Carbohydrate Sulfation As a Mechanism for Fine-Tuning Siglec Ligands. *ACS Chem Biol*, *16*(11), 2673-2689. doi:10.1021/acscchembio.1c00501
- Kirwan, P., Turner-Bridger, B., Peter, M., Momoh, A., Arambepola, D., Robinson, H. P., & Livesey, F. J. (2015). Development and function of human cerebral cortex neural networks from pluripotent stem cells in vitro. *Development*, *142*(18), 3178-3187. doi:10.1242/dev.123851

- Kurz, S., Aoki, K., Jin, C., Karlsson, N. G., Tiemeyer, M., Wilson, I. B., & Paschinger, K. (2015). Targeted release and fractionation reveal glucuronylated and sulphated N- and O-glycans in larvae of dipteran insects. *J Proteomics*, *126*, 172-188. doi:10.1016/j.jprot.2015.05.030
- Kurz, S., Sheikh, M. O., Lu, S., Wells, L., & Tiemeyer, M. (2021). Separation and Identification of Permethylated Glycan Isomers by Reversed Phase NanoLC-NSI-MS(n). *Mol Cell Proteomics*, *20*, 100045. doi:10.1074/mcp.RA120.002266
- Lee, J., Ha, S., Kim, M., Kim, S. W., Yun, J., Ozcan, S., . . . An, H. J. (2020). Spatial and temporal diversity of glycome expression in mammalian brain. *Proc Natl Acad Sci U S A*, *117*(46), 28743-28753. doi:10.1073/pnas.2014207117
- Liu, F., Zaidi, T., Iqbal, K., Grundke-Iqbal, I., Merkle, R. K., & Gong, C. X. (2002). Role of glycosylation in hyperphosphorylation of tau in Alzheimer's disease. *FEBS Lett*, *512*(1-3), 101-106. doi:10.1016/s0014-5793(02)02228-7
- McDowell, C. T., Klamer, Z., Hall, J., West, C. A., Wisniewski, L., Powers, T. W., . . . Drake, R. R. (2021). Imaging Mass Spectrometry and Lectin Analysis of N-Linked Glycans in Carbohydrate Antigen-Defined Pancreatic Cancer Tissues. *Mol Cell Proteomics*, *20*, 100012. doi:10.1074/mcp.RA120.002256
- McNaughton, D., Knight, W., Guerreiro, R., Ryan, N., Lowe, J., Poulter, M., . . . Mead, S. (2012). Duplication of amyloid precursor protein (APP), but not prion protein (PRNP) gene is a significant cause of early onset dementia in a large UK series. *Neurobiol Aging*, *33*(2), 426 e413-421. doi:10.1016/j.neurobiolaging.2010.10.010
- Mehta, N., Porterfield, M., Struwe, W. B., Heiss, C., Azadi, P., Rudd, P. M., . . . Aoki, K. (2016). Mass Spectrometric Quantification of N-Linked Glycans by Reference to Exogenous Standards. *J Proteome Res*, *15*(9), 2969-2980. doi:10.1021/acs.jproteome.6b00132

- Menendez, L., Kulik, M. J., Page, A. T., Park, S. S., Lauderdale, J. D., Cunningham, M. L., & Dalton, S. (2013). Directed differentiation of human pluripotent cells to neural crest stem cells. *Nat Protoc*, *8*(1), 203-212. doi:10.1038/nprot.2012.156
- Michelle Dookwah, S. K. W., Mayumi Ishihara, Seok-Ho Yu, Heidi Ulrichs, Michael J. Kulik, Nadja Zeltner, Stephen Dalton, Kevin A. Strauss, Kazuhiro Aoki, Richard Steet, Michael Tiemeyer. (2021). Neural-specific alterations in glycosphingolipid biosynthesis and cell signaling associated with two human ganglioside GM3 Synthase Deficiency variants. *bioRxiv*.  
doi:<https://doi.org/10.1101/2021.07.29.454399>
- Mizuno, S., Ogishima, S., Kitatani, K., Kikuchi, M., Tanaka, H., Yaegashi, N., & Nakaya, J. (2016). Network Analysis of a Comprehensive Knowledge Repository Reveals a Dual Role for Ceramide in Alzheimer's Disease. *PLoS One*, *11*(2), e0148431. doi:10.1371/journal.pone.0148431
- Nagamine, S., Yamazaki, T., Makioka, K., Fujita, Y., Ikeda, M., Takatama, M., . . . Ikeda, Y. (2016). Hypersialylation is a common feature of neurofibrillary tangles and granulovacuolar degenerations in Alzheimer's disease and tauopathy brains. *Neuropathology*, *36*(4), 333-345. doi:10.1111/neup.12277
- Noel, A., Ingrand, S., & Barrier, L. (2017). Ganglioside and related-sphingolipid profiles are altered in a cellular model of Alzheimer's disease. *Biochimie*, *137*, 158-164. doi:10.1016/j.biochi.2017.03.019
- Orlando, R., Lim, J. M., Atwood, J. A., 3rd, Angel, P. M., Fang, M., Aoki, K., . . . Wells, L. (2009). IDAWG: Metabolic incorporation of stable isotope labels for quantitative glycomics of cultured cells. *J Proteome Res*, *8*(8), 3816-3823. doi:10.1021/pr8010028

- Palmigiano, A., Barone, R., Sturiale, L., Sanfilippo, C., Bua, R. O., Romeo, D. A., . . . Garozzo, D. (2016). CSF N-glycoproteomics for early diagnosis in Alzheimer's disease. *J Proteomics*, *131*, 29-37. doi:10.1016/j.jprot.2015.10.006
- Raghunathan, R., Hogan, J. D., Labadorf, A., Myers, R. H., & Zaia, J. (2020). A glycomics and proteomics study of aging and Parkinson's disease in human brain. *Sci Rep*, *10*(1), 12804. doi:10.1038/s41598-020-69480-3
- Saljo, K., Barone, A., Vizlin-Hodzic, D., Johansson, B. R., Breimer, M. E., Funa, K., & Teneberg, S. (2017). Comparison of the glycosphingolipids of human-induced pluripotent stem cells and human embryonic stem cells. *Glycobiology*, *27*(4), 291-305. doi:10.1093/glycob/cww125
- Sarbu, M., Vukelic, Z., Clemmer, D. E., & Zamfir, A. D. (2018). Ion mobility mass spectrometry provides novel insights into the expression and structure of gangliosides in the normal adult human hippocampus. *Analyst*, *143*(21), 5234-5246. doi:10.1039/c8an01118d
- Shi, Y., Kirwan, P., & Livesey, F. J. (2012). Directed differentiation of human pluripotent stem cells to cerebral cortex neurons and neural networks. *Nat Protoc*, *7*(10), 1836-1846. doi:10.1038/nprot.2012.116
- Si-Tayeb, K., Noto, F. K., Sepac, A., Sedlic, F., Bosnjak, Z. J., Lough, J. W., & Duncan, S. A. (2010). Generation of human induced pluripotent stem cells by simple transient transfection of plasmid DNA encoding reprogramming factors. *BMC Dev Biol*, *10*, 81. doi:10.1186/1471-213X-10-81
- Slegers, K., Brouwers, N., Gijssels, I., Theuns, J., Goossens, D., Wauters, J., . . . Van Broeckhoven, C. (2006). APP duplication is sufficient to cause early onset Alzheimer's dementia with cerebral amyloid angiopathy. *Brain*, *129*(Pt 11), 2977-2983. doi:10.1093/brain/awl203

- Stanley, P., Schachter, H., & Taniguchi, N. (2009). N-Glycans. In nd, A. Varki, R. D. Cummings, J. D. Esko, H. H. Freeze, P. Stanley, C. R. Bertozzi, G. W. Hart, & M. E. Etzler (Eds.), *Essentials of Glycobiology*. Cold Spring Harbor (NY).
- Wang, J. R., Gao, W. N., Grimm, R., Jiang, S., Liang, Y., Ye, H., . . . Jiang, Z. H. (2017). A method to identify trace sulfated IgG N-glycans as biomarkers for rheumatoid arthritis. *Nat Commun*, *8*(1), 631. doi:10.1038/s41467-017-00662-w
- Williams, S. E., Noel, M., Lehoux, S., Cetinbas, M., Xavier, R. J., Sadreyev, R., . . . Mealer, R. G. (2020). The restricted nature of protein glycosylation in the mammalian brain. *bioRxiv*, 2020.2010.2001.322537. doi:10.1101/2020.10.01.322537
- Williams, S. E., Noel, M., Lehoux, S., Cetinbas, M., Xavier, R. J., Sadreyev, R. I., . . . Mealer, R. G. (2022). Mammalian brain glycoproteins exhibit diminished glycan complexity compared to other tissues. *Nat Commun*, *13*(1), 275. doi:10.1038/s41467-021-27781-9
- Xie, R., Dong, L., Du, Y., Zhu, Y., Hua, R., Zhang, C., & Chen, X. (2016). In vivo metabolic labeling of sialoglycans in the mouse brain by using a liposome-assisted bioorthogonal reporter strategy. *Proc Natl Acad Sci U S A*, *113*(19), 5173-5178. doi:10.1073/pnas.1516524113
- Yanagisawa, K., & Ihara, Y. (1998). GM1 ganglioside-bound amyloid beta-protein in Alzheimer's disease brain. *Neurobiol Aging*, *19*(1 Suppl), S65-67. doi:10.1016/s0197-4580(98)00032-3
- Yu, H., Gonzalez-Gil, A., Wei, Y., Fernandes, S. M., Porell, R. N., Vajn, K., . . . Schnaar, R. L. (2017). Siglec-8 and Siglec-9 binding specificities and endogenous airway ligand distributions and properties. *Glycobiology*, *27*(7), 657-668. doi:10.1093/glycob/cwx026

Yuzwa, S. A., Shan, X., Macauley, M. S., Clark, T., Skorobogatko, Y., Vosseller, K., & Vocadlo, D. J. (2012). Increasing O-GlcNAc slows neurodegeneration and stabilizes tau against aggregation. *Nat Chem Biol*, 8(4), 393-399.

doi:10.1038/nchembio.797

Zhang, Q., Ma, C., Chin, L. S., & Li, L. (2020). Integrative glycoproteomics reveals protein N-glycosylation aberrations and glycoproteomic network alterations in Alzheimer's disease. *Sci Adv*, 6(40). doi:10.1126/sciadv.abc5802

CHAPTER THREE

SIGLEC LIGAND EXPRESSION AT THE CHOROID PLEXUS MODULATES  
NEUROINFLAMMATION IN ALZHEIMER'S DISEASE

---

Adapted from:

**Rosenbalm KE**, Nix DB, Paschall AV, Bakshi B, Fernandes SM, Schroten H, Ishikawa H, Avci FY, Tiemeyer M. Siglec ligand expression at the choroid plexus modulates neuroinflammation in Alzheimer's disease (2022) To be submitted to *J Neurosci*

## Abstract

The pathology of Alzheimer's disease (AD) is complex and involves incompletely understood inflammatory responses. The contributions of inflammatory cells, either resident in the brain (microglia) or recruited from peripheral sources (monocytes/macrophages), are an emerging interest with regard to the initiation and progression of AD. The choroid plexus (CP), which comprises an important part of the interface between the peripheral blood and the cerebrospinal fluid, functions as an immune gateway in the brain and has been proposed to regulate trafficking, activation, and differentiation of inflammatory cells. In a mouse model for aggressive familial AD, we observed upregulated expression of ligands for Siglec-F on CP epithelial cells. Siglec-F, like other members of the Siglec family, binds sialylated glycans to modulate innate and adaptive immune responses in many inflammatory contexts. To explore the role of Siglec ligand expression in normal human CP and in human neurodegenerative disease progression, we have undertaken targeted glycomic and glycoproteomic analysis of Siglec-F and Siglec-9 counterreceptors expressed by choroid plexus papilloma cells (HIBCPP) as well as by 3-D choroid plexus tissue derived from patient induced pluripotent stem cells (choroid plexus organoids, which we call chorganoids). Specific endoglycosidase digestion and orthogonal biochemical analysis indicates that human CP cells present keratan sulfate ligands for Siglec-9, as well as structurally related ligands for Siglec-F, on polypeptide backbones including low-density lipoprotein receptor-related protein 1 (LRP1) and galectin-3 binding protein/Mac-2 binding protein/90k tumor associated antigen (Gal-3BP). Gal-3BP ligands for Siglec-9 purified from HIBCPP cell media induce inflammatory cell responses using a murine bone marrow derived hematopoietic cell-based screening platform. The identification of these Siglec ligands in

a unique tissue setting presents opportunities for investigating the response of inflammatory cells to disease-related glycan expression.

### **Key words**

glycosylation, Alzheimer's disease, choroid plexus, Siglec, innate immunity, macrophage, toll-like receptor

## **Introduction**

In Alzheimer's disease, A $\beta$  plaques, derived from enzymatic processing of amyloid precursor protein (APP), along with neurofibrillary tangles (NFTs), derived from abnormal accumulations of hyperphosphorylated tau protein, induce inflammation and cell death through their interactions with toll-like receptors and immune cells (Itagaki, McGeer, Akiyama, Zhu, & Selkoe, 1989). Immune surveillance of neural tissue, whether by cellular components of the innate or adaptive immune systems, can significantly influence brain function through targeted cell interactions, cytokine release, and altered blood-brain barrier integrity (Ransohoff, Kivisakk, & Kidd, 2003). Accordingly, the role of inflammation in the pathophysiology of degenerative brain disorders is the subject of increased attention.

Neuroinflammation is a crucial mechanism of progression in Alzheimer's disease where immuno-regulatory molecules are involved in pathogenesis. Among the regulators, Siglecs (sialic acid-binding immunoglobulin-like lectins) are cell-surface transmembrane proteins expressed on immune cells that induce signals to inhibit or to activate inflammation. Cellular expression of Siglec receptors and subsequent engagement of their recognized glycan ligands imparts various cell-type specific consequences, including induction of apoptosis, sequestration of signaling molecules, or endocytosis of extracellular signals (Bochner, 2009a; Kawasaki, Rademacher, & Paulson, 2010; Kiwamoto et al., 2015a; McMillan, Sharma, Richards, Hegde, & Crocker, 2014; Tateno et al., 2007; Vyas et al., 2002). This modulatory activity of Siglec receptors suggests that the

brain glycome, which includes glycan ligands that engage Siglecs, may influence the inflammatory status of the tissue.

To assess the role of glycosylation in AD and its influence on neuroinflammation, we have characterized glycan ligands for murine Siglec-F and human Siglec-9 in brain tissue. We discovered the ligands are expressed in a punctate pattern on the epithelium of the choroid plexus (CP), where their density appears to be increased at the 5xFAD mouse CP relative to WT. Siglec-F and -9 receptors are expressed on monocytes and macrophages as well as T cells, neutrophils, and other cell types (Macauley et al., 2014), which can infiltrate the parenchyma via the blood-CSF barrier. The activation of these Siglecs is commonly associated with inhibition of an inflammatory reaction (J. Q. Zhang, Nicoll, Jones, & Crocker, 2000; M. Zhang et al., 2007). Here, we demonstrate the Siglec-F ligand and its protein carrier expressed by human CP culture induce an inflammatory phenotype in murine leukocytes. We have also illustrated that Siglec ligand expression can be modulated in response to TLR signaling and the inflammatory climate of surrounding tissues. Thus, we propose that glycan binding to Siglecs on extravasating macrophages at the CP can modulate their inflammatory status and provides a potential avenue for therapeutic intervention in AD.

## **Experimental procedures**

### **Reagents**

Reagents are from Sigma Aldrich unless otherwise noted. All antibodies and blocking buffer [4% (w/v) BSA, 10% (v/v) Goat Serum, 0.12 mg/mL unconjugated goat anti-mouse IgG (Jackson Labs)] were filtered through 0.2  $\mu$ m SFCA filters (Corning) prior to IF. Siglec-F Fc (R&D Systems) or Siglec-9 Fc (Dr. Ronald Schnaar) was pre-complexed to goat anti-human HRP for immunohistochemistry (IHC) and WB or goat anti-human

AlexaFluor for immunofluorescence (IF) imaging. LRP1  $\alpha$ -chain (Abcam 8G1) was used under non-denaturing conditions, LRP1  $\beta$ -chain (Abcam), Iba1 (Wako), Prealbumin/TTR (Dako), AQP1 (Santa Cruz), CD206 (Abcam), SNA (Roche), MAA (Roche), Gal-3BP (Bioss), ZO-1 (Invitrogen), Actin (Santa Cruz), Otx2 (R&D Systems) were antibodies used in this study. Samples and slides were digested with 1 $\mu$ L of 44.5U/ $\mu$ L *Vibrio cholera* sialidase (Dr. Ronald Schnaar) in 0.1 M PIPES 4mM CaCl<sub>2</sub> pH 6.0 buffer prior to immunoassay.  $\alpha$ 2,3- specific sialidase (Prozyme) was used according to manufacturer's recommendation. PNGaseF (Dr. Kelly Moremen) digestion of samples and slides was performed in 0.1 M sodium phosphate pH 7.5 buffer for a minimum of 4 hrs. Keratanase I (Dr. Ronald Schnaar) digestion was completed in 100 mM sodium phosphate pH 7.4 at 37°C for the desired time using 500 mU/mL of enzyme activity.

## **Mice**

B6SJLF1/J wild-type mice and 5xFAD transgenic mice (B6SJL-Tg(APP<sup>Sw</sup>FILon, PSEN1\*<sup>M146L</sup>\*<sup>L286V</sup>)6799Vas/J) were used for our experiments (Jackson Laboratory MMRRCC strain #034840). Mice were anesthetized with CO<sub>2</sub> and decapitated. Brains were harvested and washed with ice-cold 1x PBS; the olfactory bulb and cerebellum were removed prior to separating hemispheres. Eight to ten week-old mice were used for mass spectrometry, quantitative RT-PCR, and protein purification; each hemisphere was separately snap frozen in liquid nitrogen before storage at -80°C. Sixteen week-old mice were used for IHC and incubated in formaldehyde overnight prior to mounting in wax or sucrose gradient incubation and storage at 4°C.

## **Cells**

Induced pluripotent stem cells (iPSCs) were cultured as previously described (Michelle Dookwah, 2021). K3 NCD iPSCs (Si-Tayeb et al., 2010) and APP<sup>DP2</sup> iPSCs (Israel et al., 2012) (Coriell GM24675) were cultured in HAIF-based media (Menendez et

al., 2013). Human malignant choroid plexus cell line (HIBCPP) (Ishiwata et al., 2005) was obtained from Dr. Christian Schwerk and cultured as previously described in medium with or without serum (Dinner et al., 2016). Raw264.7 cells were grown in DMEM with 10% FBS. Phagocytosis assays were completed in complete growth media with EZ-Red *E. coli* fluorescent particles (3  $\mu$ L/well) (BioVision) for 4 hr.

### **Chorganoid differentiation**

CP tissue was differentiated as described previously (Sakaguchi et al., 2015). Dissociated iPSCs (9000 cells) were aggregated with inversion via hanging drop method. After 1 day, they were each transferred to one well of a 96 well ultra-low adhesion U-bottom plate. Cells were cultured using serum-free embryoid body-like culture with quick aggregation (SFEBq) method for an additional 17 days in the presence of IWR-1-*endo* (Wnt inhibitor), SB431542 (TGF $\beta$  inhibitor) and Y-27632 (ROCK inhibitor).

After 18 days, aggregates were transferred to non-adhesive culture dish and further cultured in suspension in the presence of N-2 supplement, CHIR 99021 (GSK3 inhibitor) and BMP4 (Watanabe et al., 2016). Generation of choroid plexus tissue was validated by IHC.

### **Immunohistochemistry**

Brains stored in 30% sucrose (w/v) were frozen in Optimal Cutting Temperature compound (Tissue-Tek) prior to sectioning on a microtome-cryostat. The 20- $\mu$ m sections were adhered onto SuperFrost Gold Plus (Fisher Scientific) and placed at -20°C overnight before use. For immunofluorescent staining, slides were placed at RT for 30 min prior to post-fixation in acetone. Sections were hydrated in 1x PBS and permeabilized in PBS containing 0.1% Triton X-100 (v/v). Prolong Diamond antifade mountant (ThermoFisher) was allowed to cure overnight in the dark before sealing coverslips. Brains mounted in wax were sectioned at 5 $\mu$ m into ribbons and floated in a water bath to adhere onto

SuperFrost Gold Plus slides and kept at RT overnight before use. For IHC, sections were hydrated in Xylene (3x), 100% EtOH, 95% EtOH (v/v), and 70% EtOH (v/v). Antigen retrieval was performed using 10 mM sodium citrate buffer pH 6.0 for 20 min at 100°C. Sections were washed in 1x PBS and permeabilized in PBS containing 0.1% Triton X-100 prior to incubation with Dual Endogenous Enzyme Blocker (DAKO) for 10 min at RT. Sections were stained with 3,3'-Diaminobenzidine (DAB) and mounted in 70% Glycerol (v/v).

Chorganoids were fixed with 2% glutaraldehyde in 0.1M phosphate buffer for 20 min. Fixative was aspirated, and chorganoids were resuspended in 30% sucrose (w/v) overnight. Spheres were placed in brain paste in 30% sucrose or directly into freezing medium in a cryomold. Molds were snap frozen with dry ice and stored at -80°C until they were sectioned on Leica cryostat.

HIBCPP cells were grown on round glass coverslips (Fisher Scientific, 12-545) in a 12 well plate to desired confluency. Cells were washed with PBS and fixed for 20 minutes at room temperature with 4% paraformaldehyde. After washing with PBS, cells were blocked with 4% BSA (w/v), 10% serum (v/v) in PBS-0.1% Triton X-100 (v/v). Prolong Diamond mounting medium (Invitrogen, P36970) cured overnight before coverslips were sealed. Images were obtained using Olympus FV1200 confocal microscope, and images were normalized and prepared in Slidebook 5.0 x64 software.

### **Immunoprecipitation and LC-MS/MS**

One hundred µg of whole brain lysate was incubated with 20 µL of 50% slurry of protein A/G beads (Pierce) for 1hr at 4°C to remove all non-specific interactions. For LRP1 immunoprecipitation (IP), cleared lysate was added to an Amicon 10K spin filter (Thermo) and buffer exchanged to 50 mM ammonium bicarbonate prior to overnight incubation with PNGaseF at 37°C. Digested lysate was washed with PBS and collected by inversion.

Lysate was incubated with 5µg of antibody or fusion protein overnight at 4°C before combining with fresh protein A/G beads and incubated for 1hr at room temperature. After incubation, beads were washed with PBS and boiled in Laemmli buffer (Bio-Rad) to release bound protein. For fusion protein overlays samples were separated using SDS-PAGE prior to transfer to PVDF. For proteomic identification, eluted protein was separated using SDS-PAGE and visualized using G250-CBB prior to excision. Excised protein bands were then reduced, carbamidomethylated, and digested with modified trypsin (Promega) overnight at 37°C. Peptides were purified using Sep-Pak C18 cartridge (Waters) chromatography and dried in a SpeedVac prior. LC-MS/MS analysis was performed on an LTQ-Orbitrap Discovery equipped with a nanospray ion source by a data-dependent scan. Alternatively, samples were analyzed using Orbitrap Fusion or Orbitrap Fusion Lumos (Thermo Fisher). Obtained data were analyzed with Proteome Discoverer (Thermo Fisher) 1.4 using Sequest and a false discovery rate of 0.1% or Byonic (Protein Metrics). Post processing was performed using ProteoIQ (Premier Biosoft).

### **Anion exchange chromatography**

Keratan sulfate-modified ligand was purified as previously described (Holland, Meehan, Redmond, & Dawkins, 2004). Conditioned HIBCPP media was resuspended in five volumes of 7M urea, 0.1% CHAPS (w/v), 50mM sodium acetate pH 6.0 (UCA). A 5mL column of Sepharose Q Fast Flow (Sigma Aldrich) was equilibrated with UCA, and the sample was loaded a total of 3X. The column was washed with UCA and eluted in a step gradient of UCA containing 5mM, 50mM, 500mM NaCl. Elutions were buffer exchanged into 50mM sodium acetate pH6.0 and concentrated with 30kD MW spin filter (Amicon).

### **Periodate treatment**

Mild periodate treatment of ligand was completed in phosphate buffer pH 7.4 containing 2mM NaIO<sub>4</sub> for 30 minutes at room temperature in the dark (Razi & Varki,

1999). The reaction was quenched with 20% glycerol, where vehicle treatment included periodate and glycerol without ligand.

## **ELISA**

Ninety-six well polystyrene plates (Thermo Fisher Scientific) were coated with antibody diluted in sodium phosphate well coating buffer. Wells were blocked with BSA Fraction V (Calbiochem) in sucrose buffer before samples were incubated. Secondary antibody-AP signal was detected with pNPP substrate (Sigma Aldrich) and data was acquired at 405nm.

## **Western Blotting**

Whole brains were weighed and homogenized in 10 volumes of 0.32 M sucrose using a Potter-Elvehjem pestle. Homogenate was centrifuged at 1,000g, 4°C for 10 min. Supernatant was transferred into a separate tube and centrifuged again at 20,000g, 4°C for 30 min. Resulting pellet was suspended in 1 volume of 0.32 M sucrose and homogenized a second time using the Potter-Elvehjem pestle before adding 10 volumes of 5 mM sodium phosphate buffer and centrifuging at 20,000g, 4°C for 30 min. Pellet was resuspended in 2 volumes of 0.32 M sucrose and placed at -80°C. Protein concentration was determined by BCA assay.

Confluent HIBCPP or NCC cells were cultured in medium lacking serum for 24 hr prior to collection. Pellets were obtained by scraping and rinsed with PBS. Cells were lysed in 0.5M Tris-HCl buffer with 1mM DTT and 0.5% NP-40.

## **Flow Cytometry**

C57BL/6 mice were euthanized and femoral bone marrow was collected. BMDCs were plated in 96 well culture at a seeding density of  $5 \times 10^5$  cells/mL and stimulated with 20 ng/mL of GM-CSF for six days. Ligand challenges were completed for 24 hr following

stimulation. Cells were stained in PBS with CD11b-FITC (BioLegend), CD206-FITC (BioLegend), Siglec-F-PE (BD Pharmingen), Arg-1-PE (eBioscience), CD11b-PE (BioLegend), Gr1-PECy5 (BioLegend), iNOS-APC (eBioscience), CD45-APCCy7 (BioLegend), Ghost Red 710 (Tonbo 13-0871-T100), CD38 (BD Horizon). Cells with intracellular markers were fixed and permeabilized (eBioscience 00-5523-00) prior to staining. Samples were washed and analyzed with flow cytometry CytoFLEX S (Beckman Coulter, Hialeah, Florida). Isotype control antibody-stained samples were used as negative staining controls where appropriate and single stain controls were used for compensation. Flow cytometry data was analyzed using FlowJo Single Cell Analysis software (Version 10.2. Ashland, OR). Briefly, live CD45<sup>+</sup> immune cells were gated and percentages of immune populations were derived from these gates.

## Results

### 1. Siglec-F ligand is enriched at the mouse choroid plexus

Many cell types that reside in the central nervous system (CNS) express Siglec receptors; however, the brain regions or cell types that display their ligands remain undefined. To identify Siglec ligands, we used chimeric constructs where the ectodomain of a Siglec is fused to the Fc domain of an IgG antibody for visualization (Kelm et al., 1994). Using chimeric constructs for Siglec-3, -E, and -F ligands, we probed paraffin embedded murine brain tissue sections for their glycans ligands and were unable to find significant alterations for Siglec-3 or -E ligands between WT and 5xFAD (data not shown). However, we did find substantial changes in ligands for Siglec-F, as there was more overall staining in the 5xFAD brain sections compared to WT (**Fig. 3.1C**). To ensure that all binding was sialic acid dependent, we treated the sections with pan-sialidase, and all epitope detection was lost (**Fig. 3.1B**). We also treated tissue sections with PNGaseF to

remove N-glycans, since glycomic analysis of mouse brain tissue showed broad changes in many categories of N-glycosylation (data not shown). After treatment with PNGaseF, we saw a substantial decrease in Siglec-F Fc staining, indicating that a portion of the ligand is presumably a sialylated N-linked glycan (**Fig. 3.1B**). The most striking density of staining was observed at the apical CP in 5xFAD brains compared to WT. This staining could also be found on the ependymal surface of the ventricle where the CP originates (**Fig. 3.1B**). To further describe the localization and abundance of this endogenous ligand, we used fluorescent confocal microscopy on cryosections of lateral ventricles (**Fig. 3.1D**). Apical expression of the ligand is increased ~2 fold ( $p=0.001$ ) at the 5xFAD CP when normalized to aquaporin-1 (APQ1) expression (**Fig. 3.1E**). The ligand's staining pattern is visualized as individual puncta and appears to extend into the ventricle (**Fig. 3.1D**). Altogether, we have identified the presence of a glycan ligand for Siglec-F at the CP that is upregulated in the 5xFAD model.

## **2. LRP1 is modified with Siglec-F ligand in murine brain**

The endogenous ligands for Siglec-F has been elusive and altogether different from all well-defined targets identified so far using the Consortium for Functional Glycomics (CFG) glycan binding array (Patnode et al., 2013; Tateno, Crocker, & Paulson, 2005). Proposed epitopes for Siglec-F recognition appeared to be sialylated, sulfated glycans (Yu et al., 2017). To further define the endogenous ligand in this murine model, whole brain lysates were used for western blot analysis. Binding above the 250kD marker covers a large area with a smeared appearance commonly associated with glycosylated proteins (**Fig. 3.2A**). Both WT and 5xFAD whole brain lysates demonstrated minor sensitivity towards PNGaseF digestion (**Fig. 3.2B**). To date, all reported endogenous ligands have been O-linked glycans in mucin domains (Kiwamoto et al., 2015a), suggesting a N-glycan ligand is a novel finding. To further elucidate the sialic acid linkage,

whole brain lysates were either treated with pan- or  $\alpha$ 2,3- specific sialidase prior to western blot analysis. Siglec-F Fc binding was abolished in the case of pan-sialidase treatment, whereas binding was incompletely lost after treatment with  $\alpha$ 2,3-specific sialidase, indicating the ligand is mostly comprised of  $\alpha$ 2,3-linked sialic acid residues (**Fig. 3.2B**). For validation purposes, we used the lectins MAA and SNA based on their preferences to recognize  $\alpha$ 2,3- and  $\alpha$ 2,6-linked sialic acid residues respectively (data not shown). The linkage analysis is consistent with previous work showing ST3GAL3 is required for ligand production in mouse lung tissue (Guo et al., 2011). To elucidate if sulfation has an impact on Siglec-F binding, solvolysis was performed on whole brain lysates. Upon solvolysis, a reduction in the dispersed smear appearance and a more discrete band was observed suggesting that sulfation is not required for binding but does produce additional ligands (**Fig. 3.2B**).

To identify the glycoprotein(s) recognized by Siglec-F, we used whole brain homogenates for Siglec-F Fc immunoprecipitation. LC/MS-based proteomics revealed low density lipoprotein receptor 1 (LRP1) was identified as a top candidate in both WT and 5xFAD lysates (**Fig. 3.2C**). To verify that LRP1 carries the glycan ligand for Siglec-F, we digested whole brain lysate using PNGaseF prior to immunoprecipitation with a LRP1 antibody specific for the  $\alpha$ -chain and visualized by Siglec-F Fc overlay. For both WT and 5xFAD, LRP1 is shown to have 2 major glycoforms above the 250kD marker (**Fig. 3.2D**). Our finding that LRP1 is differentially glycosylated in 5xFAD and can be modified with the glycan ligand for Siglec-F suggest the receptor is likely to be found with the capacity and ability to interact at the CP.

To visualize LRP1 localization in the brain, confocal analysis of fluorescently labeled frozen brain sections revealed predominant apical and mosaic expression patterns at the CP in WT. In contrast, CP from 5xFAD brains demonstrated a large

increase in LRP1 expression when compared to WT that was almost exclusively on the basal membrane (**Fig. 3.2E**); a staining pattern which has been previously reported in rat brain (Kounnas, Haudenschild, Strickland, & Argraves, 1994). There was also substantial colocalization with PECAM-1 located on the fenestrated capillaries in the CP (data not shown). When sections were digested with PNGaseF prior to probing, the expression pattern changed in 5xFAD from strictly basal to both basal and apical, indicating that a new pool of protein was unveiled. The expression pattern was not affected for WT nor was there an increase in fluorescence at the apical membrane (**Fig. 3.2E**).

The total fluorescence observed after PNGaseF treatment in WT brains did not fluctuate to more closely resemble that of 5xFAD. This finding does not correlate to the changes seen for specific glycan epitopes, such as those that bind Siglec-F, and supports the theory of cell type specific glycosylation that is tightly regulated. To determine if the overall amount of LRP1 is equal between WT and 5xFAD, we used a second antibody for LRP1 directed towards the 85-kD  $\beta$ -chain and found no difference in fluorescence (**Fig. 3.2F**). Overall, our data show that LRP1 is specifically increased at the basal surface of CP in 5xFAD along with an increase of a differentially glycosylated form on the apical surface. This result suggests that LRP1 may have different functions at the apical and basal surfaces and that additional protein carriers of the Siglec-F ligand may be present at the apical surface of the CP.

### **3. LRP1 is modified with Siglec-F ligand in human stem cells**

To explore the expression of Siglec-F ligand in human tissue, we analyzed Siglec-F Fc reactivity in patient derived stem cells. Similar to murine brain, we observed Siglec-F ligand as high MW species with a significant enrichment in AD patient cells (**Fig. 3.3A**). We also observed a ~3-fold increase in Siglec-F ligand in AD cell conditioned media

relative to control media (**Fig. 3.3B**), where we also saw a significant quantity of Siglec-F ligand secreted from human neuroblastoma cells into conditioned media (data not shown).

Ligand staining of iPSCs demonstrates a similar punctate pattern seen at the epithelium of the mouse CP, suggesting the ligand may be packaged in vesicles (**Fig. 3.3C**). Although much of the Siglec ligand is expressed on the cell membrane and/or associated with the ECM, co-staining of intracellular ligand with markers in the secretory pathway demonstrates co-localization within endosomal compartments (**Fig. 3.3C**), more so than lysosomes (data not shown). This finding supports the punctate staining pattern observed at the mouse CP as well as associated with human cells.

To determine protein carriers of this ligand, we employed a similar approach to the mouse brain and immunoprecipitated glycoproteins with Siglec-F Fc from iPSC lysates. With LC/MS, we identified several known Siglec protein carriers, including mucins (Kiwamoto et al., 2015b; Tanida et al., 2013), LRP1 (this study), and DMBT1 (Gonzalez-Gil et al., 2021). To confirm LRP1 as a Siglec-F counterreceptor in human iPSCs, we used a LRP1- $\alpha$  chain antibody to pulldown purified protein and then probed with Siglec-F Fc, detecting a defined band >250kD (**Fig. 3.3E**). Furthermore, we were curious if the disparity in Siglec-F ligand density between control and AD cells could be attributed to the amount of present. LRP1- $\alpha$  has been observed to be regulated by membrane shedding (Q. Liu et al., 2009). However, densitometry analysis of the transmembrane LRP1- $\beta$  protein demonstrated comparable amounts of protein between samples (**Fig. 3.3F**), suggesting the increased Siglec-F ligand expression observed in AD cells is occurring on the level of glycan expression.

Lastly, by perturbing LRP1 detection by removing N-glycans with PNGaseF, we observed different pools of glycoprotein in AD vs. control cells like that seen at the mouse CP. Removing N-glycans from LRP1- $\alpha$  almost completely abolishes antibody recognition

in control iPSC lysate, while N-glycan removal reveals an upper MW species remains detectable in AD (**Fig. 3.3F**). This finding suggests LRP1- $\alpha$  is differentially glycosylated in AD, recapitulating our discovery in the mouse brain with human cells. This protein carrier identification, although novel, does not recognize the tissue-specific counterreceptor of interest at the apical surface of the CP epithelium.

#### **4. Siglec ligands are expressed on Galectin-3 binding protein at the CP**

To explore the expression of CP Siglec ligands in human choroid plexus tissue, we generated 3-dimensional iPSC-derived “chorganoids” using adaptations from previously published differentiation schemes (Sakaguchi et al., 2015; Watanabe et al., 2016; Watanabe et al., 2012). Pluripotent patient-derived stem cells were first aggregated by hanging drop for 24 hours and then cultured for 42 DIV (Foty, 2011). CP identity was confirmed by immunofluorescence of fundamental markers: AQP1, OTX2, TTR, and ZO-1 (**Fig. 3.4A**) (Lun et al., 2015). Aquaporin-1 is a water channel protein expressed on the apical surface of the CP epithelium, Otx2 is a transcription factor required for CP development and maintenance, transthyretin/pre-albumin is a CP-specific transport protein produced in the epithelium, and zonula occludens 1 forms tight junctions at the blood-CSF barrier.

In chorganoid lysates, Siglec-F ligand expression for both NDC K3 and APP<sup>DP2</sup> cultures was found on a high MW smear of several species >250kD. Intensity of Siglec ligand expression between control and diseased cultures appears comparable. For Siglec-9 ligand expression, however, we observed a ~60kD MW glycoprotein that is smaller than protein carriers normally associated with Siglec ligands (**Fig. 3.4B**) (H. Liu et al., 2020). We found that all Siglec ligand binding analyzed was sensitive to digestion by neuraminidase (data not shown).

Recently, the Siglec-8 ligand in the airway was shown to be a sialylated keratan sulfate (KS) structure (Gonzalez-Gil et al., 2018). Additionally, deficiency of sulfotransferase GlcNAc6ST1, encoded by *chst2*, was found to be beneficial against AD by mitigating A $\beta$  pathology (Z. Zhang et al., 2017). Reduced density of microglial Siglec ligands is predicted to increase phagocytosis and offer protection against neurodegeneration. In chorganoids, we found that Siglec-9 ligands were sensitive to digestion with keratanase I (KI), which cleaves  $\beta$ 1-4 Gal-GlcNAc( $\pm$ 6S). Interestingly, we have observed that AD CP tissue is more sensitive to digestion with KI than NDC tissue, suggesting a greater proportion of the CP Siglec ligand is sialylated KS in AD (**Fig. 3.4B**).

Because chorganoids are heterogeneous in nature and are not subject to manipulation through media conditions, we obtained a human choroid plexus papilloma cell line (HIBCPP) (Ishiwata et al., 2005). These cells exhibit appropriate CP physiological markers and can create functional blood-CSF barrier models (**Fig. 3.4C**) (Bernd et al., 2015; Dinner et al., 2016). Whole cell lysates from HIBCPP produce Siglec-F and -9 ligands in the high MW range observed in additional cell types. Conditioned media harvested from these cells shows that they produce Siglec ligands in the high MW range but also robustly secrete ligands on a mid MW species approximately 60kD (**Fig. 3.4D**).

HIBCPP Siglec ligands are completely sensitive to neuraminidase as expected but exhibit differential sensitivity to KI and PNGaseF. The Siglec-9 Fc sensitive epitope is more resistant to KI digestion over a 48 hr time course, where binding is only completely abolished with additional enzyme supplementation after 24 hr. The Siglec-F HIBCPP ligand is immediately cleaved within 4 hr of KI treatment, indicating the glycan is more susceptible to enzyme. The Siglec-F ligand also appears slightly more sensitive to PNGaseF treatment, suggesting a greater proportion of the ligand modifies an N-linked glycosylation site (**Fig. 3.4D**).

A major barrier to studying Siglec-glycan interactions is the low affinity, where multivalent presentation of Siglecs and their glycan counterreceptors is often required to enhance avidity (Rodrigues et al., 2020). To optimize purification of the secreted HIBCPP Siglec ligand, we opted to target KS through anion exchange chromatography where elution was optimized to 500 mM salt condition (**Fig. 3.4E**) (Holland et al., 2004; Yanagishita, Midura, & Hascall, 1987). The purified KS Siglec ligand was subjected to buffer exchange and in-gel trypsin digestion for proteomics. Our top hits that were not common highly abundant serum proteins or contaminants and were also the appropriate MW included galectin-3 binding protein and 78kD glucose-regulated protein (**Fig. 3.4E**). Because Gal-3BP was previously found to be a Siglec-9 ligand carrier in tumor cell extracts, we chose to explore its involvement as a CP glycoprotein (Laubli, Alisson-Silva, et al., 2014). Through a reciprocal immunoprecipitation experiment, we confirmed that a mid MW range protein carrier of Siglec-9 ligand is Gal-3BP (**Fig. 3.4F**). This result was also recapitulated by immunofluorescence imaging of HIBCPP cultures, where extracellular staining of Siglec-F and Siglec-9 Fc constructs displayed a high degree of co-localization with Gal-3BP extracellular staining overlaid with an intracellular DAPI reference (**Fig. 3.4F**). The staining pattern for each glycan ligand remains punctate but displays notable differences in localization. Siglec-9 Fc staining appears to form in sheets over cells, possibly due to raft aggregation or cell cycle fluctuations, while Siglec-F Fc appears homogeneously presented by the entire cell population.

Since LRP1 immunostaining did not co-localize with Siglec-F ligand at the mouse lateral CP, we visualized Siglec ligand expression among Gal-3BP localization in murine brain. Gal-3BP localization displayed a similar pattern as seen with Siglec ligands at the epithelium with extracellular puncta associating with apical surface. We also observed a high degree of co-localization between Gal-3BP and Siglec-F ligand at the CP of the fourth ventricle, where the Siglec-9 epitope co-localized at extracellular puncta but included a

dense epithelial canopy of glycan that did not co-localize with Gal-3BP. This result suggests that additional Siglec ligand carriers are present at the mouse CP and that the glycan epitopes for Siglec-F and -9 are not completely synonymous (**Fig. 3.4G**).

We also observed Siglec ligand expression in human CSF samples obtained via lumbar punch biopsy. Human CSF contained soluble Siglec-9 ligand glycoproteins similar in MW range observed in chorganoids and secreted by HIBCPP cultures as well as soluble Gal-3BP. Adjusted Siglec-9 Fc signal normalized to monomeric TTR expression trends toward reduced ligand amount in AD patients, though additional control codes are needed (**Fig. 3.4H**). Siglec-9 signaling has been shown to be involved in pathology of cancer and chronic obstructive pulmonary disease (COPD), suggesting the NDCs used here may also have altered Siglec ligand expression (Haas et al., 2019; Rodriguez et al., 2021; Zeng et al., 2017).

### **5. Siglec ligand expression at the CP is responsive to inflammation**

To explore the alteration of CP Siglec ligands during inflammation, chorganoids were stimulated with TLR4 agonist LPS derived from *E. coli* and TLR2 agonist hyaluronic acid fragments (36kD HA) (**Fig. 3.5A**). Siglec ligand expression was analyzed by immunofluorescence imaging of intact chorganoids. Both LPS and HA stimulation induced Siglec-9 ligand expression on the apical surface of chorganoids (**Fig. 3.5B**).

To explore the alteration of CP Siglec ligands during inflammation, HIBCPP cultures were challenged with TLR agonists and antagonists as well as disease-relevant elicitors such as A $\beta$ . Previously in a blood-CSF barrier study modeling meningitis infection, TLR expression detected in HIBCPP included TLR1, 2, 3, 4, 5, 6 and 10. They also expressed co-receptors CD14 and MD2 as well as adapter MyD88 (Borkowski et al., 2014). Furthermore, TLR4 stimulation via LPS has been shown to increase Siglec-E ligand expression on mouse aortas as well as primary mouse aortic endothelial cells in a dose-

dependent manner (H. Liu et al., 2020). NF- $\kappa$ B signaling was also blocked with TPCK, preventing LPS stimulation from altering Siglec-E ligand expression.

Serum-free conditioned media was analyzed for Siglec ligand expression following 24 hour stimulations. After full spectrum TLR agonists and A $\beta$  monomers and oligomers did not significantly stimulate or inhibit ligand expression by immuno-overlay blot analysis, we hypothesized HIBCPP cultures were producing and/or secreting ligands near maximum capacity (**Fig. 3.5C**).

We explored down-regulation of Siglec ligand expression using a pan-TLR inhibitor for MyD88 homodimerization. Twenty-four hr treatment of HIBCPP cultures with the inhibitor peptide completely abolished Siglec ligand secretion into the media of the Gal-3BP<sup>60kD</sup> species, where the antennapedia control peptide did not significantly alter expression from vehicle treatment (**Fig. 3.5D**). Interestingly, MyD88 inhibition did not appear to significantly alter Siglec ligand modification to the high MW protein carrier. The effect of TLR inhibition on subcellular localization was also demonstrated by 3-D reconstruction. Treatment with the inhibitor translocated Siglec ligand intracellularly where it can be seen in closer association with the nucleus, where vehicle treated cells express their ligand in an extracellular canopy (**Fig. 3.5D**).

To assess the effect of MyD88 inhibition on the cellular glycome, we surveyed lysate reactivity to concanavalin A (ConA), which binds high mannose and bisected hybrid N-glycans, and wheat germ agglutinin (WGA), which binds terminal GlcNAc and sialic acid residues. Despite inhibiting Siglec ligand presentation on the Gal-3BP<sup>60kD</sup> species, MyD88 inhibition did not affect HIBCPP lysate glycosylation overall (**Fig. 3.5E**). Supporting an absence of Siglec-9 ligand in the media, we also observed a considerable decrease in Gal-3BP<sup>60kD</sup> in the media of MyD88 inhibited cells which was not recapitulated in the lysate (**Fig. 3.5E**).

Another mechanism for modulation of Siglec ligand expression at the CP was demonstrated by Siglec ligand co-culture with the secretome of neural crest cells (NCCs). NCCs are a neural progenitor lineage of the peripheral nervous system. Culturing HIBCPP tissue with conditioned media from NCCs reduced the amount of Siglec ligand presented on Gal-3BP<sup>60kD</sup> in the media. Incubating conditioned NCC media with purified Gal-3BP<sup>S9L</sup> resulted in a similar effect (**Fig. 3.5F**). After denaturing secreted NCC proteins with heat, recovery of Siglec ligand presentation from purified Gal-3BP<sup>SF&9L</sup> was observed, suggesting involvement of a protein effector such as a neuraminidase (**Fig. 3.5F**). Similarly, co-incubation of high volume (10x) conditioned NCC media with purified G3BP<sup>SF&9L</sup> abolished Siglec ligand binding by overlay completely (data not shown).

## **6. Siglec-F engagement induces a pro-inflammatory phenotype**

To explore the biological impact of Siglec ligand expression from the CP, we challenged mouse primary BMDCs with purified Gal-3BP<sup>SFL</sup>. Red blood cells were lysed from extracted bone marrow, and residual cells were stimulated with GM-CSF for six days prior to 24 hr challenges, where GM-CSF stimulation has been shown to induce Siglec-F expression (Tateyama et al., 2019). Challenges included ligand, mild periodate-treated ligand, and vehicle-treated. Contrary to our hypothesis from the 5xFAD model, our immunophenotyping data suggest Gal-3BP<sup>SFL</sup> invokes pro-inflammatory signaling in mouse leukocytes. Siglec-F ligand challenged CD45<sup>+</sup> cells showed increased viability as well as greater M1 (Gr1, iNOS, CD38) marker expression and reduced M2 (CD206, Arg-1) marker expression (**Fig. 3.6A**). The lowest concentration of ligand, 10 µg/mL, induced a diminished response for most markers, suggesting this concentration may not be relevant for potential therapeutic intervention. The effect of sialidase-treated ligand (data not shown) and mild-periodate treatment to oxidize sialic acids (**Fig. 3.6A**) was variable, indicating additional negative controls such as antibody blockage are needed.

We also used Raw264.7 cells to monitor phagocytosis. Twenty-four hr challenge of murine macrophages demonstrated purified ligand reduced phagocytic activity in a dose dependent manner (**Fig. 3.6B**), as suggested previously (H. Liu et al., 2020). High dose of ligand significantly reduced phagocytosis, while low dose enhanced activity to greater than vehicle-treated control. Likewise, periodate-treated ligand enhanced phagocytosis (data not shown).

### **Discussion**

In this study, we demonstrated that immunostimulatory Siglec ligands at the CP were N- and O-glycans with varying structural features of a keratan sulfate modification and presented on LRP1 and Gal-3BP among other proteins. Although additional studies are required to target Siglec-9 receptors on human leukocytes, Siglec-F ligands activated murine immune cells which may be a therapeutic target in AD to dampen neuroinflammation.

The biological activity of Siglecs is activated by their sialoglycan counterreceptors, so understanding the structure of the ligands is important for predicting physiological outcomes. Here, we have incomplete structural information about the Siglec-F and Siglec-9 tissue specific ligands. All ligands studied appear to be partially sensitive to PNGaseF digestion, implying the Siglec epitope can modify N- and O-glycans at the CP. Siglec-F and -9 ligands exhibit differential susceptibility to keratanase I digestion, and no sensitivity to keratanase II digestion or 5D4 binding. Keratanase I prefers a lower sulfation density than keratanase II, suggesting the epitope is not completely sulfated or rather, the epitope contains a short addition of poly lactosamine. A small keratan sulfate chain would be consistent with the MW of our Gal-3BP<sup>SF&9L</sup> cleavage product, as a KS GAG alone can account for >40kD (Fu et al., 2016). Further characterization of the glycan can be

completed with lectin array technology and mass spectrometry, though the KS modification can complicate MS analysis.

We have identified LRP1 and Gal-3BP as tissue-specific protein carriers of Siglec ligands in brain tissue. Additional protein carriers certainly exist including phosphacan (Gonzalez-Gil et al., 2022), versican (this study), GRP78 (this study) which has been found to be secreted when cells are under stress (Vig et al., 2019), and mucins (Beatson et al., 2016; Belisle et al., 2010; Kiwamoto et al., 2015b). The solubility of Gal-3BP<sup>SF&9L</sup> and secretion into the CSF from the CP indicates it may be present in other parts of the brain via the glymphatic system as well as in serum, making it a possible biomarker for neuroinflammation.

Our finding that MyD88 inhibition prevents secretion of Gal-3BP<sup>SF&9L</sup> suggests that TLRs may have a role in modulating the secretory pathway in AD. It has been widely established that TLR signaling can mediate cytokine and chemokine secretion (Jozsef, Khreiss, El Kebir, & Filep, 2006; B. S. Liu, Cao, Huizinga, Hafler, & Toes, 2014; Schaefer, Desouza, Fahey, Beagley, & Wira, 2004). However, TLRs have also been able to induce secretion of antiviral proteins, antimicrobial peptides, and defensins as well as influence expression of cell surface receptors (Abrahams et al., 2006; Jia et al., 2004; Redfern, Reins, & McDermott, 2011). Siglec-F and -9 were both shown to strongly interact with TLR4 (G. Y. Chen et al., 2014), which may allude to our negative result for Siglec ligand expression modulation in the presence of TLR agonists if Siglec receptors prefer to interact with TLRs directly (**Fig. 3.5C**). Modulation of Gal-3BP<sup>SF&9L</sup> secretion could be a TLR-mediated mechanism to compensate or to contribute to neuroinflammation through Siglec signaling or through Gal-3BP dependent signaling.

Our immunophenotyping data suggest Gal-3BP<sup>SFL</sup> acts as a pro-inflammatory effector with immune cells. We observed reduced leukocyte apoptosis, reduced macrophage phagocytosis, and increased expression of M1 markers (**Fig. 3.6**). Siglec-F

receptor presentation decreased in cultures challenged with the ligand (**Fig. 3.6A**), suggesting the receptor was bound and internalized (O'Sullivan, Carroll, Cao, Salicru, & Bochner, 2018; Tateno et al., 2007). Ongoing experiments will help to demonstrate macrophage differentiation is Siglec-mediated by performing receptor blockade with Siglec-F Fc. We also will investigate downstream ITAM signaling in immune cells with detection of phosphorylated proteins using antibodies recognizing phosphotyrosine and phospho-Src family kinases. However, an additional possibility for the macrophage phenotype observed could be attributed to Gal-3BP.

Gal-3BP plasma levels have been associated with many infectious and autoimmune/inflammatory diseases such as HIV, rheumatoid arthritis, asthma, cancer, coronary artery disease, inflammatory bowel disease, and hepatitis C (Artini et al., 1996; Gleissner et al., 2016; Kalayci et al., 2004; Natoli et al., 1993). The protein itself, independent of Siglec signaling activities, has been shown to induce pro-inflammatory cytokine production (Ozaki et al., 2004; Xu et al., 2019). Some studies have suggested that Gal-3BP can act as a negative regulator of NF- $\kappa$ B, making its Siglec ligand addition a possible inhibitory feedback mechanism by activation of this signaling pathway induced by some Siglecs (C. S. Hong et al., 2019; H. Liu et al., 2020).

To further elucidate the role of Gal-3BP as an immunostimulatory molecule with and without Siglec ligand presentation, genetic manipulations of Gal-3BP can be utilized. Knockdown of *lgals3bp* with shRNA (Xu et al., 2019) and knockout with CRISPR-Cas9 genome editing system (C. S. Hong et al., 2019) mice have been produced. These models have demonstrated increased sensitivity to LPS-induced proinflammatory cytokine release via NF- $\kappa$ B activation. *Lgals3bp* knockout HIBCPP cell line would be a valuable tool to characterize secretion and activity of Gal-3BP at the CP.

Our finding of neuraminidase-regulated presentation of Siglec ligands also presents an interesting opportunity for exploration of feedback mechanisms for Siglecs

and other sialylated glycoproteins. The prominence of gangliosides and glycoproteins presenting polysialic acids in the mammalian brain has established a fundamental role for neuraminidases modulating synaptic plasticity, myelination, ion channel signaling, and neuron regeneration among other functions (Pshezhetsky & Ashmarina, 2018). The effect of neuraminidases on Siglec-mediated signaling in the brain has not been thoroughly considered.

Neuraminidases NEU1-4 have different but overlapping substrate specificities and expression patterns. NEU1 is present on the plasma membrane and in the lysosome, while NEU2 is cytosolic. NEU3 is also expressed on the plasma membrane but prefers gangliosides as a substrate. NEU4 is present on internal cellular membranes. NEU1 and NEU4 are active against oligosaccharides and glycoproteins, making them candidates for modifying Siglec ligands. Postnatal inflammatory exposure in rats has been shown to increase the activity of NEU1 and NEU4, resulting in reduced sialylated glycoproteins in brain tissue (Demina et al., 2018). The hyper-inflammatory environment in AD may stimulate neuraminidase production which could alter downstream Siglec receptor engagement.

Furthermore, in addition to Siglecs, evidence exists to suggest TLRs themselves can be substrates for neuraminidases. TLR4 is activated by desialylation, where activation of TLRs can be attenuated by sialidase inhibitors (Allendorf, Franssen, & Brown, 2020; Amith et al., 2010). Upon LPS stimulation, NEU1 translocated to the cell surface, co-localized with TLR4, and led to reduced Siglec Fc binding to leukocytes (G. Y. Chen et al., 2014). It has been suggested that this process functions to disarm the Siglec-mediated negative regulation of TLR function.

Exploring Siglec function through mouse models is not ideal, as Siglecs have demonstrated rapid evolution in humans thus creating different expression profiles and ligand-binding capacities (McCord & Macauley, 2022). Likewise, mice express Neu5Gc in

addition to Neu5Ac. Neu5Gc is the major sialic acid in many mouse tissues, and some Siglecs show preferential binding for Neu5Gc with incompletely understood relevancy to human brain studies (Crocker, Paulson, & Varki, 2007). Immunophenotyping experiments targeting Siglec-9 using primary human PBMCs would reveal the utility of Gal-3BP<sup>S9L</sup> as a therapeutic resource.

Neuroinflammation is a molecular trigger of AD, which is the seventh leading cause of death in the United States and the most common cause of dementia in the aging population. AD pathogenesis is undoubtedly complex, and treatment options are underwhelming at the present time. Most treatments target symptoms, while new disease-modifying therapies have yet to demonstrate impacts on clinical outcomes. Increasing evidence has revealed roles for inflammatory processes in AD pathogenesis, including findings of GWAS and links between systemic inflammation and obesity to AD risk. Our future studies on the implications of Siglec ligand expression and its effect on infiltrating immune cells at the CP may reveal novel targets for the treatment of AD and other neuroinflammatory or neurodegenerative disorders.

## Figures

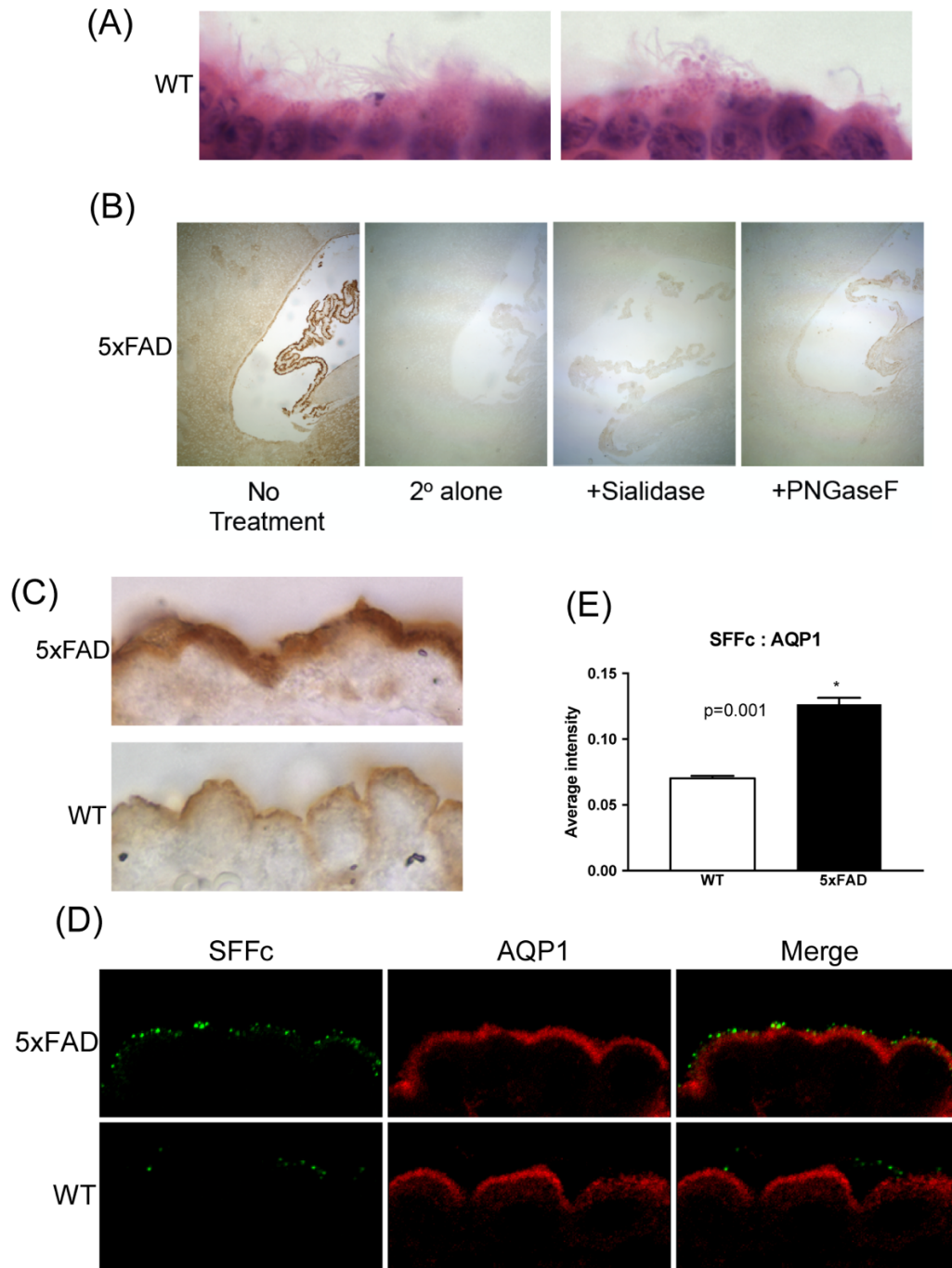
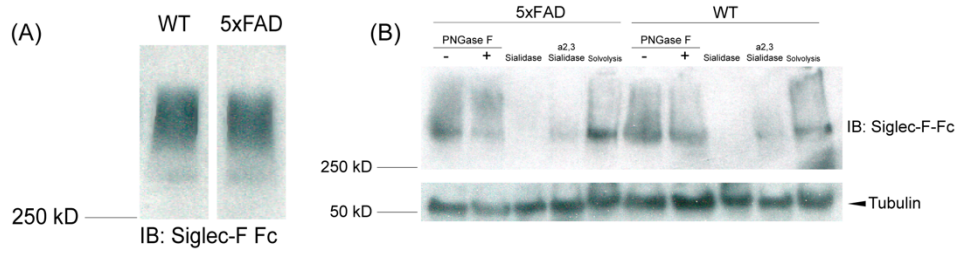


### Fig. 3.1. Siglec-F ligand is increased at the 5xFAD CP

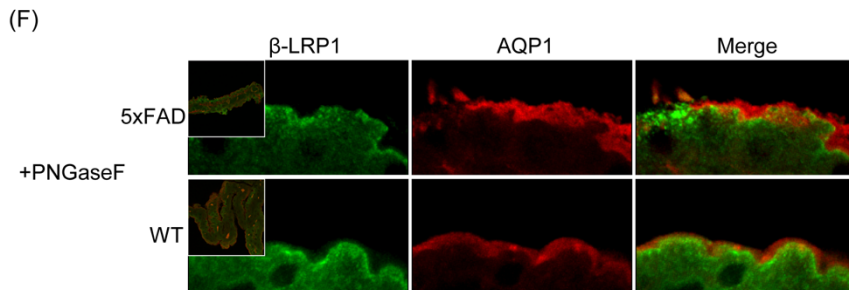
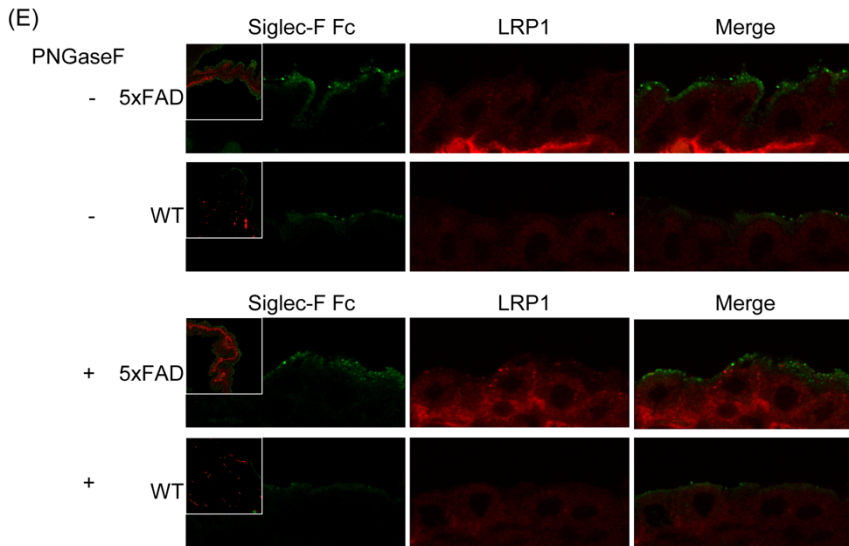
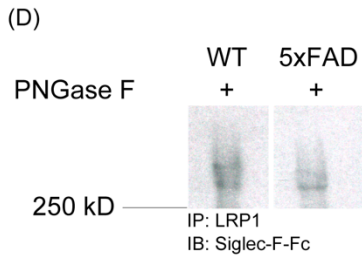
H&E staining of the CP demonstrates the apical surface of the epithelium is in contact with the CSF and is ciliated. A fenestrated capillary bed is also found below the basal surface (A). DAB staining of 5xFAD brain sections highlights accumulation of Siglec ligand at the CP and ependyma, which was sensitive to sialidase digestion and partially sensitive to PNGaseF digestion (B). This Siglec-F ligand staining at the CP was increased relative to WT (C). Confocal microscopy shows Siglec-F Fc staining occurs in puncta associated with

the apical surface (**D**). When normalized to AQP1 staining intensity, a ~2 fold increase ( $p=0.001$ ) in the ligand is seen in AD (**E**).



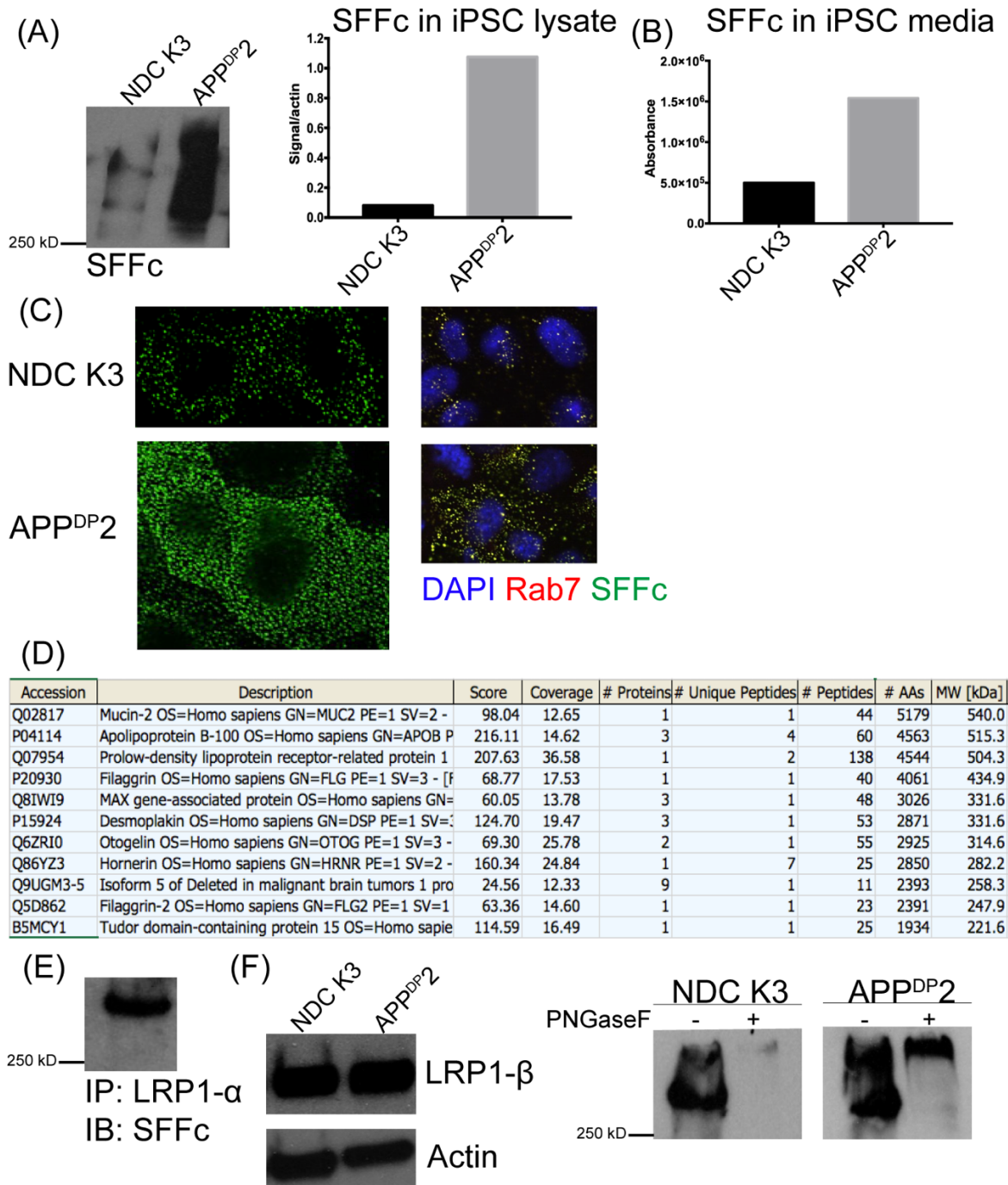
(C)

Accession	Description	Score	Coverage	# Proteins	# Unique Peptides	# Peptides	MW [kDa]
A2ASS6	Titin OS=Mus musculus GN=Ttn PE=1 SV=1 - [TITIN_MOUSE]	23.34	9.97	3	1	252	3904.1
Q9QX20	Microtubule-actin cross-linking factor 1 OS=Mus musculus GN=Me	26.04	8.28	4	2	46	831.4
E9Q401	Ryanodine receptor 2 OS=Mus musculus GN=Ryr2 PE=1 SV=1 - [	5.64	11.22	2	1	34	564.5
Q9QYX7	Protein piccolo OS=Mus musculus GN=Pclo PE=1 SV=4 - [PCLO_f	23.13	11.21	1	1	39	550.5
Q9QXS1	Plectin OS=Mus musculus GN=Plec PE=1 SV=3 - [PLEC_MOUSE]	558.13	22.13	2	34	101	533.9
Q9JHU4	Cytoplasmic dynein 1 heavy chain 1 OS=Mus musculus GN=Dync	318.03	17.66	1	19	73	531.7
Q91ZX7	Prolow-density lipoprotein receptor-related protein 1 OS=Mus mu	32.51	27.26	1	4	85	504.4
O88737	Protein bassoon OS=Mus musculus GN=Bsn PE=1 SV=4 - [BSN_N	142.05	11.54	1	8	38	418.6
V9GX34	Protein Csm2 (Fragment) OS=Mus musculus GN=Csm2 PE=1 S	40.46	4.82	1	1	9	372.4
Q62059	Versican core protein OS=Mus musculus GN=Vcan PE=1 SV=2 - [	55.16	6.20	6	5	19	366.6



### **Fig. 3.2. LRP1 is modified with the ligand for Siglec-F in murine brain tissue**

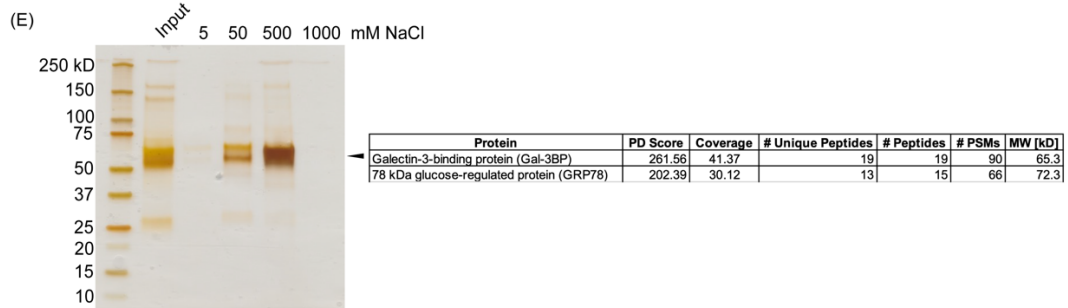
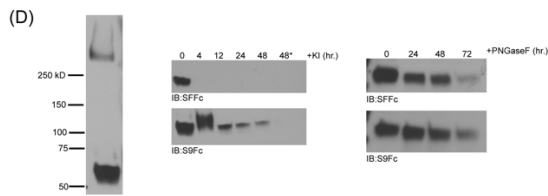
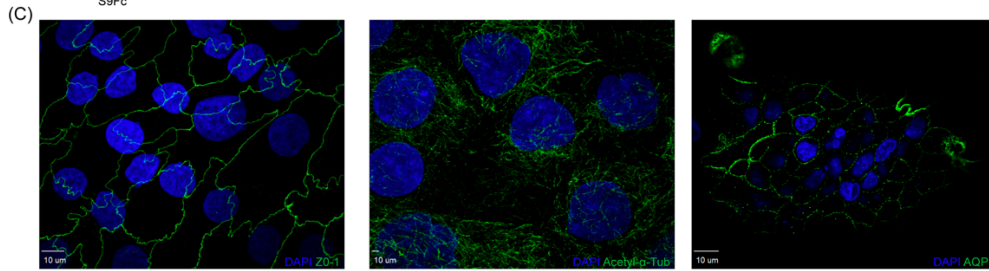
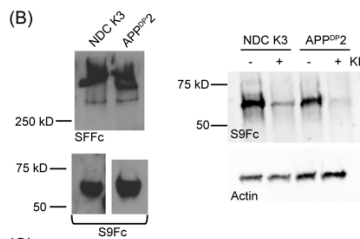
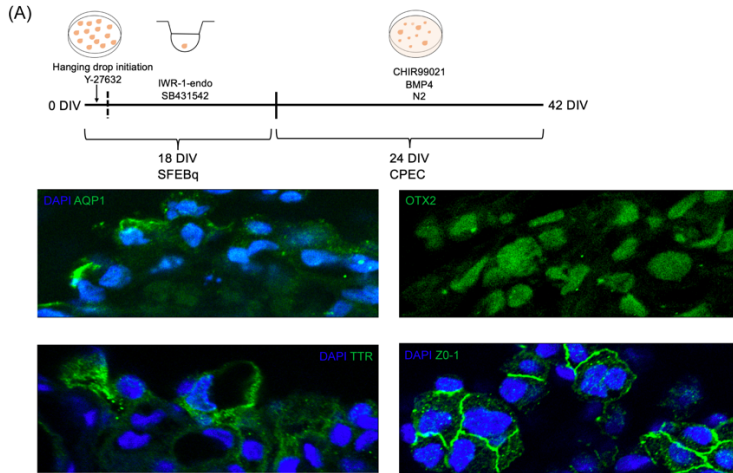
SDS-PAGE analysis and subsequent Siglec-F Fc overlay of brain homogenate demonstrates Siglec-F binds high MW (>250kD) smear of glycoproteins (**A**). PNGaseF treatment reduces Siglec-F recognition of the faster migrating material in 5xFAD. Pan-sialidase treatment completely abolishes all binding in both WT & 5xFAD, while  $\alpha$ 2-3 specific sialidase removes a significant amount of binding. Removal of sulfate via solvolysis appears to collapse the smear into a tighter band of higher intensity, demonstrating that sulfate isn't required for binding (**B**). LC-MS/MS of in-gel digested material following Siglec-F Fc immunoprecipitation revealed LRP1 as a carrier protein candidate (**C**) among additional glycoproteins. Immunoprecipitation of LRP1 with Siglec-F overlay confirms LRP1 as a carrier (**D**). 5xFAD CP sections have an intense pool of LRP1 at the basal surface (**E**). Very little apical LRP1 is detected in 5xFAD unless the section is first treated with PNGaseF, suggesting that the anti-LRP1 epitope is sensitive to glycosylation and therefore that LRP1 is alternatively glycosylated in 5xFAD model (**E**). The expression of LRP1 when probed for the  $\beta$ -chain is more concentrated at the apical surface in 5xFAD (**F**). This result is not fully understood, however, this may be a pool of rapidly endocytosed LRP1 during a signaling event.



### Fig. 3.3. Siglec-F ligand also modifies LRP1 in human iPSCs

SDS-PAGE separation of proteins and Siglec-F Fc immunoblotting of iPSC lysates identifies high MW (>250kD) protein carriers with markedly increased glycan epitope in AD patient cells (A). Siglec-F Fc reactivity was also detected in the media by ELISA (B). Fluorescence microscopy confirmed enrichment of Siglec-F Fc signal in AD iPSCs and found puncta to co-localize with Rab7<sup>+</sup> compartments (C). Siglec-F Fc immunoprecipitation and proteomics identified LRP1 as a counterreceptor in AD iPSC lysate (D). Reciprocal immunoprecipitation with  $\alpha$ -LRP1 confirmed LRP1's candidacy (E).

Western blot of LRP1- $\beta$  displays comparable amounts of protein present in iPSCs, while LRP1- $\alpha$  displays sensitivity to PNGaseF with separate pools of glycoprotein present (**E**).



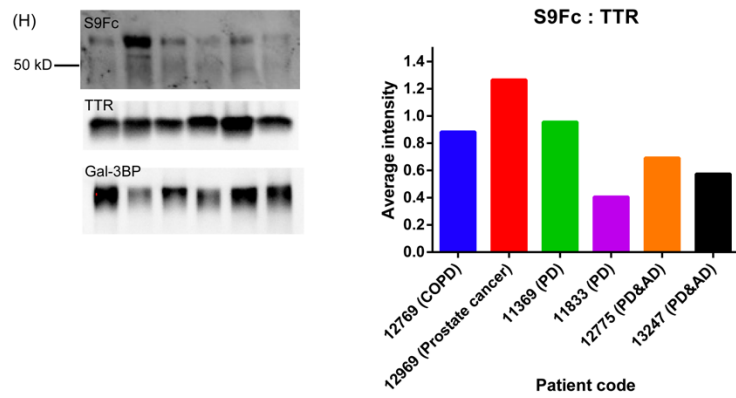
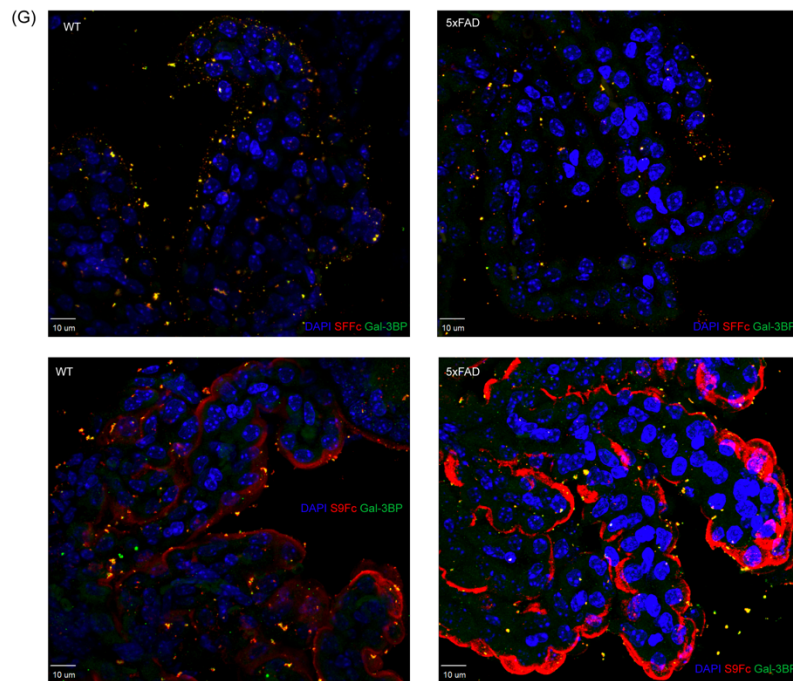
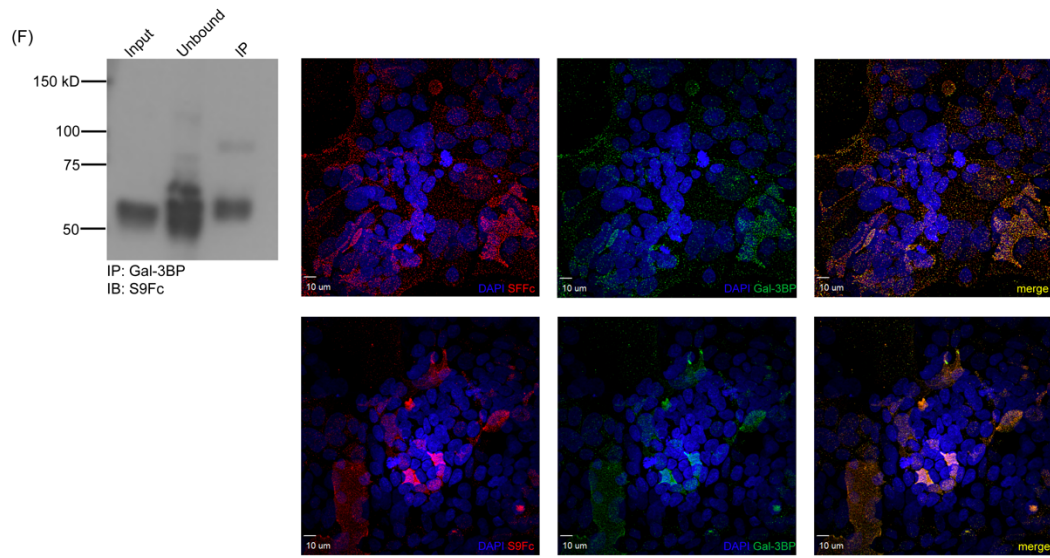


**Fig 3.4. Gal-3BP is a Siglec ligand carrier at the CP**

Chorganoids were differentiated from healthy iPSCs and expressed functionally appropriate markers (A). Chorganoid lysates displayed different protein carriers for Siglec-F and -9 based on protein MW reactivity. The Siglec-9 ligands also displayed distinct keratanase I sensitivity between NDC and AD cultures (B). Fluorescence microscopy of HIBCPP cells shows they express functionally characteristic CP proteins including tight junction protein ZO-1, microtubule and ciliary protein acetylated alpha tubulin, and water channel AQP1 (C). HIBCPP cell conditioned media contains Siglec ligands on >250 kD high MW smear as well as a ~60 kD species (D). HIBCPP Siglec ligands are minimally sensitive to removal of N-glycans with PNGaseF (D). Enzyme was supplemented every 24 hours to account for PNGaseF half-life. HIBCPP Siglec ligands are sensitive to digestion by keratanase I over time with loss of Siglec-F ligand binding within 4 hours and loss of Siglec-9 ligand binding in 48 hours with additional enzyme supplementation at 24 hours\* (D). The ~60 kD species was purified from conditioned HIBCPP media by anion exchange chromatography and eluted by NaCl gradient. LC-MS/MS identified candidates not highly abundant in serum with PD scores >200 from the 500 mM eluted material (E).  $\alpha$ -Gal-3BP immunoprecipitation and Siglec-9 Fc overlay in addition to immunofluorescence imaging upheld Gal-3BP identification (F). Confocal images of murine CP from the 4<sup>th</sup> ventricle exhibited co-localization between Gal-3BP and Siglec Fc constructs (G). Siglec-9 Fc reactive species were additionally detected in human CSF (H).

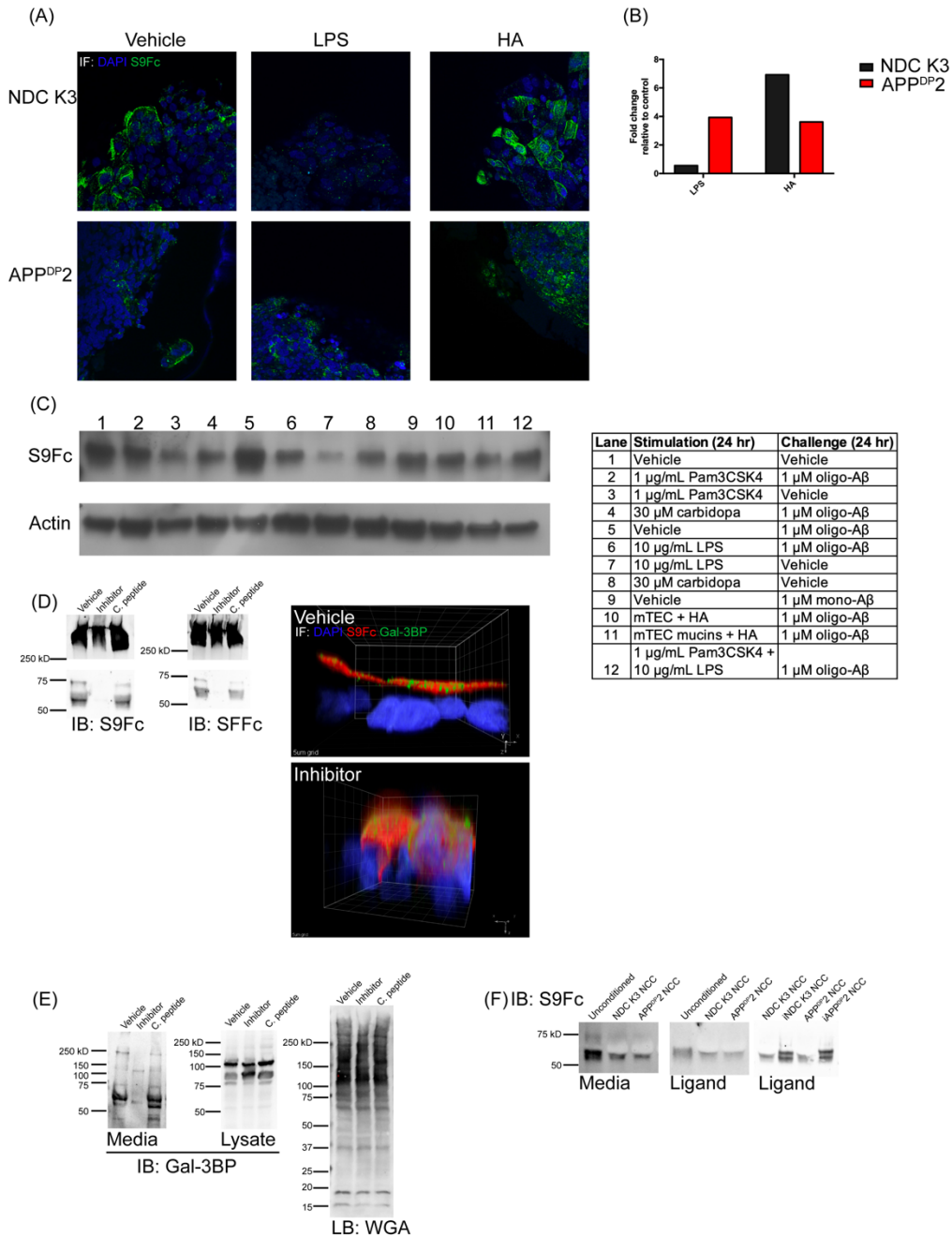


### Fig. 3.5. Siglec ligand expression is sensitive to TLR signaling

Z-stacks of apical Siglec-9 ligand expression on chorganoids was responsive to stimulation with TLR agonists for 24 hr (A). Quantified Siglec-9 Fc signal was induced to a great degree by 35kD HA fragments than LPS (B). Gal-3BP<sup>S9L</sup> secretion from HIBCPP was not induced by TLR priming (24 hr) or Aβ challenge (additional 24 hr) (C). Twenty-four hr treatment of HIBCPP with 100 µM MyD88 inhibition inhibited secretion of Gal-3BP<sup>SF&9L</sup> while the antennapedia control peptide did not have an effect. Three-dimensional 60X reconstruction of HIBCPP demonstrated mis-localization of Gal-3BP in inhibited cultures (D). Western blot analysis confirms Gal-3BP is not present in inhibited media but remains in lysate (E). Twenty-four hr treatment of HIBCPP cells with conditioned serum-

free neural crest cell (NCC) media reduces Gal-3BP<sup>SL</sup>. This effect is reversed by inactivating (iNCC) media prior to HIBCPP challenge (**F**).

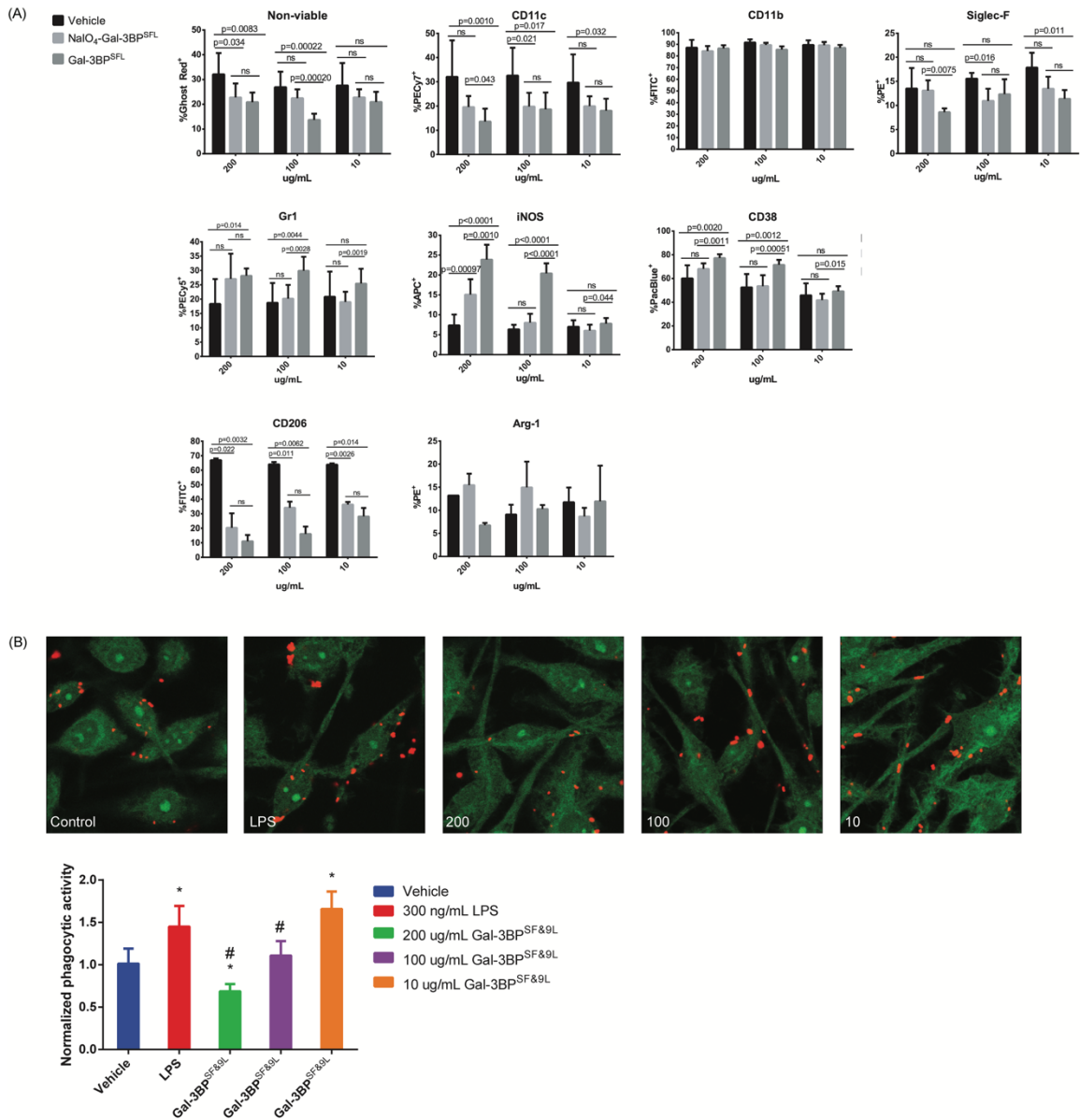


**Fig. 3.6. Siglec-F engagement induces a pro-inflammatory phenotype in mouse leukocytes**

Flow cytometry analysis of mouse PBMCs stimulated with vehicle (50 mM sodium acetate) purified Gal-3BP<sup>SF</sup>&9L, or periodate-treated Gal-3BP<sup>SF</sup>&9L where cell populations were characterized (top row), M1-like markers were measured (middle row), and M2-like markers were measured (bottom row) (A). All gated populations were Ghost Red<sup>-</sup> and CD45<sup>+</sup>. Raw264.7 cells were stimulated with purified Gal-3BP<sup>SF</sup>&9L at varying concentrations or LPS (300ng/mL) for 24 hr before treatment with *E. coli* particles for 4 hr. High concentration stimulation with ligand significantly decreased phagocytosis (mean ± SD, \*p<0.05 vs. vehicle, #p<0.05 vs. LPS, n=4) (B).

## References

- Abrahams, V. M., Schaefer, T. M., Fahey, J. V., Visintin, I., Wright, J. A., Aldo, P. B., . . . Mor, G. (2006). Expression and secretion of antiviral factors by trophoblast cells following stimulation by the TLR-3 agonist, Poly(I : C). *Hum Reprod*, *21*(9), 2432-2439. doi:10.1093/humrep/del178
- Allendorf, D. H., Franssen, E. H., & Brown, G. C. (2020). Lipopolysaccharide activates microglia via neuraminidase 1 desialylation of Toll-like Receptor 4. *J Neurochem*, *155*(4), 403-416. doi:10.1111/jnc.15024
- Amith, S. R., Jayanth, P., Franchuk, S., Finlay, T., Seyrantepe, V., Beyaert, R., . . . Szewczuk, M. R. (2010). Neu1 desialylation of sialyl alpha-2,3-linked beta-galactosyl residues of TOLL-like receptor 4 is essential for receptor activation and cellular signaling. *Cell Signal*, *22*(2), 314-324. doi:10.1016/j.cellsig.2009.09.038
- Artini, M., Natoli, C., Tinari, N., Costanzo, A., Marinelli, R., Balsano, C., . . . Iacobelli, S. (1996). Elevated serum levels of 90K/MAC-2 BP predict unresponsiveness to alpha-interferon therapy in chronic HCV hepatitis patients. *J Hepatol*, *25*(2), 212-217. doi:10.1016/s0168-8278(96)80076-6
- Beatson, R., Tajadura-Ortega, V., Achkova, D., Picco, G., Tsourouktsoglou, T. D., Klausning, S., . . . Burchell, J. M. (2016). The mucin MUC1 modulates the tumor immunological microenvironment through engagement of the lectin Siglec-9. *Nat Immunol*, *17*(11), 1273-1281. doi:10.1038/ni.3552
- Belisle, J. A., Horibata, S., Jennifer, G. A., Petrie, S., Kapur, A., Andre, S., . . . Patankar, M. S. (2010). Identification of Siglec-9 as the receptor for MUC16 on human NK cells, B cells, and monocytes. *Mol Cancer*, *9*, 118. doi:10.1186/1476-4598-9-118

- Bernd, A., Ott, M., Ishikawa, H., Schroten, H., Schwerk, C., & Fricker, G. (2015). Characterization of efflux transport proteins of the human choroid plexus papilloma cell line HIBCPP, a functional in vitro model of the blood-cerebrospinal fluid barrier. *Pharm Res*, 32(9), 2973-2982. doi:10.1007/s11095-015-1679-1
- Bochner, B. S. (2009). Siglec-8 on human eosinophils and mast cells, and Siglec-F on murine eosinophils, are functionally related inhibitory receptors. *Clin Exp Allergy*, 39, 317-324.
- Borkowski, J., Li, L., Steinmann, U., Quednau, N., Stump-Guthier, C., Weiss, C., . . . Schwerk, C. (2014). Neisseria meningitidis elicits a pro-inflammatory response involving IkappaBzeta in a human blood-cerebrospinal fluid barrier model. *J Neuroinflammation*, 11, 163. doi:10.1186/s12974-014-0163-x
- Chen, G. Y., Brown, N. K., Wu, W., Khedri, Z., Yu, H., Chen, X., . . . Liu, Y. (2014). Broad and direct interaction between TLR and Siglec families of pattern recognition receptors and its regulation by Neu1. *Elife*, 3, e04066. doi:10.7554/eLife.04066
- Crocker, P. R., Paulson, J. C., & Varki, A. (2007). Siglecs and their roles in the immune system. *Nat Rev Immunol*, 7(4), 255-266. doi:10.1038/nri2056
- Demina, E. P., Pierre, W. C., Nguyen, A. L. A., Londono, I., Reiz, B., Zou, C., . . . Lodygensky, G. A. (2018). Persistent reduction in sialylation of cerebral glycoproteins following postnatal inflammatory exposure. *J Neuroinflammation*, 15(1), 336. doi:10.1186/s12974-018-1367-2
- Dinner, S., Borkowski, J., Stump-Guthier, C., Ishikawa, H., Tenenbaum, T., Schroten, H., & Schwerk, C. (2016). A Choroid Plexus Epithelial Cell-based Model of the

Human Blood-Cerebrospinal Fluid Barrier to Study Bacterial Infection from the Basolateral Side. *J Vis Exp*(111). doi:10.3791/54061

Foty, R. (2011). A simple hanging drop cell culture protocol for generation of 3D spheroids. *J Vis Exp*(51). doi:10.3791/2720

Fouet, G., Gout, E., Wicker-Planquart, C., Bally, I., De Nardis, C., Dedieu, S., . . . Rossi, V. (2020). Complement C1q Interacts With LRP1 Clusters II and IV Through a Site Close but Different From the Binding Site of Its C1r and C1s-Associated Proteases. *Front Immunol*, 11, 583754. doi:10.3389/fimmu.2020.583754

Fu, L., Sun, X., He, W., Cai, C., Onishi, A., Zhang, F., . . . Liu, Z. (2016). Keratan sulfate glycosaminoglycan from chicken egg white. *Glycobiology*, 26(7), 693-700. doi:10.1093/glycob/cww017

Gleissner, C. A., Erbel, C., Linden, F., Domschke, G., Akhavanpoor, M., Doesch, A. O., . . . Korosoglou, G. (2016). Galectin-3 binding protein plasma levels are associated with long-term mortality in coronary artery disease independent of plaque morphology. *Atherosclerosis*, 251, 94-100. doi:10.1016/j.atherosclerosis.2016.06.002

Gonzalez-Gil, A., Li, T. A., Porell, R. N., Fernandes, S. M., Tarbox, H. E., Lee, H. S., . . . Schnaar, R. L. (2021). Isolation, identification, and characterization of the human airway ligand for the eosinophil and mast cell immunoinhibitory receptor Siglec-8. *J Allergy Clin Immunol*, 147(4), 1442-1452. doi:10.1016/j.jaci.2020.08.001

Gonzalez-Gil, A., Porell, R. N., Fernandes, S. M., Wei, Y., Yu, H., Carroll, D. J., . . . Schnaar, R. L. (2018). Sialylated keratan sulfate proteoglycans are Siglec-8 ligands in human airways. *Glycobiology*, 28(10), 786-801. doi:10.1093/glycob/cwy057

- Granados-Duran, P., Lopez-Avalos, M. D., Hughes, T. R., Johnson, K., Morgan, B. P., Tamburini, P. P., . . . Grondona, J. M. (2016). Complement system activation contributes to the ependymal damage induced by microbial neuraminidase. *J Neuroinflammation*, *13*(1), 115. doi:10.1186/s12974-016-0576-9
- Guo, J. P., Brummet, M. E., Myers, A. C., Na, H. J., Rowland, E., Schnaar, R. L., . . . Bochner, B. S. (2011). Characterization of Expression of Glycan Ligands for Siglec-F in Normal Mouse Lungs. *Am J Respir Cell and Molec Biol*, *44*, 238-243.
- Haas, Q., Boligan, K. F., Jandus, C., Schneider, C., Simillion, C., Stanczak, M. A., . . . von Gunten, S. (2019). Siglec-9 Regulates an Effector Memory CD8(+) T-cell Subset That Congregates in the Melanoma Tumor Microenvironment. *Cancer Immunol Res*, *7*(5), 707-718. doi:10.1158/2326-6066.CIR-18-0505
- Holland, J. W., Meehan, K. L., Redmond, S. L., & Dawkins, H. J. (2004). Purification of the keratan sulfate proteoglycan expressed in prostatic secretory cells and its identification as lumican. *Prostate*, *59*(3), 252-259. doi:10.1002/pros.20002
- Hong, C. S., Park, M. R., Sun, E. G., Choi, W., Hwang, J. E., Bae, W. K., . . . Chung, I. J. (2019). Gal-3BP Negatively Regulates NF-kappaB Signaling by Inhibiting the Activation of TAK1. *Front Immunol*, *10*, 1760. doi:10.3389/fimmu.2019.01760
- Inohara, H., Akahani, S., Koths, K., & Raz, A. (1996). Interactions between galectin-3 and Mac-2-binding protein mediate cell-cell adhesion. *Cancer Res*, *56*(19), 4530-4534. Retrieved from <https://www.ncbi.nlm.nih.gov/pubmed/8813152>
- Ishiwata, I., Ishiwata, C., Ishiwata, E., Sato, Y., Kiguchi, K., Tachibana, T., . . . Ishikawa, H. (2005). Establishment and characterization of a human malignant choroids plexus papilloma cell line (HIBCPP). *Hum Cell*, *18*(1), 67-72. doi:10.1111/j.1749-0774.2005.tb00059.x

- Israel, M. A., Yuan, S. H., Bardy, C., Reyna, S. M., Mu, Y., Herrera, C., . . . Goldstein, L. S. (2012). Probing sporadic and familial Alzheimer's disease using induced pluripotent stem cells. *Nature*, *482*(7384), 216-220. doi:10.1038/nature10821
- Itagaki, S., McGeer, P. L., Akiyama, H., Zhu, S., & Selkoe, D. (1989). Relationship of microglia and astrocytes to amyloid deposits of Alzheimer disease. *J Neuroimmunol*, *24*(3), 173-182. Retrieved from <http://www.ncbi.nlm.nih.gov/pubmed/2808689>
- Jia, H. P., Kline, J. N., Penisten, A., Apicella, M. A., Gioannini, T. L., Weiss, J., & McCray, P. B., Jr. (2004). Endotoxin responsiveness of human airway epithelia is limited by low expression of MD-2. *Am J Physiol Lung Cell Mol Physiol*, *287*(2), L428-437. doi:10.1152/ajplung.00377.2003
- Jozsef, L., Khreiss, T., El Kebir, D., & Filep, J. G. (2006). Activation of TLR-9 induces IL-8 secretion through peroxynitrite signaling in human neutrophils. *J Immunol*, *176*(2), 1195-1202. doi:10.4049/jimmunol.176.2.1195
- Kalayci, O., Birben, E., Tinari, N., Oguma, T., Iacobelli, S., & Lilly, C. M. (2004). Role of 90K protein in asthma and TH2-type cytokine expression. *Ann Allergy Asthma Immunol*, *93*(5), 485-492. doi:10.1016/S1081-1206(10)61417-2
- Kawasaki, N., Rademacher, C., & Paulson, J. C. (2010). CD22 regulates adaptive and innate immune responses of B cells. *J Innate Immun*, *3*(4), 411-419. doi:000322375 [pii]
- 10.1159/000322375
- Kelm, S., Pelz, A., Schauer, R., Filbin, M. T., Tang, S., de Bellard, M. E., . . . et al. (1994). Sialoadhesin, myelin-associated glycoprotein and CD22 define a new

family of sialic acid-dependent adhesion molecules of the immunoglobulin superfamily. *Curr Biol*, 4(11), 965-972. doi:10.1016/s0960-9822(00)00220-7

Kiwamoto, T., Katoh, T., Evans, C. M., Janssen, W. J., Brummet, M. E., Hudson, S. A., . . . Bochner, B. S. (2015a). Endogenous airway mucins carry glycans that bind Siglec-F and induce eosinophil apoptosis. *J Allergy Clin Immunol*, 135(5), 1329-1340 e1321-1329. doi:10.1016/j.jaci.2014.10.027

Kiwamoto, T., Katoh, T., Evans, C. M., Janssen, W. J., Brummet, M. E., Hudson, S. A., . . . Bochner, B. S. (2015b). Endogenous airway mucins carry glycans that bind Siglec-F and induce eosinophil apoptosis. *J Allergy Clin Immunol*, 135(5), 1329-1340 e1329. doi:10.1016/j.jaci.2014.10.027

Kounnas, M. Z., Haudenschild, C. C., Strickland, D. K., & Argraves, W. S. (1994). Immunological localization of glycoprotein 330, low density lipoprotein receptor related protein and 39 kDa receptor associated protein in embryonic mouse tissues. *In Vivo*, 8(3), 343-351. Retrieved from <http://www.ncbi.nlm.nih.gov/pubmed/7803716>

Laubli, H., Alisson-Silva, F., Stanczak, M. A., Siddiqui, S. S., Deng, L., Verhagen, A., . . . Varki, A. (2014). Lectin galactoside-binding soluble 3 binding protein (LGALS3BP) is a tumor-associated immunomodulatory ligand for CD33-related Siglecs. *J Biol Chem*, 289(48), 33481-33491. doi:10.1074/jbc.M114.593129

Liu, B. S., Cao, Y., Huizinga, T. W., Hafler, D. A., & Toes, R. E. (2014). TLR-mediated STAT3 and ERK activation controls IL-10 secretion by human B cells. *Eur J Immunol*, 44(7), 2121-2129. doi:10.1002/eji.201344341

Liu, H., Zheng, Y., Zhang, Y., Li, J., Fernandes, S. M., Zeng, D., . . . Jia, Y. (2020). Immunosuppressive Siglec-E ligands on mouse aorta are up-regulated by LPS

via NF-kappaB pathway. *Biomed Pharmacother*, 122, 109760.

doi:10.1016/j.biopha.2019.109760

Liu, Q., Zhang, J., Tran, H., Verbeek, M. M., Reiss, K., Estus, S., & Bu, G. (2009). LRP1 shedding in human brain: roles of ADAM10 and ADAM17. *Mol Neurodegener*, 4, 17. doi:10.1186/1750-1326-4-17

Lun, M. P., Johnson, M. B., Broadbelt, K. G., Watanabe, M., Kang, Y. J., Chau, K. F., . . . Lehtinen, M. K. (2015). Spatially heterogeneous choroid plexus transcriptomes encode positional identity and contribute to regional CSF production. *J Neurosci*, 35(12), 4903-4916. doi:10.1523/JNEUROSCI.3081-14.2015

Macauley, M. S., Crocker, P. R., & Paulson, J. C. (2014). Siglec-mediated regulation of immune cell function in disease. *Nat Rev Immunol*, 14(10), 653-666. doi:10.1038/nri3737

McCord, K. A., & Macauley, M. S. (2022). Transgenic mouse models to study the physiological and pathophysiological roles of human Siglecs. *Biochem Soc Trans*. doi:10.1042/BST20211203

McMillan, S. J., Sharma, R. S., Richards, H. E., Hegde, V., & Crocker, P. R. (2014). Siglec-E Promotes beta2-Integrin-dependent NADPH Oxidase Activation to Suppress Neutrophil Recruitment to the Lung. *J Biol Chem*, 289(29), 20370-20376. doi:10.1074/jbc.M114.574624

Menendez, L., Kulik, M. J., Page, A. T., Park, S. S., Lauderdale, J. D., Cunningham, M. L., & Dalton, S. (2013). Directed differentiation of human pluripotent cells to neural crest stem cells. *Nat Protoc*, 8(1), 203-212. doi:10.1038/nprot.2012.156

- Michelle Dookwah, S. K. W., Mayumi Ishihara, Seok-Ho Yu, Heidi Ulrichs, Michael J. Kulik, Nadja Zeltner, Stephen Dalton, Kevin A. Strauss, Kazuhiro Aoki, Richard Steet, Michael Tiemeyer. (2021). Neural-specific alterations in glycosphingolipid biosynthesis and cell signaling associated with two human ganglioside GM3 Synthase Deficiency variants. *bioRxiv*.  
doi:<https://doi.org/10.1101/2021.07.29.454399>
- Natoli, C., Dianzani, F., Mazzotta, F., Balocchini, E., Pierotti, P., Antonelli, G., & Iacobelli, S. (1993). 90K protein: a new predictor marker of disease progression in human immunodeficiency virus infection. *J Acquir Immune Defic Syndr (1988)*, 6(4), 370-375. Retrieved from <https://www.ncbi.nlm.nih.gov/pubmed/8095982>
- Nomura, K., Vilalta, A., Allendorf, D. H., Hornik, T. C., & Brown, G. C. (2017). Activated Microglia Desialylate and Phagocytose Cells via Neuraminidase, Galectin-3, and Mer Tyrosine Kinase. *J Immunol*, 198(12), 4792-4801.  
doi:10.4049/jimmunol.1502532
- O'Sullivan, J. A., Carroll, D. J., Cao, Y., Salicru, A. N., & Bochner, B. S. (2018). Leveraging Siglec-8 endocytic mechanisms to kill human eosinophils and malignant mast cells. *J Allergy Clin Immunol*, 141(5), 1774-1785 e1777.  
doi:10.1016/j.jaci.2017.06.028
- Ozaki, Y., Kontani, K., Teramoto, K., Fujita, T., Tezuka, N., Sawai, S., . . . Ohkubo, I. (2004). Involvement of 90K/Mac-2 binding protein in cancer metastases by increased cellular adhesiveness in lung cancer. *Oncol Rep*, 12(5), 1071-1077.  
Retrieved from <https://www.ncbi.nlm.nih.gov/pubmed/15492795>
- Patnode, M. L., Cheng, C. W., Chou, C. C., Singer, M. S., Elin, M. S., Uchimura, K., . . . Rosen, S. D. (2013). Galactose 6-O-sulfotransferases are not required for the

generation of Siglec-F ligands in leukocytes or lung tissue. *J Biol Chem*, 288(37), 26533-26545. doi:10.1074/jbc.M113.485409

Pshezhetsky, A. V., & Ashmarina, M. (2018). Keeping it trim: roles of neuraminidases in CNS function. *Glycoconj J*, 35(4), 375-386. doi:10.1007/s10719-018-9837-4

Ransohoff, R. M., Kivisakk, P., & Kidd, G. (2003). Three or more routes for leukocyte migration into the central nervous system. *Nat Rev Immunol*, 3(7), 569-581. doi:10.1038/nri1130

Razi, N., & Varki, A. (1999). Cryptic sialic acid binding lectins on human blood leukocytes can be unmasked by sialidase treatment or cellular activation. *Glycobiology*, 9(11), 1225-1234. doi:10.1093/glycob/9.11.1225

Redfern, R. L., Reins, R. Y., & McDermott, A. M. (2011). Toll-like receptor activation modulates antimicrobial peptide expression by ocular surface cells. *Exp Eye Res*, 92(3), 209-220. doi:10.1016/j.exer.2010.12.005

Rodrigues, E., Jung, J., Park, H., Loo, C., Soukhtehzari, S., Kitova, E. N., . . . Macauley, M. S. (2020). A versatile soluble siglec scaffold for sensitive and quantitative detection of glycan ligands. *Nat Commun*, 11(1), 5091. doi:10.1038/s41467-020-18907-6

Rodriguez, E., Boelaars, K., Brown, K., Eveline Li, R. J., Kruijssen, L., Bruijns, S. C. M., . . . van Kooyk, Y. (2021). Sialic acids in pancreatic cancer cells drive tumour-associated macrophage differentiation via the Siglec receptors Siglec-7 and Siglec-9. *Nat Commun*, 12(1), 1270. doi:10.1038/s41467-021-21550-4

Sakaguchi, H., Kadoshima, T., Soen, M., Narii, N., Ishida, Y., Ohgushi, M., . . . Sasai, Y. (2015). Generation of functional hippocampal neurons from self-organizing

human embryonic stem cell-derived dorsomedial telencephalic tissue. *Nat Commun*, 6, 8896. doi:10.1038/ncomms9896

Schaefer, T. M., Desouza, K., Fahey, J. V., Beagley, K. W., & Wira, C. R. (2004). Toll-like receptor (TLR) expression and TLR-mediated cytokine/chemokine production by human uterine epithelial cells. *Immunology*, 112(3), 428-436. doi:10.1111/j.1365-2567.2004.01898.x

Si-Tayeb, K., Noto, F. K., Sepac, A., Sedlic, F., Bosnjak, Z. J., Lough, J. W., & Duncan, S. A. (2010). Generation of human induced pluripotent stem cells by simple transient transfection of plasmid DNA encoding reprogramming factors. *BMC Dev Biol*, 10, 81. doi:10.1186/1471-213X-10-81

Tanida, S., Akita, K., Ishida, A., Mori, Y., Toda, M., Inoue, M., . . . Nakada, H. (2013). Binding of the sialic acid-binding lectin, Siglec-9, to the membrane mucin, MUC1, induces recruitment of beta-catenin and subsequent cell growth. *J Biol Chem*, 288(44), 31842-31852. doi:10.1074/jbc.M113.471318

Tateno, H., Crocker, P. R., & Paulson, J. C. (2005). Mouse Siglec-F and human Siglec-8 are functionally convergent paralogs that are selectively expressed on eosinophils and recognize 6 -sulfo-sialyl Lewis X as a preferred glycan ligand. *Glycobiology*, 15, 1125-1135.

Tateno, H., Li, H., Schur, M. J., Bovin, N., Crocker, P. R., Wakarchuk, W. W., & Paulson, J. C. (2007). Distinct endocytic mechanisms of CD22 (Siglec-2) and Siglec-F reflect roles in cell signaling and innate immunity. *Mol Cell Biol*, 27(16), 5699-5710. doi:10.1128/MCB.00383-07

Tateyama, H., Murase, Y., Higuchi, H., Inasaka, Y., Kaneoka, H., Iijima, S., & Nishijima, K. I. (2019). Siglec-F is induced by granulocyte-macrophage colony-stimulating

- factor and enhances interleukin-4-induced expression of arginase-1 in mouse macrophages. *Immunology*, 158(4), 340-352. doi:10.1111/imm.13121
- Vig, S., Buitinga, M., Rondas, D., Crevecoeur, I., van Zandvoort, M., Waelkens, E., . . . Overbergh, L. (2019). Cytokine-induced translocation of GRP78 to the plasma membrane triggers a pro-apoptotic feedback loop in pancreatic beta cells. *Cell Death Dis*, 10(4), 309. doi:10.1038/s41419-019-1518-0
- Vyas, A. A., Patel, H. V., Fromholt, S. E., Heffer-Lauc, M., Vyas, K. A., Dang, J., . . . Schnaar, R. L. (2002). Gangliosides are functional nerve cell ligands for myelin-associated glycoprotein (MAG), an inhibitor of nerve regeneration. *Proc Natl Acad Sci U S A*, 99(12), 8412-8417. doi:10.1073/pnas.072211699
- Watanabe, M., Fung, E. S., Chan, F. B., Wong, J. S., Coutts, M., & Monuki, E. S. (2016). BMP4 acts as a dorsal telencephalic morphogen in a mouse embryonic stem cell culture system. *Biol Open*, 5(12), 1834-1843. doi:10.1242/bio.012021
- Watanabe, M., Kang, Y. J., Davies, L. M., Meghpara, S., Lau, K., Chung, C. Y., . . . Monuki, E. S. (2012). BMP4 sufficiency to induce choroid plexus epithelial fate from embryonic stem cell-derived neuroepithelial progenitors. *J Neurosci*, 32(45), 15934-15945. doi:10.1523/JNEUROSCI.3227-12.2012
- Xu, G., Xia, Z., Deng, F., Liu, L., Wang, Q., Yu, Y., . . . Liu, S. (2019). Inducible LGALS3BP/90K activates antiviral innate immune responses by targeting TRAF6 and TRAF3 complex. *PLoS Pathog*, 15(8), e1008002. doi:10.1371/journal.ppat.1008002
- Yanagishita, M., Midura, R. J., & Hascall, V. C. (1987). Proteoglycans: isolation and purification from tissue cultures. *Methods Enzymol*, 138, 279-289. doi:10.1016/0076-6879(87)38023-1

- Yu, H., Gonzalez-Gil, A., Wei, Y., Fernandes, S. M., Porell, R. N., Vajn, K., . . . Schnaar, R. L. (2017). Siglec-8 and Siglec-9 binding specificities and endogenous airway ligand distributions and properties. *Glycobiology*, *27*(7), 657-668.  
doi:10.1093/glycob/cwx026
- Zeng, Z., Li, M., Wang, M., Wu, X., Li, Q., Ning, Q., . . . Xie, J. (2017). Increased expression of Siglec-9 in chronic obstructive pulmonary disease. *Sci Rep*, *7*(1), 10116. doi:10.1038/s41598-017-09120-5
- Zhang, J. Q., Nicoll, G., Jones, C., & Crocker, P. R. (2000). Siglec-9, a novel sialic acid binding member of the immunoglobulin superfamily expressed broadly on human blood leukocytes. *J Biol Chem*, *275*(29), 22121-22126.  
doi:10.1074/jbc.M002788200
- Zhang, M., Angata, T., Cho, J. Y., Miller, M., Broide, D. H., & Varki, A. (2007). Defining the in vivo function of Siglec-F, a CD33-related Siglec expressed on mouse eosinophils. *Blood*, *109*(10), 4280-4287. doi:10.1182/blood-2006-08-039255
- Zhang, Z., Takeda-Uchimura, Y., Foyez, T., Ohtake-Niimi, S., Narentuya, Akatsu, H., . . . Uchimura, K. (2017). Deficiency of a sulfotransferase for sialic acid-modified glycans mitigates Alzheimer's pathology. *Proc Natl Acad Sci U S A*, *114*(14), E2947-E2954. doi:10.1073/pnas.1615036114

CHAPTER FOUR  
GLYCOMIC ANALYSIS OF SITE-SPECIFIC GLYCOSYLATION FOR SARS-COV-2  
SPIKE PROTEIN

---

Adapted from:

**Rosenbalm KE**, Tiemeyer M, Wells L, Aoki K, Zhao P (2020) *STAR Protoc*

## **Abstract**

This protocol describes an integrated approach for analyzing site-specific N- and O-linked glycosylation of SARS-CoV-2 spike protein by mass spectrometry. Glycoproteomics analyzes intact glycopeptides to examine site-specific microheterogeneity of glycoproteins. Glycomics provides structural characterization on any glycan assignments by glycoproteomics. This procedure can be modified and applied to a variety of N- and/or O-linked glycoproteins. Combined with bioinformatics, the glycomics-informed glycoproteomics may be useful in generating 3D molecular dynamics simulations of certain glycoproteins alone or interacting with one another.

### **Key words**

mass spectrometry, glycomics, glycoproteomics, SARS-CoV-2, spike

## **Introduction**

This protocol was used in a recent publication (Zhao et al., 2020) to characterize site-specific microheterogeneity of glycosylation for a recombinant trimer SARS-CoV-2 spike mimetic immunogen and for a soluble version of human ACE2. The analysis quantitated the site-specific N-linked and O-linked glycosylation for SARS-CoV-2 spike as well as human ACE2 proteins. In combination with bioinformatic analyses of natural variants and with existing 3D-structures of both glycoproteins, the results generated molecular dynamics simulations of each glycoprotein alone and interacting with one another and highlighted roles for glycans in sterically masking polypeptide epitopes and directly modulating Spike-ACE2 interactions. Additionally, this protocol has broad applicability for a variety of glycoproteins that can be enriched and purified.

Prior to the experiment, clean glassware and plastic sample tubes, prepare solvents and reaction buffers and store them as stock. These may be done several months in advance with the buffers stored at room temperature (20~25 °C) or 4 °C. Protein

reduction, alkylation reagents and proteases should be added to the buffers right before their respective steps of the experiments.

## Experimental Procedures

### Reagents

- *5% Acetic acid stock solution*

Reagent	Final Concentration	Volume
Acetic acid, glacial	5%	50 mL
Ultrapure water	95%	950 mL
<b>Total</b>	<b>n/a</b>	<b>1 L</b>

Note: Store in a clean glass bottle at room temperature (20~25 °C).

- *10% Acetic acid stock solution*

Reagent	Final Concentration	Volume
Acetic acid, glacial	10%	100 mL
Ultrapure water	90%	900 mL
<b>Total</b>	<b>n/a</b>	<b>1 L</b>

Note: Store in a clean glass bottle at room temperature (20~25 °C).

- *20% 2-Propanol stock solution*

Reagent	Final Concentration	Volume
2-Propanol, HPLC grade	20%	20 mL
Ultrapure water	80%	80 mL
<b>Total</b>	<b>n/a</b>	<b>100 mL</b>

Note: Store in a clean glass bottle at room temperature (20~25 °C).

- *40% 2-Propanol stock solution*

Reagent	Final Concentration	Volume
2-Propanol, HPLC grade	40%	40 mL
Ultrapure water	60%	60 mL
<b>Total</b>	<b>n/a</b>	<b>100 mL</b>

Note: Store in a clean glass bottle at room temperature (20~25 °C).

- *50 mM Sodium hydroxide stock solution*

Reagent	Final Concentration	Volume
Sodium hydroxide solution, 50% w/w	50 mM	0.13 mL

Ultrapure water	n/a	49.87 mL
<b>Total</b>	<b>n/a</b>	<b>50 mL</b>

Note: Store in a clean plastic tube at 4 °C.

Note: The sodium hydroxide solution (50%, w/w) is viscous and needs to be treated with care.

▪ *1 M Hydrochloric acid stock solution*

Reagent	Final Concentration	Volume
Hydrochloric acid, 37%, ACS reagent	1 M	82 mL
Ultrapure water	n/a	918 mL
<b>Total</b>	<b>n/a</b>	<b>1 L</b>

Note: Store in a clean glass bottle at room temperature (20~25 °C).

▪ *1 M Sodium hydroxide stock solution*

Reagent	Final Concentration	Volume
Sodium hydroxide solution, 50% w/w	1 M	53 mL
Ultrapure water	n/a	947 mL
<b>Total</b>	<b>n/a</b>	<b>1 L</b>

Note: Store in a clean plastic bottle at 4 °C.

Note: The sodium hydroxide solution (50%, w/w) is viscous and needs to be treated with care.

▪ *10% Acetic acid in methanol stock solution*

Reagent	Final Concentration	Volume
Acetic acid, glacial	10%	5 mL
Methanol, HPLC grade	90%	45 mL
<b>Total</b>	<b>n/a</b>	<b>50 mL</b>

Note: Store in a clean glass bottle at room temperature (20~25 °C).

▪ *1 mM Sodium hydroxide in 50% methanol stock solution*

Reagent	Final Concentration	Volume
Sodium hydroxide solution, 50% w/w	1 mM	5.3 µL
Methanol, HPLC grade	50%	50 mL
Ultrapure water	50%	50 mL
<b>Total</b>	<b>n/a</b>	<b>100 mL</b>

Note: Store in a clean glass bottle at room temperature (20~25 °C).

Note: The sodium hydroxide solution (50%, w/w) is viscous and needs to be treated with care.

## Method Details

***Prepare clean glassware and plastic tubes***

1. Prepare ultrapure water by passing deionized water through 0.22- $\mu\text{m}$  Millipak® membrane filter.
2. Soak all glassware (glass pipettes, bottles, and tubes) in ultrapure water, sonicate for 45 min, and discard water
3. Soak all glassware in 50% methanol, sonicate for 45 min, and discard methanol.
4. Soak all glassware in 100% methanol, sonicate for 45 min, and discard methanol.
5. Air dry all glassware.
6. Rinse all plastic sample tubes with 100% methanol
7. Air dry all plastic sample tubes.

***Prepare solvents and reaction buffers***

8. Prepare 10 mL of trypsin reaction buffer: 100 mM Tris-HCl, 10 mM calcium chloride, pH 8.2. Store in a clean glass bottle at room temperature (20~25 °C).
9. Prepare 10 mL of PNGase F reaction buffer: 100 mM sodium phosphate, pH 7.5. Store in a clean glass bottle at room temperature (20~25 °C).
10. Activate cation exchange resin:
  - a. Soak 20 g of cation exchange resin in 200 mL of 1 M hydrochloric acid.
  - b. Decant the supernatant and wash the resin with 200 mL of ultrapure water twice.
  - c. Remove water and soak the resin in 200 mL of 1 M sodium hydroxide.
  - d. Decant the supernatant and wash the resin with 200 mL of ultrapure water twice.
  - e. Remove water and soak the resin in 200 mL of 1 M hydrochloric acid.
  - f. Decant the supernatant and wash the resin with ultrapure water till its pH becomes neutral.
11. Add 5% of acetic acid to the resin to make 50/50 (v/v) slurry.

**CRITICAL:** Use ultrapure water to prepare for any solvents and reaction buffers. All glassware and plastic tubes need to be pre-washed and dried.

### ***Trypsin digestion of glycoproteins***

It is crucial to use pre-washed, clean glassware such as glass tubes and glass pipettes as well as clean plastic tubes in order to reduce the amount of contaminant during sample preparation. Those contaminants may interfere with glycan profiling by MS analysis. The product from trypsin digestion contains peptides, salts, and other contaminants that may interfere with the subsequent PNGaseF digestion and therefore needs to be purified.

1. Prepare 2 mg/mL trypsin solution in trypsin reaction buffer and mix on vortex mixer.
2. Reconstitute the purified glycoproteins (25 µg of SARS-CoV-2 spike protein) in 200 µL trypsin buffer.
3. Heat the sample for 5 min at 98 °C prior to digestion.
4. Cool down on ice and add 25 µL trypsin solution to the sample
5. Incubate the sample at 37 °C for 18 h.
6. Stop the reaction by boiling the sample for 5 min.
7. Cool down on ice and add equal volume (225 µL) of 10% acetic acid to the sample.
8. Equilibrate a C18 cartridge with 3 mL of 100% acetonitrile, followed by 3 mL of 5% acetic acid.
9. Load the sample onto the cartridge, and discard the flow-through.
10. Rinse the sample tube with 0.5 mL of 5% acetic acid for three times, apply each rinse to the cartridge, and discard the flow-through.
11. Wash the cartridge with an additional 5 mL of 5% acetic acid, and discard the flow-through.
12. Elute and collect glycopeptides into three separate 2-mL screw cap tubes:
  - a. First elution with 2 mL of 20% 2-propanol
  - b. Second elution with 2 mL of 40% 2-propanol

- c. Third elution with 2 mL of 100% 2-propanol
13. Evaporate water and 2-propanol with a vacuum concentrator.
  14. Reconstitute the dried second elution (40% 2-propanol elution) in 0.5 mL of 5% acetic acid and pooled with the first elution (20% 2-propanol elution). The third elution (100% 2-propanol) can be used to prepare O-linked glycans.
  15. Evaporate water and acetic acid with a vacuum concentrator.
  16. Store the dry glycopeptides at -20 °C until use.

**Note:** It can be helpful to briefly vortex digestion solution every 15 min for the first hour.

**Note:** Use glass pipettes for any organic solvents and acid solutions.

**Pause point:** Dry glycopeptides can be stored at -20 °C for 3~4 weeks.

#### ***Isolating N-linked glycans released by PNGaseF digestion***

N-linked glycans are released from glycopeptides by enzymatic digestion with PNGase F and purified using C18 cartridges. The purified N-linked glycans are ready for permethylation.

1. Reconstitute dry glycopeptides in 20  $\mu$ L PNGase F reaction buffer with vortexing and sonication.
2. Add 28  $\mu$ L of ultrapure water and adjust pH to 7.5 with additional PNGase F reaction buffer if necessary. Adjust total volume of the sample by evaporating excessive buffer with a vacuum concentrator.
3. Add 2  $\mu$ L PNGase F (0.75 mg/mL) and incubate for 18 h at 37 °C.
4. After incubation, evaporate the reaction with a vacuum concentrator.
5. Reconstitute the sample in 0.2 mL of 5% acetic acid.
6. Equilibrate a C18 cartridge with 3 mL of 100% acetonitrile, followed by 3 mL of 5% acetic acid.
7. Place a clean screw cap glass tube under the cartridge, load the sample, and collect the flow-through.

8. Rinse the sample tube with 0.2 mL of 5% acetic acid for three times, apply each rinse to the cartridge and collect the flow-through.
9. Elute with an additional 1.2 mL of 5% acetic acid and collect for a total elution volume of 2 mL.
10. Elute and collect residual glycopeptides with 2 mL of 100% 2-propanol.
11. Dry the purified glycans by lyophilization.
12. Combine elution from steps 12c and 26 in a glass tube with screw top, and dry under nitrogen stream. The combined glycopeptides can be used to prepare O-linked glycans.
13. Store the dry glycans and glycopeptides at -20 °C until use.

**Note:** Use glass pipettes for any organic solvents and acid solutions.

**Pause point:** Dry glycans and glycopeptides can be stored at -20 °C for 3~4 weeks.

### ***Releasing O-linked glycans by reductive $\beta$ -elimination***

O-linked glycans are released from deglycosylated glycopeptides obtained from steps 1 through 29 by reductive  $\beta$ -elimination. After reaction, the product contains a large amount of sodium and borate salts as well as small peptides and other contaminants, and therefore needs to be purified. Following desalting and C18 purification, O-linked glycans are ready for permethylation.

17. Preparation of reaction reagents for reductive  $\beta$ -elimination.
  - a. Prepare 1 M sodium borohydride in 50 mM sodium hydroxide in a glass tube.
  - b. Add 0.3 mL of the sodium borohydride solution to the O-linked glycopeptides from step 27.
  - c. Cap the glass tube with a PTFE-lined screw cap and dissolve the glycopeptides by sonication for 30 s.
18. Incubate at 45 °C for 18 h.

19. Remove the glass tube from incubation and place it on ice for 10 min.
  20. Keep the tube on ice while adding 10% acetic acid dropwise into the sample solution until bubbling stops. Vortex and centrifuge the tube repeatedly to avoid any spillover caused by bubbling.
  21. Prepare a small glass column by breaking the tip of a pasteur glass pipette using a ceramic cutter.
  22. Plug the bottom of the glass column with some glass wool, and transfer the activated resin to the glass column (1 mL bed volume).
  23. Wash the resin with 5 mL of 5% acetic acid.
  24. Place a clean glass tube under the glass column for collection, load the sample onto the column, and collect the flow-through.
  25. Elute glycans with additional 3 mL of 5% acetic acid and collect the flow-through.
  26. Dry the glycans by lyophilization.
  27. Add 200-300  $\mu$ L of 10% acetic acid in methanol to the dried glycans. Evaporate under nitrogen stream at 37 °C.
  28. Repeat step 40 for three to five times.
  29. Reconstitute the dry glycans in 200  $\mu$ L of 5% acetic acid.
  30. Equilibrate a C18 cartridge with 3 mL of 100% acetonitrile, followed by 5 mL of 5% acetic acid.
  31. Place a clean glass tube under the cartridge for collection, load the sample, and collect the flow-through.
  32. Elute with additional 3 mL of 5% acetic acid and collect the flow-through.
  33. Dry the glycans by lyophilization.
  34. Store the dry glycans at -20 °C until use.
- Note:** Use glass pipettes for any organic solvents and acid solutions.

**Note:** When terminating the reductive  $\beta$ -elimination with 10% acetic acid, the neutralizing reaction can generate a large volume of bubbles in a short period of time and cause spills. Therefore, the acetic acid needs to be slowly added dropwise with intermittent vortexing and centrifugation.

**Pause point:** Dry glycans can be stored at  $-20\text{ }^{\circ}\text{C}$  for 3~4 weeks.

### ***Permethylation of purified N- and O-linked glycans***

Following lyophilization, the purified dry glycans are permethylated for MS analysis.

#### **35. Prepare the base solution for permethylation**

- a. Transfer 300  $\mu\text{L}$  of sodium hydroxide solution (50%, w/w) to a clean glass tube with screw top.
- b. Add 600  $\mu\text{L}$  of anhydrous methanol to the same tube and vortex for 30 s.
- c. Add 4 mL of anhydrous dimethyl sulfoxide and vortex for 30 s.
- d. Centrifuge for 30 to 60 s.
- e. Remove and discard the supernatant with a glass pipette.
- f. Repeat steps c through e for three to five times until the base slurry becomes translucent.
- g. Dissolve the precipitated base in 3 mL of anhydrous dimethyl sulfoxide by pipetting with a new clean glass pipette

#### **36. Permethylate the dry glycans**

- a. Add 100  $\mu\text{L}$  of anhydrous dimethyl sulfoxide to the dry glycans with a glass pipette and sonicate for 30 s to dissolve the glycans.
- b. Transfer 200  $\mu\text{L}$  of the base solution to the glycans with a glass pipette.
- c. Add 50  $\mu\text{L}$  of methyl iodine quickly with a glass syringe.
- d. Vortex vigorously for 5 min.
- e. Place the sample tube on ice.
- f. Add 2 mL of dichloromethane to the glycans with a clean glass pipette.

- g. Add 2 mL of ultrapure water to the glycans with a glass pipette.
- h. Vortex for 30 s, and centrifuge for 30 s.
- i. Remove and discard the supernatant (the water phase).
- j. Repeat steps g through i for three to five times.
- k. After removing water phase as much as possible, transfer the lower phase (organic phase) carefully with a new clean glass pipette to a new glass tube.
- l. Dry the sample solution under nitrogen stream at 37 °C.

37. Store the permethylated glycans at -20 °C until use.

**Note:** Use plastic pipettes for the sodium hydroxide solution.

**Note:** Use glass pipettes for any organic solvents and acid solutions.

**Note:** The base solution can be stored up to 6 h at room temperature (20~25 °C).

**Note:** Methyl iodine used in permethylation is stored at 4 °C and needs to sit at room temperature (20~25 °C) for at least 30 min prior to the reaction.

**Pause point:** Permethylated glycans can be stored at -20 °C for 3~4 months.

### ***Analyzing N- and O-linked glycans by mass spectrometry***

The permethylated glycans are reconstituted and analyzed by directly infused into a mass spectrometer. Data annotation and assignment of glycan accession identifiers are performed manually and can be facilitated by softwares.

38. Reconstitute permethylated glycans in 100% methanol: glycans derived from the equivalent of 5~15 µg of purified glycoproteins are reconstituted in 30~50 µL of 100% methanol.

39. Transfer 10 µL of the reconstituted glycans to a small glass vial using a clean glass syringe.

40. Add 40 µL of 1 mM sodium hydroxide or sodium acetate in 50% methanol to the glycans and mix by vortexing.

41. Glycans are loaded into a glass syringe, directly infused into the nano-electrospray ion source of an LTQ-Orbitrap Discovery™ mass spectrometer (Thermo Fisher Scientific), and analyzed by MS/MS.
- a. The flow rate is set at 0.4-0.6  $\mu\text{L}/\text{min}$  and the capillary temperature is set at 210 °C.
  - b. The total ion mapping (TIM) functionality of the Xcalibur software package (v 2.0, Thermo Fisher Scientific) is utilized to detect and quantify the prevalence of individual glycans in the total glycan profile. Through TIM, automated MS and MS/MS spectra (at 30-40% normalized collision energy via collision induced dissociation) are acquired in collection windows that are 2.8 mass units in width. Five scans, each 150 ms in duration, are averaged for each collection window. The  $m/z$  range from 500 to 2000 is scanned in successive 2.8 mass unit windows with a window-to-window overlap of 2 mass units.
42. Glycan species are identified by manual interpretation of the raw spectra as well as by using tools such as GRITS Toolbox (Weatherly et al., 2019), GlyGen (York et al., 2020), GNOme (OBO Foundry), and GlyTouCan (Aoki-Kinoshita et al., 2016). Manual interpretation of glycan mass spectra may be carried out as reported previously (Ashline, Hanneman, Zhang, & Reinhold, 2014). N-linked glycan peaks of all charge states are deconvoluted by charge state and summed for quantification using the Xtract functionality of the Xcalibur software package (v 2.0, Thermo Fisher Scientific). O-linked glycan peaks of all charges are manually collected and summed for quantification.

**Note:** The amount of glycans required for MS analysis depends on sample quality, such as the purity and the origin of the sample (tissue or cell types). Information on the

level of glycosylation (the number of glycosylation sites and their occupancy) of the sample is also very important and sometimes unknown. The amount of injection may need to be adjusted to enhance quality of MS profile (Mehta et al., 2016).

**Note:** In TIM, the 2.8 mass unit window allows signals from the naturally occurring isotopes of individual glycans to be summed into a single response, increasing detection sensitivity for minor structures. The 2 mass unit overlap ensures that minor glycans, whose masses place them at the edge of an individual window, would be sampled in a representative fashion.

**Note:** For detail MS<sup>n</sup> analysis to determine glycan linkage, 1 mM of lithium acetate in 50% methanol is preferred.

**Note:** Manual interpretation of glycan spectra can be facilitated by the resources provided by Expasy ([www.expasy.org](http://www.expasy.org)). The computational tools provided via Expasy can help calculating the m/z values of unmodified peptides, peptides modified with glycans, and released glycans with and/or without derivatization.

**Optional:** Permethylated glycans can also be analyzed by MALDI-TOF-MS.

## Results

This protocol is designed to fully characterize the N-linked and O-linked glycosylation of a purified glycoprotein and was optimized for SARS-CoV-2 spike protein. The glycomic analysis of released glycans allows for the elucidation of glycan structures while providing a quantitative glycan profile of the target glycoprotein. The glycoproteomic analysis characterizes and quantitates site-specific glycan topologies and provides insights into the roles of glycosylation microheterogeneity. By integrating the cross-validating glycomic and glycoproteomic analyses, the use of this protocol will provide a detailed understanding of the glycosylation states of the target glycoprotein and facilitate exploring a variety of essential roles for glycosylation.

For glycomic analysis of released glycans, process the raw spectra by deconvolution and manual interpretation. The explicit identities of individual monosaccharide residues are assigned based on known human biosynthetic pathways. Data annotation and assignment of glycan accession identifiers are performed manually and can be facilitated by GRITS Toolbox (Weatherly et al., 2019), GlyTouCan (Tiemeyer et al., 2017), GNOme (OBO Foundry), and GlyGen (Kahsay et al., 2020; York et al., 2020). Quantification are performed based on peak intensities. N-linked glycan peaks of all charge states are deconvoluted by charge state and summed for quantification using the Xtract functionality of the Xcalibur software package (v 2.0, Thermo Fisher Scientific). O-linked glycan peaks of all charges are manually collected and summed for quantification.

**Problem 1:** High signal intensity of singly-charged polymer peaks are observed and target species (glycans or glycopeptides) are at very low intensity.

The cause of this problem is likely polymer contamination. The source of polymer contamination may come from the glassware, plastic sample tubes, solvents, and buffers used in the sample preparation steps as well as the mass spectrometer. Make sure to clean all glassware and plastic tubes as described in the preparation steps and use HPLC grade reagents to prepare any solvents and buffers. If the source of contamination is in the mass spectrometer, replace any liquid transfer parts, and clean the ion transfer tube and lenses as recommended by the manufacturer.

**Problem 2:** Single glycan species is observed as multiple peaks differed by 14 Da in glycomic analysis

This problem is likely caused by under-permethylation of the released glycans and can be addressed by repeating the permethylation step (steps 48 through 50) for a second

time. Additional purification of glycans prior to permethylation using C18 and/or porous graphitized carbon columns is also beneficial to reduce under-permethylation.

**Problem 3:** Low signal intensity of N-linked glycans in glycomic analysis

If high-intensity signals from contaminants are detected, then additional purification may need to be performed to remove the interferences. Before N-linked glycans are permethylated, a porous graphitized carbon column can be used to remove contaminants in addition to a C18 column. After permethylation, the permethylated glycans can be purified using a C18 column before being analyzed by a mass spectrometer. If no high-intensity signal is detected in general, then the amount of starting material may need to be increased.

**Problem 4:** Low signal intensity of O-linked glycans in glycomic analysis

If high-intensity signals from sources other than O-linked glycans are detected, such as N-linked glycans or other contaminants, then additional deglycosylation of N-linked glycans may need to be performed using PNGase F or PNGaseA as well as additional purification by C18 and/or porous graphitized carbon columns. If no high-intensity signal is detected in general, then the amount of starting material may need to be increased.

**Problem 5:** Potential glycans and glycopeptides are detected at reasonable signal intensity, but no confident identification from data analysis.

A possible cause is that the mass spectrometer is out of calibration. Make sure to perform regular cleaning and calibration of the mass spectrometer and perform test runs of standard glycans or peptides prior to analyzing target proteins.

## **Discussion**

While this protocol can be applied to characterize a variety of glycoproteins individually, it may become less reliable when analyzing a mixture of glycoproteins. In glycomic analysis, glycans are released universally from the source material and can't be correlate to any individual source proteins. Glycoproteomic analysis can differentiate individual proteins in a mixture to certain extent based on their respective sequences but may fail to do so if the target proteins are highly conserved. Therefore, we highly recommend performing individual enrichment for each target protein by biochemical methods, such as immunoprecipitation, prior to starting this protocol.

## References

- Aoki-Kinoshita, K., Agravat, S., Aoki, N. P., Arpinar, S., Cummings, R. D., Fujita, A., . . . Narimatsu, H. (2016). GlyTouCan 1.0--The international glycan structure repository. *Nucleic Acids Res*, *44*(D1), D1237-1242. doi:10.1093/nar/gkv1041
- Ashline, D. J., Hanneman, A. J., Zhang, H., & Reinhold, V. N. (2014). Structural documentation of glycan epitopes: sequential mass spectrometry and spectral matching. *J Am Soc Mass Spectrom*, *25*(3), 444-453. doi:10.1007/s13361-013-0776-9
- Kahsay, R., Vora, J., Navelkar, R., Mousavi, R., Fochtman, B. C., Holmes, X., . . . Mazumder, R. (2020). GlyGen data model and processing workflow. *Bioinformatics*, *36*(12), 3941-3943. doi:10.1093/bioinformatics/btaa238
- Mehta, N., Porterfield, M., Struwe, W. B., Heiss, C., Azadi, P., Rudd, P. M., . . . Aoki, K. (2016). Mass Spectrometric Quantification of N-Linked Glycans by Reference to Exogenous Standards. *J Proteome Res*, *15*(9), 2969-2980. doi:10.1021/acs.jproteome.6b00132
- Tiemeyer, M., Aoki, K., Paulson, J., Cummings, R. D., York, W. S., Karlsson, N. G., . . . Aoki-Kinoshita, K. F. (2017). GlyTouCan: an accessible glycan structure repository. *Glycobiology*, *27*(10), 915-919. doi:10.1093/glycob/cwx066
- Weatherly, D. B., Arpinar, F. S., Porterfield, M., Tiemeyer, M., York, W. S., & Ranzinger, R. (2019). GRITS Toolbox-a freely available software for processing, annotating and archiving glycomics mass spectrometry data. *Glycobiology*, *29*(6), 452-460. doi:10.1093/glycob/cwz023

York, W. S., Mazumder, R., Ranzinger, R., Edwards, N., Kahsay, R., Aoki-Kinoshita, K. F., . . . Zhang, W. (2020). GlyGen: Computational and Informatics Resources for Glycoscience. *Glycobiology*, 30(2), 72-73. doi:10.1093/glycob/cwz080

Zhao, P., Praissman, J. L., Grant, O. C., Cai, Y., Xiao, T., Rosenbalm, K. E., . . . Wells, L. (2020). Virus-Receptor Interactions of Glycosylated SARS-CoV-2 Spike and Human ACE2 Receptor. *Cell Host Microbe*. doi:10.1016/j.chom.2020.08.004

## CHAPTER FIVE

### CONCLUSIONS AND FUTURE DIRECTIONS

#### **Scope of study**

The work described herein is defined by the characterization of glycosylation biosynthetic products and their impact on the immune system. The inflammatory response facilitated by the innate immune system is often associated with pro-inflammatory signaling. As the field of immunology has progressed, it has become increasingly apparent that anti-inflammatory counterresponses are just as vital as pro-inflammatory signaling to eliminate infection or pathological constituents. Dampening of the pro-inflammatory response or promoting the anti-inflammatory response has been well established by Siglec biology in a plethora of disease states including cancer and autoimmunity. The methods described in chapter four can be applied to disease models or patient tissues, as seen in chapter two, to characterize glycosylation and apply this glycome structural foundation to Siglec biology demonstrated in chapter three (**Fig. 5.1**).

#### **Discussion**

##### **The AD cortical glycome shows minor alterations in glycosylation**

Alterations in the glycome can affect several mechanisms on a molecular level. Glycoprotein modifications in the membrane can modulate cell-cell interactions which can have a host of implications. Similarly, glycolipid modifications can influence lipid raft composition and localization with a myriad of downstream signaling fluctuations.

Chapter two describes the global glycosylation patterns in iPSCs as well as derived cortical cultures in control cells as well as AD patient cells. The changes visualized include:

- A shift towards N-glycan complexity upon differentiation from iPSCs
- A relative increase in bisected N-glycans in AD NI cultures
- A relative increase in LewisX epitope decorating O-glycans in AD NI cultures
- A greater diversity in sulfated O-glycan structures in AD NI cultures
- A relative increase in LacCer with an accompanied decrease in gangliosides in AD NI cultures
- An indication of secretory pathway dysfunction in AD NI cultures with accumulated endosomes and uncouple Golgi complex

In our 5xFAD mouse model, we also observed forebrain depletion of N-glycosylation with a concomitant increase of free oligosaccharides (FOS). Since N-glycosylation aberrations have been observed in human AD models as well as patient tissues, FOS analysis should be completed in our human patient-derived model (Q. Zhang et al., 2020). FOS can arise from endoplasmic reticulum associated protein degradation (ERAD), suggesting the quality control machinery in the ER is detecting protein misfolding. Unfolded proteins are induced by cellular stressors and activate the unfolded protein response (UPR). The UPR alleviates ER stress and cell death by initiating ERAD. In ERAD, unfolded proteins are marked for degradation by the removal of mannose residues by ER mannosidases and terminal GlcNAc by ENGase and shuttled to the cytosol to interact with the proteasome. Enrichment of FOS in this AD model would further allude to interruptions in the early secretory pathway.

The disrupted secretory compartments seen in AD models provide a potential mechanism for the alterations seen in the AD glycome. The increase in FOS can be considered a readout of cell stress and the presence of an accumulation of misfolded proteins in the ER. Further, redistribution of the Golgi apparatus can impact trafficking, processing, and sorting of proteins required for normal cell function (Joshi, Bekier, &

Wang, 2015). Phosphorylation of Golgi stacking protein GRASP65 resulting in Golgi fragmentation has been implicated in AD, which could be characterized in our models. Given the evidence for impaired ER processing in conjunction with Golgi uncoupling, ER-Golgi tubule formation could be investigated (Barzilay, Ben-Califa, Hirschberg, & Neumann, 2005). Beyond the Golgi, the accumulation of intracellular endosomes seen in AD cells suggests later components of the secretory pathway are also disordered. In some AD models, A $\beta$  has been found to accumulate intracellularly in vesicular compartments before extracellular depositions are present (Rajendran et al., 2007). Co-localization studies of pathological proteins fragments including A $\beta$  and tau with endosomal markers should be completed in our models. Downstream consequences in glycosylation from ER, Golgi, and vesicular defects can affect many signaling processes including Siglec ligand production and presentation.

### **The AD CP shows tissue and epitope-specific changes in glycosylation**

Chapter three describes targeted manipulations in glycan structures that serve an explicit cellular function. The addition of Siglec ligands as immunological modulating structures to the epithelium of the choroid plexus as the main trafficking site for extravasating immune cells into the brain cannot be regarded as coincidental.

Probing brain sections from 5xFAD mouse model for Siglec ligands showed the most compelling change in the density of Siglec-F ligand was an increase on the CP epithelial apical surface. This ligand was found to modify LRP1 in the murine brain cortex and the basolateral region of the CP, where it is likely involved in leukocyte extravasation through interactions with  $\beta$ 2 integrin receptors (Ranganathan et al., 2011). LRP1 is also implicated in many different processes in the brain, such as A $\beta$  clearance across the BBB and BCSFB (Fujiyoshi et al., 2011) and modulation of signaling pathways through interactions with other cell surface receptors (Kanekiyo & Bu, 2014). At the apical surface

of the CP, Siglec-F ligands were shown to modify Gal-3BP. Likewise, Siglec ligands were found to modify Gal-3BP secreted from human CP cells. In all model systems, Siglec ligand engagement is completely sensitive to digestion with neuraminidase. In addition, the ligands were partially sensitive to PNGaseF, suggesting the epitope can decorate N- and O-glycosylation sites. Detailed structural analysis of glycosylation sites using LC/MS/MS with purified Gal-3BP from secreted from HIBCPP culture could help to address the positions of the modification as well as structural features of the glycan beyond composition. Negative mode ESI tandem mass spectrometry has also been used to characterize GAGs, which can be applied to KS analysis (Pepi, Sanderson, Stickney, & Amster, 2021). For therapeutic utility in the future, Siglec ligand structural characterization and mechanism may be required.

Further investigation of glycosylated species from CP should also be completed. Our current data are limited to the glycome of neuronal populations and assorted cell types of the cortex. Expertise from the Lehtinen lab allows for collection of primary mouse CSF and CP tissue. Glycomics from samples harvested from 5xFAD model would be interesting, as well as human patient biopsies, HIBCPP cells, and their conditioned media as a model system for human CSF. Given the changes established in the secretome of mouse CP based on proteomics and RNA sequencing during various developmental stages as well as ventricle localization, we would expect there to additionally be changes in the glycome (Lun et al., 2015). The heterogeneous expression pattern of the human CP has yet to be explored in detail. Furthermore, probing human CSF for Gal-3BP<sup>S9L</sup> as a biomarker for AD diagnosis or progression is currently underway, and high throughput analysis of CSF is possible using sandwich ELISAs.

As an element of the immune system, Siglec expression and signaling is finetuned in response to the environment. Siglec functionality is regulated by:

- Epitope affinity

- Ligand protein carrier expression and tissue specificity
- Receptor expression and tissue specificity

Each of these facets must be considered when applying Siglec physiology to a disease model and seeking an immunological outcome, as explored next.

### **The CP glycoterrain may influence immune cell function**

Chapter three describes targeted manipulations in glycan structures that we believe serve to induce a specific immunological response. Despite evidence of anti-inflammatory Siglec signaling in the literature and our hypothesis that Gal-3BP<sup>S9L</sup> challenged BMDCs would differentiate to an M2 phenotype based on our mouse model, our evidence suggests that Siglec signaling promoted inflammation by inducing expression of pro-inflammatory markers. A significant caveat here is that brain-resident microglia also express Siglec receptors and their signaling may contribute or counteract that of BMDCs (our model for infiltrating leukocytes from the vasculature).

Based on preliminary data from frozen sections of the 5xFAD mouse model, we found that increased SFFc signal at the CP was not accompanied with increased microglial density based on Iba1 staining. Our observation that there may have been an enrichment of CD206<sup>+</sup> cells at the 5xFAD CP relative to WT suggests epileptus associated immune cells are M2 infiltrating leukocytes. An important distinction to determine is whether Siglec ligand functionality serves to prime infiltrating leukocytes and/or if it is capable of recruiting leukocytes to the BCSFB. An interesting method to address this possibility would be to utilize two-photon imaging to survey cell movement at the BCSFB in live mice (Shiple et al., 2020). Such analysis should also be completed in Siglec-F null mice generated by the Varki lab (M. Zhang et al., 2007).

Likewise, Siglec-F <sup>-/-</sup> BMDCs would be a valuable negative control in our immunophenotyping experiment. Our current design targeted bone marrow derived

macrophages, but given the implications of Siglec-9 in particular on regulatory T cells (Tregs), we should also characterize the immune response of Tregs to Gal-3BP<sup>SFL</sup>. Tregs can be analyzed from bone marrow or spleen as a population of CD4<sup>+</sup>IL-2R/CD25<sup>+</sup>FoxP3<sup>+</sup> cells.

The role of glycosylation at the CP and its interplay with innate immune receptors/TLRs is likely multifaceted and serves many functions. The engagement of sialylated epitopes with Siglec receptors almost certainly accounts for a very limited snapshot of the tissue specific interactions occurring with glycosylated entities at the CP. Our observation of secreted neuraminidases from a neural progenitor population that can modulate the presentation of sialic acids presents an interesting opportunity to consider feedback mechanisms. The possibility of other soluble glycosidases or glycosyltransferases that can mold the glycoterrain from the ECM surface, particularly at signaling-enriched tissue epithelium such as CP, should be explored further. Such characterizations can greatly benefit neurological disease research and contribute to diagnostic and therapeutic potentials in AD.

## Figures

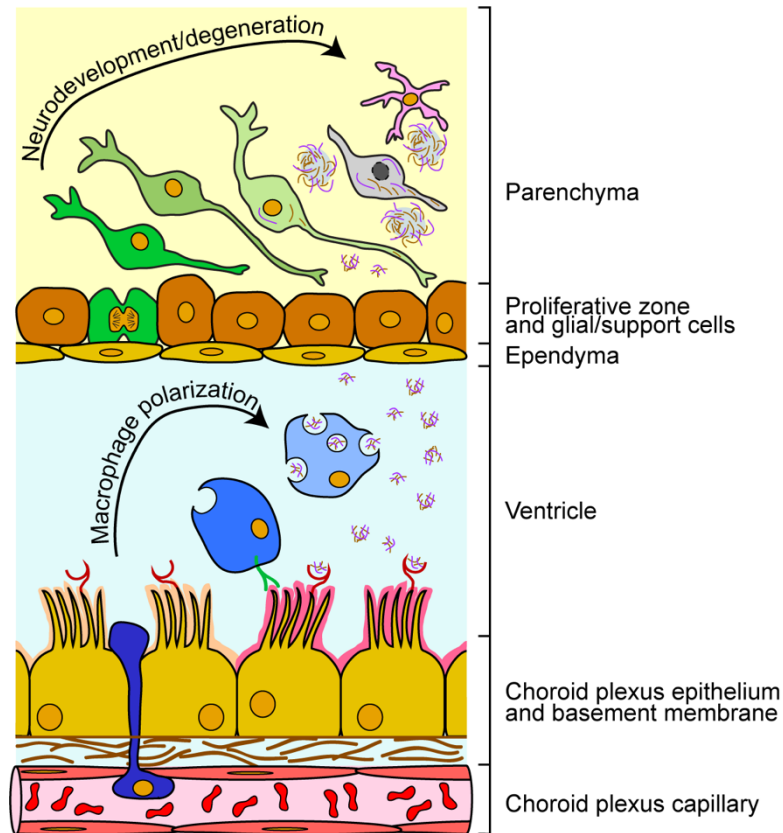


**Fig. 5.1. AD pathology produces DAMPs that interact with innate immune receptors to alter cell surface glycosylation at the CP epithelium, which functions to differentiate infiltrating leukocytes at the BCSFB**

In AD, neuronal cells in the parenchyma produce pathological elicitors such as oligomeric A $\beta$  and ptau, which percolate to the ventricles via the glymphatic system. These inflammatory derivatives interact with innate immune receptors on the CP epithelium such as TLRs and scavenger receptors. In response to inflammatory signals, the CP epithelial cells alter their presentation of glycan epitopes, including Siglec ligands. As circulating immune cells extravasate through the fenestrated capillaries of the CP and traffic through the stroma, their cell surface receptors including Siglecs interact with glycan counterreceptors. This interaction facilitates an immune response such as macrophage polarization.

## References

- Barzilay, E., Ben-Califa, N., Hirschberg, K., & Neumann, D. (2005). Uncoupling of brefeldin a-mediated coatomer protein complex-I dissociation from Golgi redistribution. *Traffic*, 6(9), 794-802. doi:10.1111/j.1600-0854.2005.00317.x
- Fujiyoshi, M., Tachikawa, M., Ohtsuki, S., Ito, S., Uchida, Y., Akanuma, S., . . . Terasaki, T. (2011). Amyloid-beta peptide(1-40) elimination from cerebrospinal fluid involves low-density lipoprotein receptor-related protein 1 at the blood-cerebrospinal fluid barrier. *J Neurochem*, 118(3), 407-415. doi:10.1111/j.1471-4159.2011.07311.x
- Joshi, G., Bekier, M. E., 2nd, & Wang, Y. (2015). Golgi fragmentation in Alzheimer's disease. *Front Neurosci*, 9, 340. doi:10.3389/fnins.2015.00340
- Kanekiyo, T., & Bu, G. (2014). The low-density lipoprotein receptor-related protein 1 and amyloid-beta clearance in Alzheimer's disease. *Front Aging Neurosci*, 6, 93. doi:10.3389/fnagi.2014.00093
- Lun, M. P., Johnson, M. B., Broadbelt, K. G., Watanabe, M., Kang, Y. J., Chau, K. F., . . . Lehtinen, M. K. (2015). Spatially heterogeneous choroid plexus transcriptomes encode positional identity and contribute to regional CSF production. *J Neurosci*, 35(12), 4903-4916. doi:10.1523/JNEUROSCI.3081-14.2015
- Pepi, L. E., Sanderson, P., Stickney, M., & Amster, I. J. (2021). Developments in Mass Spectrometry for Glycosaminoglycan Analysis: A Review. *Mol Cell Proteomics*, 20, 100025. doi:10.1074/mcp.R120.002267
- Rajendran, L., Knobloch, M., Geiger, K. D., Diemel, S., Nitsch, R., Simons, K., & Konietzko, U. (2007). Increased Abeta production leads to intracellular accumulation of Abeta in flotillin-1-positive endosomes. *Neurodegener Dis*, 4(2-3), 164-170. doi:10.1159/000101841

- Ranganathan, S., Cao, C., Catania, J., Migliorini, M., Zhang, L., & Strickland, D. K. (2011). Molecular basis for the interaction of low density lipoprotein receptor-related protein 1 (LRP1) with integrin alphaMbeta2: identification of binding sites within alphaMbeta2 for LRP1. *J Biol Chem*, 286(35), 30535-30541. doi:10.1074/jbc.M111.265413
- Shiple, F. B., Dani, N., Xu, H., Deister, C., Cui, J., Head, J. P., . . . Lehtinen, M. K. (2020). Tracking Calcium Dynamics and Immune Surveillance at the Choroid Plexus Blood-Cerebrospinal Fluid Interface. *Neuron*, 108(4), 623-639 e610. doi:10.1016/j.neuron.2020.08.024
- Zhang, M., Angata, T., Cho, J. Y., Miller, M., Broide, D. H., & Varki, A. (2007). Defining the in vivo function of Siglec-F, a CD33-related Siglec expressed on mouse eosinophils. *Blood*, 109(10), 4280-4287. doi:10.1182/blood-2006-08-039255
- Zhang, Q., Ma, C., Chin, L. S., & Li, L. (2020). Integrative glycoproteomics reveals protein N-glycosylation aberrations and glycoproteomic network alterations in Alzheimer's disease. *Sci Adv*, 6(40). doi:10.1126/sciadv.abc5802